LAPPEENRANTA UNIVERSITY OF TECHNOLOGY
LUT School of Energy Systems
LUT Mechanical Engineering

Juho Raukola

CHARACTERISTICS OF METAL ADDITIVE MANUFACTURING IN FOUR-STROKE ENGINE MANUFACTURING PROCESS

8.12.2017

Examiner: Prof. Antti Salminen
M. Sc. (Tech) Markus Välimäki
Supervisor: B. Eng. Juho Mäenpää

TIIVISTELMÄ

Lappeenrannan teknillinen yliopisto
LUT School of Energy Systems
LUT Kone

Juho Raukola

Metallin lisäävän valmistuksen tunnuspiirteet nelitahtimoottoreiden valmistusprosessissa

Diplomityö
2017

122 sivua, 53 kuvaa, 18 taulukkoa ja 3 liitettä.

Tarkastajat: Prof. Antti Salminen
DI Markus Välimäki
Valvoja: Ins. Juho Mäenpää

Hakusanat: metallin lisäävä valmistus, 3D-tulostus, DFAM, jauhepetitulostus, laser-suorakerrostus, kulurakenne, materiaaliominaisuudet

Tämä tutkimus kartoittaa metallin lisäävän valmistuksen potentiaalia ja vaatimuksia Wärtsilän moottorivalmistuksessa. Teollisen 3D-tulostuksen vaatimuksia tutkittiin suunnittelun, valmistusprosessin, kulurakenteen ja tulostettujen osien mekaanisten ominaisuuksien kannalta. Työ koostuu kirjallisuustutkimuksesta ja kokeellisesta osuudesta. Kirjallisuusosassa esitellään jauhepohjaiset tulostusprosessit ja tulostinjärjestelmät, luodaan suunnitteluohjeisto, ja löydösten perusteella muodostetaan kaksi mallia valmistuskulujen arviointiin. Lisäksi määritellään tulosteiden tyypilliset materiaaliominaisuudet, ja esitellään teollisia sovelluksia. Kokeissa tutkittiin pallografiittivaluraudan lasersuorakerrostusta nikkeliseoksilla.

Tulostinlaitteistojen pääpaino on vaihtunut prototyyppien ja piensarjojen valmistuksesta lopputuotteiden sarjavalmistukseen. Lisäävän valmistuksen avulla voidaan saavuttaa merkittäviä parannuksia moottoreiden suorituskyvyssä ja polttoainetehokkuudessa. 3D-tulostus on kuitenkin erittäin monimutkaista, ja miltei kaikki on erilaista perinteisiin menetelmiin verrattuna. Yhteensä yhdeksän eri osaamistarvetta tunnistettiin luodussa ”kannattava tulostus”-mallissa, ja sen onnistuminen vaatii intensiivistä yhteistyötä.

ABSTRACT

Lappeenranta University of Technology
LUT School of Energy Systems
LUT Mechanical Engineering

Juho Raukola

Characteristics of metal additive manufacturing in four-stroke engine manufacturing process

Master's thesis
2017

122 pages, 53 figures, 18 tables and 3 appendices.

Examiners: Prof. Antti Salminen
M. Sc. (Tech) Markus Välimäki
Supervisor: B. Eng. Juho Mäenpää

Keywords: metal additive manufacturing, 3D printing, DFAM, powder bed fusion, directed energy deposition, cost structure, mechanical properties

This study is carried out to investigate the potential and the requirements for metal additive manufacturing in Wärtsilä four-stroke engine manufacturing process. The requirements for industrial-scale implementation of AM are elaborated in design, manufacturing process, cost structure, and mechanical properties of parts. The thesis comprises a literature research, and an experimental part. In the literature part, powder-based metal AM processes, and the machinery are reviewed, comprehensive DFAM (design for additive manufacturing) guidelines are constructed, and based on cost structure research two models for part cost estimation are generated. Also, mechanical properties, and industrial applications of AM are discussed. In the experiments, directed energy deposition of nickel-based alloys on nodular cast iron is examined.

The focus of AM in industrial use has recently shifted from prototyping and small-scale production, to serial production of end-use parts. Significant increase in performance, and efficiency could be obtained in engines by AM. However, viable utilization of AM is incredibly complex ensemble of tasks, since almost everything is different to conventional manufacturing. In total, nine different expertise were identified in "feasible approach for AM" model, and intensive cooperation between all the different fields is required for successive utilization.

ACKNOWLEDGEMENTS

First, I would like to thank Wärtsilä Finland/Delivery Center Vaasa for giving me the opportunity to do this Master's thesis on the most interesting topic. I would like to show my gratitude to Professor Antti Salminen from Lappeenranta University of Technology for supervising, and for introducing me the world of laser technology, and additive manufacturing during my time as a student in LUT. Also, I would like to thank Doctor Joonas Pekkarinen for helping me with the experiments of this study. Special thanks belong to my superior and examiner of this thesis, Markus Välimäki, and to supervisor, GM of our department, Juho Mäenpää, for the valuable, down-to-earth advising during the whole thesis. Altogether, I would like to thank the whole Product Specialist team, where people were always supporting and encouraging me – it's been an honor to work with you.

I am grateful for the years I studied in Lappeenranta and for the people I met, and especially for all the persons of Koneenrakennuskilta Ry – I think you all know what we have experienced together.

Last and the foremost, I want to show my gratitude to my family for all the support you have provided me. Heidi, this last sentence is exclusively dedicated to you – you have supported me and have provided me endless inspiration by being yourself, but most importantly, you have believed in me. Thank you.

Juho Raukola

Juho Raukola

Vaasa 10.12.2017

TABLE OF CONTENTS

LIST OF SYMBOLS AND ABBREVIATIONS

AM	Additive manufacturing
ASTM	American Society for Testing and Materials
CAD	Computer adjusted design
CAGR	Compound annual growth rate
CNC	Computer numerical control
DCV	Delivery Center Vaasa
DED	Directed energy deposition, an AM method
DFAM	Design for additive manufacturing
DFMA	Design for manufacturing and assembly
DLF	Directed light fabrication, a DED-based AM method
DMD	Direct metal deposition, a DED-based AM method
DMLM	Direct metal laser melting, an AM method
DMLS	Direct metal laser sintering, an AM method
EBAM	Electron beam additive manufacturing, an AM method
EBM	Electron beam melting, a metal additive manufacturing process
FDM	Fused deposition modeling, an AM process principle
FEM	Finite element method
GA	Gas atomization, a powder manufacturing process
HAZ	Heat affected zone
HIP	Hot isostatic pressing
LBMD	Laser based metal deposition, a DED-based AM method
LFF	Laser freeform fabrication, a DED-based AM method
MAM	Metal additive manufacturing
MIT	Massachusetts Institute of Technology
PBF	Powder bed fusion, an additive manufacturing process
SLM	Selective laser melting, an AM method
SLS	Selective laser sintering, an AM method
STL	Stereolithography, file format, also an abbreviation for an AM process
VED	Volumetric energy density
WA	Water atomization, a powder manufacturing process

1 INTRODUCTION

This study was conducted to investigate the utilization potential of additive manufacturing (AM) of metals in four-stroke engine manufacturing process of Wärtsilä.

1.1 Background

Modern mechanical industry in the late 2010s is going through a major transformation as the fourth industrial revolution. Production systems are evolving to be increasingly more automated, and constantly accelerating digitalization has become a new standard for development all over the world. As the production efficiency has intensified tremendously and the productiveness of facilities has climbed, both competition in the field and demands over the performance of the products have surged even more. Thus, the up-to-date knowledge and utilization of new, vital processes are in a key role to enhance the overall productivity, profitability, and sustainability of production. One of these revolutionary technologies is additive manufacturing, which will facilitate staying competitive in the global market. (BCG 2015, p. 6-9)

Wärtsilä's power units are used to generate electricity in power plants, offshore applications, and marine industry, or as a direct power source for ships, vessels and ferries. Due to their challenging operational environment, restrictions and requirements set to the engines are strict. Emission levels have to be decreased along with fuel consumption, weight and life-cycle costs of the power unit, while the demands for performance characteristics are continuously rising. Output power per cylinder has risen over 165 % between the company's very first own model, Wärtsilä 14 in 1961, and the most recent design with the same bore size in 2017. (Wärtsilä 2017) However, the latter is still in its concept design stage, and will reach serial production readiness in the early-2020s.

Components for new engine model must follow the constraints of the desired method and in design, a trade-off between functionality and manufacturability is always present. Currently, all of the crucial mechanical components of the Wärtsilä engines are manufactured with conventional methods: casting, milling, turning and forging. The time span from initial drafting to launching of the new model in medium bore 4 stroke engines is usually several

years, and the main manufacturing methods and principles have to be selected in the early stages of designing. Although the traditional processes are usually meeting the industry requirements the most adequately, the development of manufacturing methods must be monitored continuously. Without actively probing new possibilities, the product could be designed to be manufactured using technologies which are already obsolete when the actual production begins. Furthermore, the compromises done in part level reflects an overall performance of the whole engine life-cycle, likely deteriorating engine operational statistics, efficiency of the manufacturing process, or supply-chain by creating critical vulnerabilities to the process. This can be avoided only by carefully researching the latest progress of manufacturing processes and systems and accordingly forecasting the liable trends in near future. Additive manufacturing of metallic materials appears to be such a major overhaul in novel technologies, and is expected to have a significant value-adding potential to performance of Wärtsilä engines and their manufacturing processes.

1.2 Objectives

The main objective of the study is to gather knowledge on additive manufacturing technologies and to elaborate the new possibilities these methods enable in the four-stroke engine manufacturing process in Wärtsilä Corporation. Moreover, the obtained understanding about the metal additive manufacturing is in pivotal role in the forming of Wärtsilä's AM strategy for the future.

Research questions are as follows:

- What is the status of metal additive manufacturing systems now and in the near future?
- What are the design rules required to be followed to optimize the component functionality and properties for metal additive manufacturing technologies?
- What are the characteristic costs and properties of metal additive manufactured parts and materials?
- How the metal additive manufacturing technologies should be utilized to add value to Wärtsilä's engine design and manufacturing process?

1.3 Limitations and the structure of the study

The scope of this thesis is to find the beneficent prospects of implementation of additive manufacturing of metallic materials in the medium bore four-stroke engine manufacturing process, and what kind of phenomena industrial scale utilization of AM involves. The study was limited to AM technologies utilizing only powder metal materials. The methods researched for net-shaping processes were powder bed fusion (PBF), directed energy deposition (DED), and hybrid processes which combines additive manufacturing with CNC-machining. In the literature review, the most vital methods of metal additive manufacturing for the mechanical industry are explained and onwards, the commercially available metal material AM systems are reviewed. Furthermore, comprehensive guidelines for efficient and effective design for additively manufactured products are generated, based on the functional requirements of the components and the characteristics of studied methods and materials. Moreover, the characteristic cost structure and tools for cost evaluation are elaborated, and material properties of AM materials are discussed. In the experimental part of the thesis, feasibility and manufacturability aspects of directed energy deposition (DED) of nodular cast iron with nickel-based alloys are studied. Based on the identified advantages and characteristics of metal additive manufacturing by both AM, and DED, their implementation potential for Wärtsilä engine production and manufacturing is evaluated, and a roadmap for utilization is generated.

1.4 Wärtsilä Corporation

Wärtsilä Corporation, founded in 1834 in Värtsilä, Finland, is a multinational technology company specialized in advanced energy and power solutions. Its core businesses are in the large combustion engines, and service operations in the energy field. In 2016, Wärtsilä had operations in over 70 countries, employed on average 18300 personnel, and had the net sales of 4.8 billion euros. Wärtsilä Corporation is listed in Nasdaq Helsinki, and its businesses are divided into three main divisions: Services, Marine Solutions and Energy Solutions. Their proportions of sales are 46 %, 35 %, and 22 %, respectively. According to company's strategy, Wärtsilä's mission is to shape the energy and marine markets with advanced technologies, focus on lifecycle performance, and benefit the environment. Company values are represented by three E's: energy (to capture opportunities and make things happen), excellence (to do things better than anyone else), and excitement (foster openness and trust to create excitement). Wärtsilä's vision is to be their customer's most valued business partner.

Currently in Energy Solutions division, the company has taken a major step towards hybrid energy production systems, which are comprising renewable energy sources (mainly solar, wind, and wave power) along with combustion engines. Within the system, renewables are producing the power in variable rates, and the combustion engines are used for balancing by generating adjustable power on-demand. (Wärtsilä 2017)

Marine Solutions, in turn, have developed several liquefied natural gas (LNG) engine concepts for powering cargo ships and ferries, since the Sulphur emission levels of LNG are superior when compared to engines running on fuel oil or especially heavy fuel oil. The emission standards in maritime industry have been tightened considerably, and virtually the use of heavy fuel oil has been superseded after 2020, hence increasing the market potential of sophisticated LNG power solutions for ships. (Bloomberg 2017) Increasing energy efficiency and reducing emissions is a prospective driver for implementing additive manufactured, high-performing parts into serial production engines.

1.5 Delivery Centre Vaasa

Wärtsiläs medium bore engines are manufactured in Delivery Centre Vaasa (DCV) in Vaasa, Finland, where four medium bore engine models (W20, W31, W32 and W34) are assembled. The engine models are named after their piston diameter in centimeters, which therefore vary from 20 cm to 34 cm of W34. Every single engine produced in DCV is tailor-made for client specific purposes, and is a unique configuration of the base model. Production models vary between in-line engines to V-engines, and from four up to 20 cylinders per engine. The lightest product configuration of W20 weigh approximately 8 tons, whereas the heaviest power units based on the 20-cylinder configuration of W31 can have a weight over 85 000 kilograms. Thus, the need for client customization of engines is remarkable.

1.6 Sourcing

Additive manufacturing is a relatively new method both in the field of research and industry, and the development of processes and systems is nimble. The technology is constantly evolving to become faster, cheaper, more versatile and better in quality. Up-to-date knowledge of the current situation of AM technologies is particularly important in evaluating the order of magnitude of its advantages and drawbacks in a real industrial environment. Thus, if available, sources not older than five years were used in the literature review in parts concerning the latest research in processes, materials nor systems, and their characteristics. However, some older basic seminal works has been used as a reference, such as Thomas (2009) work on design rules for additive manufacturing, hence their thesis still stays plausible and up-to-date.

2 ADDITIVE MANUFACTURING

In this chapter, additive manufacturing and its characteristics features, market, and history are reviewed.

2.1 Additive manufacturing in general

Additive manufacturing (AM, also colloquially referred as 3D printing or rapid prototyping) is a category of manufacturing technologies which add material to build the desired geometry. As ASTM has defined, additive manufacturing is a “process of joining materials to make parts from 3D model data, usually layer upon layer, as opposed to subtractive and formative manufacturing methodologies.” (SFS-ISO/ASTM 52900 2016, p. 5). The material types used for AM can vary widely and numerous substances in polymer compounds, composites, ceramics, biomaterials, and metals can be manufactured using dozens of commercially available additive techniques. Despite large quantity of different AM systems, they usually operate on one of the six main principles: filament extrusion, material jetting, powder or wire feeding, powder fusion, layer lamination, or light curing of resin.

AM gives a new kind of freedom in many fields, such as functionality design, mass-customization, manufacturing and assembly process, and supply chain. ”Energy savings, less material waste, faster design-to-build time, design optimization, reduction in manufacturing steps, and product customization are the most important advantages of AM.” (Jamshidinia, Sadek & Kelly 2015, p. 22) Since the additive manufacturing process itself is always operating without tools, even major geometry changes to the design are effortlessly implemented. In fact, as opposite to conventional subtractive manufacturing methods, increasing complexity generally expedites the process as the machine needs to process less material. Consequently, in contrast with conventional methods, complex shapes and surfaces containing lots of details are in fact usually easier to manufacture using AM than producing plain solid block of material.

Control of AM machines is always based on 3D CAD geometry. The geometry of the workpiece is designed with modeling software and the data is then converted into a printer compatible form, at present usually a .STL (strereolithography) format. The file format

conversion restructures the solid model and feature data of CAD into a set of triangles and their corresponding normal vectors, thus approximating the design surface geometry. As represented in figure 1, number 1 is the original CAD geometry of a sphere and numbers 2-4 are .STL conversions with different resolutions. The most accurate .STL, number 4, contains 16 times the data of number 2, which has a direct correlation to the file size.

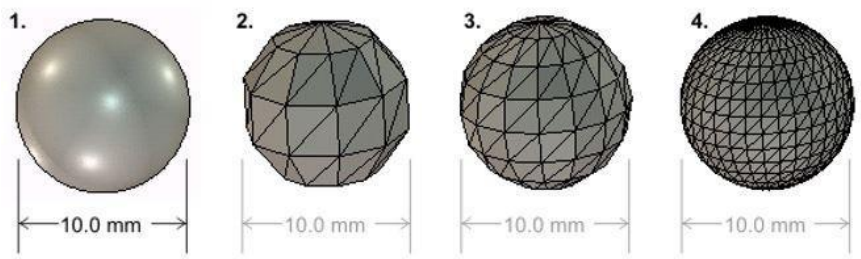

Figure 1. The effect of .STL file resolution to geometrical accuracy and file size. (Solidworks 2015)

The manufacturing resolution is defined when the .STL-geometry is sliced into thin cross-section layers according to the desired layer thickness, and the data is transferred to the AM machine. As demonstrated in figure 2, the geometry is eventually consisted of thin cross-section layers joined together, which is giving additively manufactured products their characteristic appearance with stair-stepping effect.

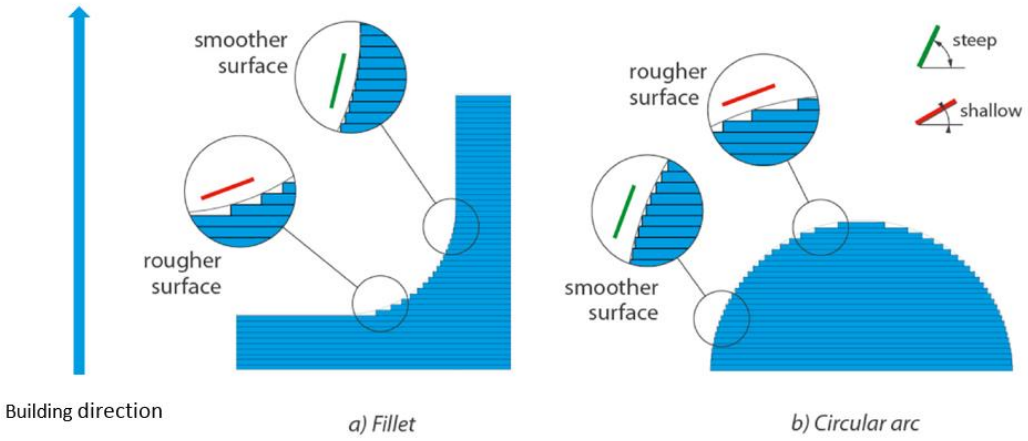

Figure 2. Stair-stepping effect in sliced geometry and its characteristic impact on surface quality. (Modified: VTT 2016, p. 10)

2.1.1 Recent trending

When new technology is emerged to the general public, and the knowledge and hard data over the ultimate limitations and boundaries have not been studied yet enough, initial expectations for the method are often exaggerated. Over the time, the inflated beliefs eventually collapse, and the technology will start its developing process towards maturity. One instrument for explaining this phenomenon is Gartner Hype Cycle, which delineates the maturity and adoption level of novel technologies and applications, such as additive manufacturing. The graph can be used to recognize the development phases of novel initiates to evaluate their real utilization value, and to put the bold promises given in innovation hype in perspective. Commonly, the new possibilities of technologies are overestimated in the short run and the effects are underestimated in the long run. Thus, knowing the present position in the hype cycle is essential in interpreting the prevailing conceptions in media, industry, and research regarding the AM technologies. Moreover, this supports making right time decisions regarding further research and implementation of AM.

As represented in figure 3, the AM industry has been under a major hype since 2012, when 3D printing, in general, was on the crest of a wave. Vital applications for additive manufacturing were seen almost infinitely and most of the crucial restrictions concerning the methods were neglected, which was naturally leading to unrealistic expectations towards the technology. When the implementation problems concretized, the hype eventually crashed down and started one’s slow progress in feasibility as the methods are matured and developed more.

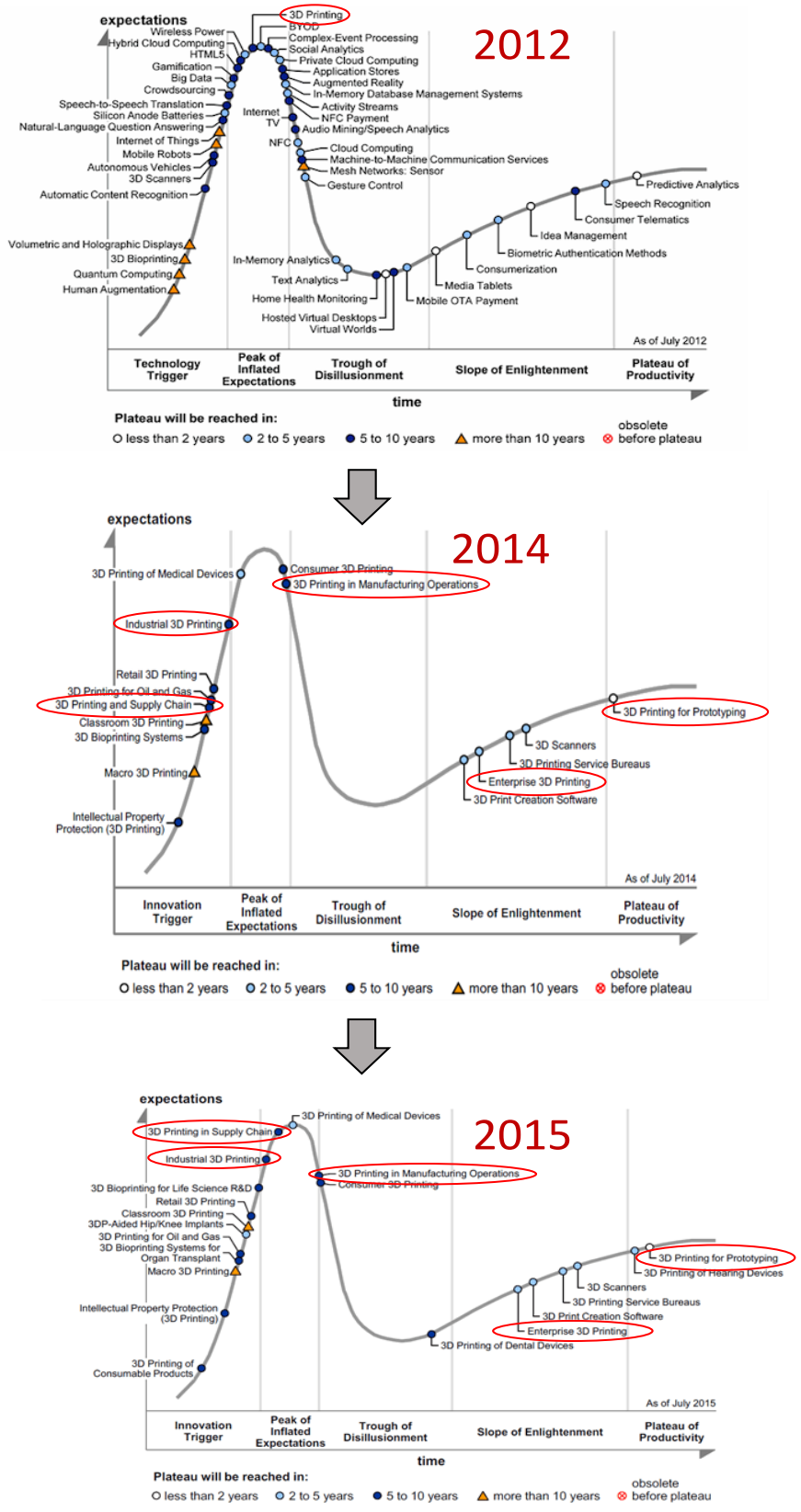

Figure 3. Evolution in global interest regarding areas of metal additive manufacturing (circled in red) represented in Gartner hype curve between 2012 and 2015. (Modified: Gartner 2012; Gartner 2014; Gartner 2015)

According to Gartner's predictions from 2014 and 2015, the areas including metal printing intended for end-use products (industrial 3D printing, 3D printing in supply chain, and 3D printing in manufacturing operations) were all seen to reach plateau of productivity at beginning of the 2020s, while the commercial feasibility for more contributory purposes for AM (prototyping and enterprise 3D printing) were seen only 2 to 5 years ahead. In turn, Wohlers annual forecast for the future of AM in 2016 predicts, that in 2020, a significant share of 10 % of industrial operations will include robot-made additive manufactured parts and functions in their end-products. It was also forecasted that product introduction timelines would be reduced by 25 % with the leverage of 3D printing, and remarkable 75 % of manufacturing operations around the globe would exploit additively manufactured jigs, tools, and fixtures in the manufacturing processes of components. (3ders 2016)

2.1.2 Market

The market in additive manufacturing has been growing extraordinary fast in the recent years. In 2011 the whole AM market, comprising system manufacturers, service providers, materials and consumer products, valued USD 1,5 billion in revenue, while during 2015 the total value surpassed USD 5,2 billion globally. (MC Cue 2016) As seen in the figure 4, in 2015, compound annual growth rate (CAGR) for the market was 25.9 %, thus aggregating the index for the previous three years starting from 2013 to 33.8 %. Over the past 27 years, total AM market CAGR is impressive 26.2 %. (EY 2015, p. 60)

The market of additive manufacturing systems has been dominated by the non-metallic material processes from the very beginning, mainly due to strong consumer market of polymer systems, and high prices and low productivity of metal AM machines. Nonetheless, the lead of non-metallic AM is constantly reduced thanks to implementation of metal systems in industry, and the metal system sales was about one third of the total sales revenues of the AM systems in 2016. (EY 2015, p. 56; Context 2016)

Despite the continually accelerating growth of additive manufacturing in recent years, it still comprised only 0.05 % of all manufacturing industry and about 1 % of machine system sales in 2016. (Koenig 2017)

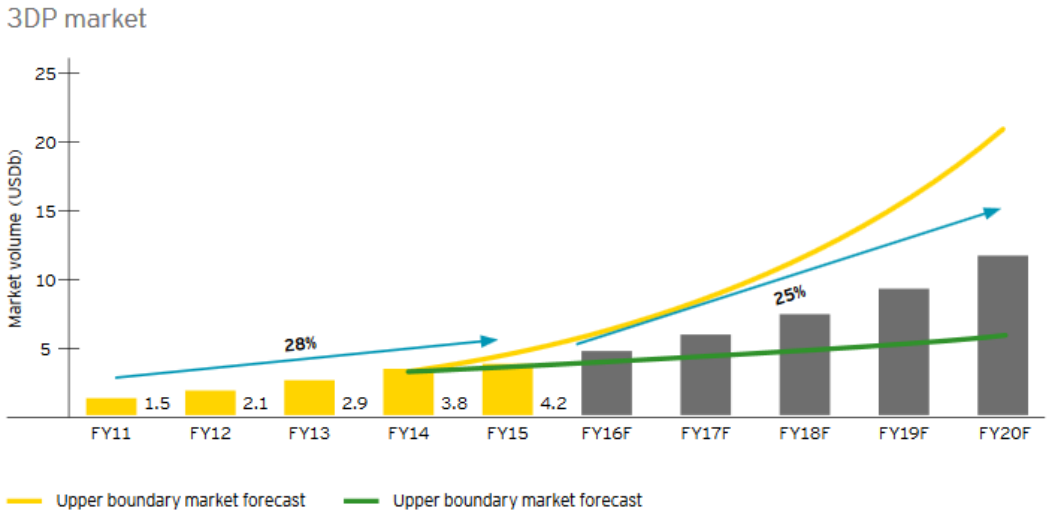

Figure 4. Value growth forecast for additive manufacturing market with realized and estimated CAGR percentages. Values in yellow are actual market values of the past years, while the gray values are the estimates for future. (EY 2015, p. 60)

2.2 History and methods

In the following chapter, the main milestones in the evolution of additive manufacturing are discussed based on the findings in the literature. At times, the progress in development with the additive methods has been parallel and coexistent, hence it is difficult to unambiguously clarify the original inventor of the methods. However, the most influential discoveries were identified similarly in several references.

2.2.1 Stereolithography (STL)

The initial concept of additive manufacturing has over 30 years of history, the first AM-relating patents dating back to the end of the 1970's. Strereolitography (STL) was invented in 1983 and patented the next year by Charles Hull in the USA, and the method is regarded as the first actual additive manufacturing process. Although multiple parallel patents in Japan, France and USA describing a similar laser-based fabrication of 3D objects were issued the same year, Hull's patent has been considered as the most trailblazing. (Davis 2014; Gibson, Rosen & Stucker 2015, p. 37) The process utilized solidification of ultraviolet sensitive liquid polymers by curing a thin 2D-layer of resin with a laser, layer by layer. The first commercial systems using the STL process emerged in 1987, and were developed by 3D Systems. (Davis 2014; Wohlers & Gornet 2014, p. 1) The company, 3D Systems, was founded by Hull, being the first enterprise fully concentrated on AM, and it is currently the

second largest AM firm by revenue in market. (EY 2016, p. 57) The .STL file format still used in the state-of-the-art machinery stems from the original format developed by Hull in the mid-1980s. (Davis 2014)

Figure 5. The first 3D printed object, which took several months to manufacture in 1983. (3D Systems 2014)

2.2.2 Powder bed fusion (PBF)

The first additive manufacturing method for metallic materials, powder bed fusion (PBF), was also coming from the United States. Patent for selective laser sintering (SLS) was firstly issued in 1986, and the process became commercially available in 1992 by DTM Co. As represented in figure 6, the technique dispersed powdered material on substrate and melted the 3D-CAD-derived cross-section with laser beam, providing a new way to produce dense and complex structures with fairly good mechanical properties. (Savini & Savini 2015; Wohlers & Gornet 2014, p. 2; Gibson, Rosen & Stucker 2015, p. 37) Even though multiple abbreviations are used by system manufacturers to describe their machine operating principles, such as direct metal laser sintering (DMLS), selective laser melting (SLM), direct metal laser melting (DMLM), selective laser sintering (SLS) and laserCUSING, they are essentially all the same process. Electron beam melting (EBM) diverges from the above-mentioned processes, since an electron beam is exploited as a heat source instead of a laser. However, EBM is still an application of powder bed fusion.

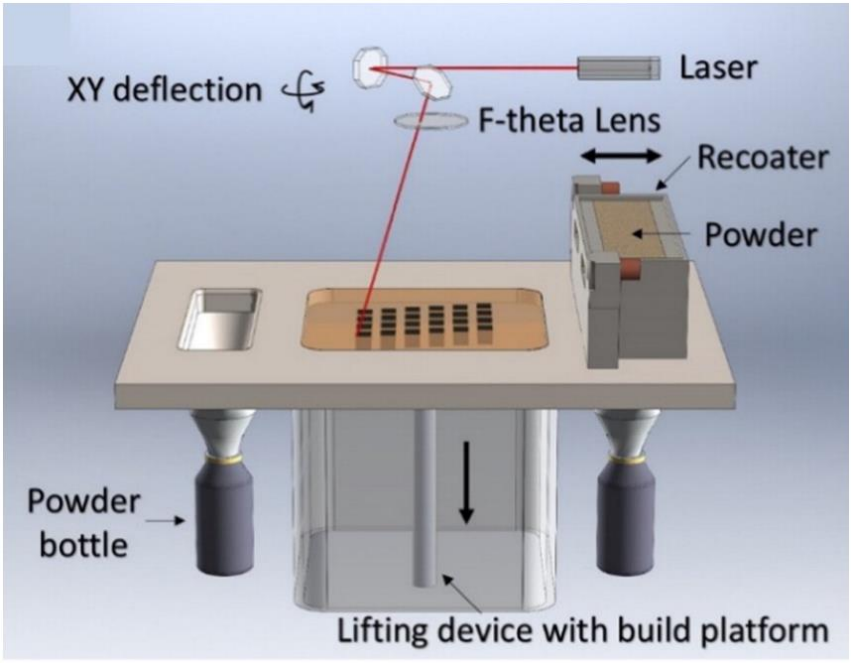

Figure 6. Schematic of powder bed fusion (PBF) system. (Modified: Sun et al. 2016, p. 198)

2.2.3 Directed energy deposition (DED)

One of the latest technologies in the field of AM is directed energy deposition (DED), which is an advanced application of laser cladding. Suitable materials for DED include several ceramics and polymers, while metallic materials are the most exploited in industry. Directed energy deposition applies heat energy from laser or electron beam to melt the surface of base material, simultaneously feeding wire or fine particles to beam with the carrier gas. The additive material is penetrated in the melt pool and it fuses to the base material, thus forming a new layer of solidified material as the process head moves forward. (Mudge & Wald 2007, p. 44; Gibson, Rosen & Stucker 2015, p. 245-246)

In figure 7, one of the main advantages of the DED over the powder bed process is shown– the ability to add material to already existing geometries, and different base materials than the powder material. Hereby, the process allows, along with substrate plates, the use of pre-machined billets or parts needing repairing as the work pieces for additively manufacturing new surfaces, functionalities, and geometries on them. (Mudge & Wald 2007, p. 44-45)

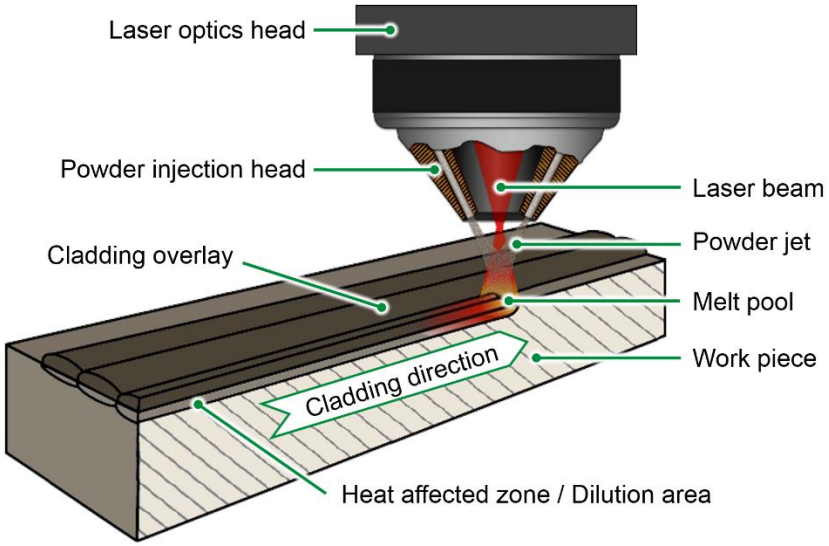

Figure 7. Directed energy deposition (DED), an advanced application of laser cladding, process principle and work piece deposition with powder material. (Flame Spray Technologies 2017)

According to Koch & Mazumder (1993), the initial concept of additive manufacturing by laser cladding was invented in 1993 at the University of Illinois, USA. Laser engineered net shaping (LENS) is usually regarded the first commercial AM application of DED and although different laser cladding technologies had been used in aviation industry since the year 1981, it was invented not until the year 1996 and was commercialized in 1997. (Mudge & Wald 2007, p. 44-45) Several organizations have developed their own DED-based processes, such as directed light fabrication (DLF), direct metal deposition (DMD), 3D laser cladding, laser generation laser-based metal deposition (LBMD) and laser freeform fabrication (LFF), even though they are principally similar processes.

3 AM OF METAL MATERIALS

The components of Wärtsilä medium bore engines are operating under the constant presence of oil, humidity, solvents and heat, along with a vicious fatiguing stress originated from rotating masses of an engine. The rigorous requirements can be effectively met by carefully optimizing crucial material characteristics, which in general are high hardness, creeping strength, fatigue and yield strength and elastic modulus. In manufacturing and assembly operations, the materials for tools and lifting devices must have an exemplary strength to weight-ratio, besides reliable and predictable behavior in cyclic stress conditions.
Albeit the multiple material and process alternatives and their advantages among the AM technologies, the requirements of company purposes are best met with AM of metallic materials.

Although the design and process principles of metal AM are somewhat similar to 3D printing of polymers, the whole manufacturing process is significantly more complex and expensive. Heat dissipation and heat related failures in structures, demand for overhang supports, along with laborious post processing are all characteristic to metal additive manufacturing (MAM). Feasible utilization of MAM requires vast proficiency in design and manufacturing to produce constant quality products efficiently.

As the laser- and EB-based MAM systems are currently the most popular and suitable for constructing a wide range of metallic materials and functional properties, the next chapter studies only the laser- and EB-based AM of metallic materials. The later research concentrates on powder bed fusion (PBF) and directed energy deposition (DED) with both laser and electron beam (EB) as the energy source, and their commercially available systems and their properties.

3.1 Processes

AM of metals can be divided into three broad categories which are powder bed systems, powder feed systems, and wire feed systems, the latter two belonging to DED processes. The main principles of these three types of systems are the same: an energy source (laser or electron beam, in wire feed systems even plasma arc) melts the feed material layer by layer and deposits it to previously solidified layers or substrate. The part is gradually generated by finite thickness 2D cross sections derived from the original geometry. The part is strongly welded to the base plate, which is always used for proper fixing and conducting the heat off the workpiece. (Gibson, Rosen & Stucker 2015, p. 108-110)

3.1.1 Powder bed fusion (PBF)

Powder bed fusion is an AM method where fine grains of metal (or with some laser-based systems, also polymer) are spread in a thin, usually 20µm – 80 µm thick layer which is hereafter leveled carefully with a recoater blade or roller. The powder is then melted using laser or electron beam following the path derived from 2D cross-section slice of the 3D geometry of manufactured component. Depending on the machine, the maximum laser output varies from 200 W to approximately 1 kW per beam and multiple lasers are often utilized to enhance the building rate, whereas electron beams are usually 3 kW at maximum power. The chamber is pumped out of air and filled with shielding gas (usually argon or nitrogen) to avoid oxidization, while EBM chamber usually operates under a vacuum environment. (Jamshidinia, Sadek & Kelly 2015, p. 22)

Figure 8. EOS M290 powder bed fusion machine, and its operator in protective gear in order to avoid exposure to harmful metal powder. (Pocketnewsalert 2017)

The build speed in powder bed fusion depends only on volumetric energy density (VED), which can be measured as the suitable energy density for additive manufacturing of certain powder material. Ciurana, Hernandez & Delgado's (2013) definition for VED is expressed in equation 1,

$$VED = \frac{P}{v\sigma t}\left[\frac{J}{mm^3}\right] \quad [1]$$

which is defined as the ratio between laser power P and the product of scan speed v, laser beam diameter σ and powder bed layer thickness t. The volumetric energy density can also be expressed through defect boundaries as a relation of scanning velocity and processing heat power (figure 9). If the metal powder is exposed to excessive heat, it starts to evaporate and generates an unwanted keyhole formation. If in turn the scanning velocity is immoderately high, the powder grains are no longer fused properly, resulting in un-melted defects. The build speed cannot be increased unreasonably with the right proportions of parameters either, due to balling up phenomena. It is caused by the characteristics of melt pool, which is scattered into droplets of molten material instead of one, stable pool when the power and velocity are both too high. (Everton et al. 2016, p. 433-434; Saunders 2017a)

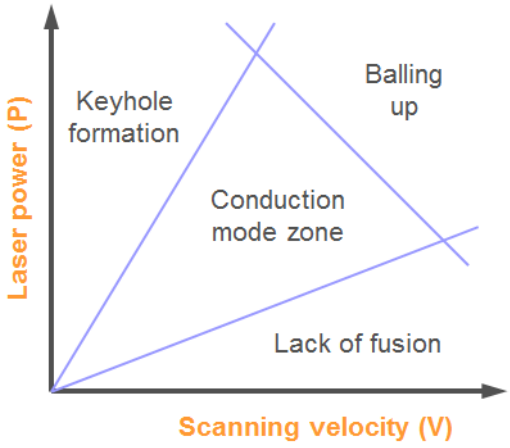

Figure 9. The optimal processing parameter window for MAM is a delicate relation of velocity and laser power. Staying in material-specific conduction mode zone is crucial in producing fully dense, defect-free parts. (Saunders 2017a)

The powder itself does not support the formed structure and works as an insulator, due to great amount of gas it contains between the grains. Additional lattice-like support structures are mostly needed to be designed in the part before manufacturing to ensure a proper contact to the substrate and to facilitate the detaching, yet parts can be also produced directly on the base plate. Supports both conduct the laser's heat off the part and support its overhanging structures, and are removed in post-processing. Sufficient heat conduction prevents overheating of a workpiece and prevents cracks resulted from thermal and internal stresses inside the structure. (Gibson, Rosen & Stucker 2015, 2015, p. 135, 53)

Figure 10. Lattice support structures are needed in parts manufactured with powder bed fusion for anchoring, heat dissipation and supporting overhanging sections. (Fabricating and Metalworking 2016)

3.1.2 Directed energy deposition (DED)

Directed energy deposition (DED, also referred as laser metal deposition (LMD)) forms a 3D geometry by feeding additive material to base material melt pool, unlike the PBF processes which utilize a pre-laid layer of material. The process differs from conventional cladding by utilizing 3D CAD data to determine the process path in three dimensions, which is not usually used in traditional deposition processes. (Gibson, Rosen & Stucker 2015, p. 245)

Characteristic, rotationally symmetric build geometry of DED is presented in figure 11.

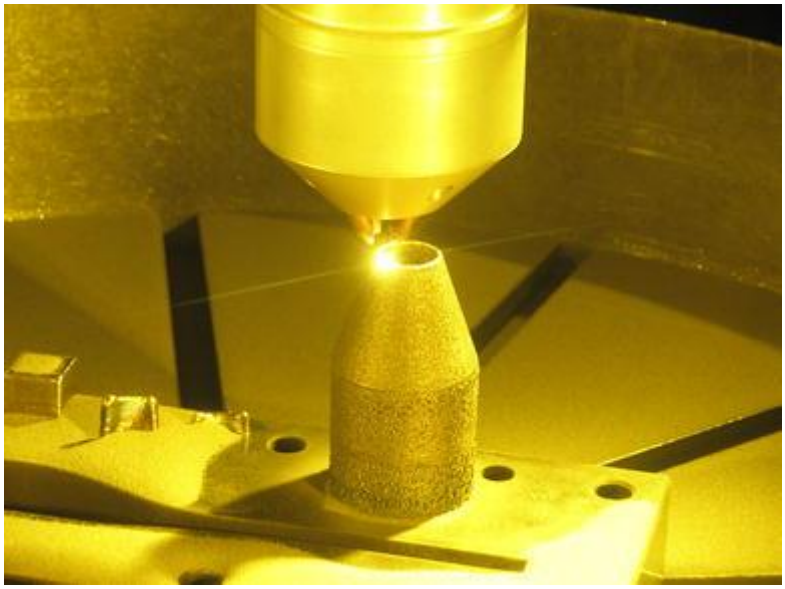

Figure 11. Typical rotationally symmetric geometry manufactured using powder-fed directed energy deposition. (Vartanian & McDonald 2016)

The solidified layer thicknesses with powder feeding vary usually from 200 µm to 500 µm and, with wire feeding even more, consequently leading to 10 times rougher resolution than powder bed processes. However, this is also notably increasing building rate, which with powder-fed DED processes can reach values of several kilograms per hour of solidified material. For instance, INCONEL718 has been deposited at the rate of 3,5 kg/h, although this was achieved using specialized research machinery (Zhong et al. 2015, p. 88). Wire-fed EB processes are the fastest MAM methods in the matter of deposition rates up to 19,8 kg per hour, compared to 325-480 g/hour building rate of PBF. However, wire-fed EB parts are manufactured with highly coarse surface and always must be machined for end use applications. (Ding et al. 2015, p. 3; Gibson, Rosen & Stucker 2015, p. 266; Zhong et al. 2015, p. 88)

Typical surface roughness values for each process are 10-16 µm for PBF, 40 µm for DED with thin layer thickness and minimal deposition speed, and up to 90 µm with decreased resolution and maximal building rate. (Guo, Ge & Lin 2015, p. 17)

Wire feed systems are capable of larger building rates and utilization of more inexpensive additive materials than powder-DED systems, but the parts need more post-processing due to coarse surface quality. Wire-fed systems are often used to manufacture near net-shaped billets to be machined to final dimensions, rather than producing as-consolidated end products. They also lack any complex internal shapes or functionalities, and the parts are usually rib-on-plate (figure 12) or rotationally symmetric structures (figure 11). (Frazier 2015, p. 1919-1920; (Gibson, Rosen & Stucker 2015, p. 256)

Typical process-specific values for metal AM processing are presented in table 1, and the ancillary treating demands are categorised by process later in table 2.

Table 1. Characteristic values for metal additive manufacturing methods. Processes are denoted with abbreviations, where PBF (powder bed fusion), DED (directed energy deposition), and for energy source EB (electron beam). Sources: ([1] Machine suppliers' internet pages, optimal geometry for fast deposition; [2] *as-build: Gu 2015, p. 17; Bossuyt & Fournier 2016)*

Process	**Build speed [kg/h]** [1]	**Surface roughness [µm]** [2, 3]	**System price [k€]**
PBF (Laser, Powder)	0,4	5-16	200-1200
DED (Laser, Powder)	1	20-90	200-800
PBF (EB, Powder)	0,5	20-25	500-800
DED (Laser, Wire)	0,7	> 50	300-1000
DED (EB, Wire)	19,8	> 200	> 1800
DED (Arc, Wire)	6	> 200	100-1000

Table 2. Ancillary processes for metal AM technologies. Processes are denoted with abbreviations, where PBF (powder bed fusion), DED (directed energy deposition), and for utilized energy source EB (electron beam). For heat treatments, S stands for stress relief treatment right after manufacturing, and A for more extensive heat treatments, such as solution annealing, and aging. (Gibson, Rosen & Stucker 2015)

Process	**Powder conditioning**	**Machining**	**Cutting**	**Support removal**	**Heat treatment**
PBF (Laser, Powder)	X	(X)	X	X	S, A
DED (Laser, Powder)	X	X	(X)	(X)	S, A
PBF (EB, Powder)	X	(X)	X	X	A
DED (Laser, Wire)		X	X		S, A
DED (EB, Wire)		X	X		S, A
DED (Arc, Wire)		X	X		S,A

Figure 12. Titanium rib-on-plate structure additively manufactured using wire feed DED and post-processed by machining. (GKN 2017)

One of the most prominent advantages of directed energy deposition over the PBF is its utility for repairing worn-out or broken parts. The damaged surfaces or even features can be replaced with the same material, or it can be replaced with layer of material with preferable property profile for the part's performance. DED can also be utilized to manufacture functionally graded materials (FGM) by gradually mixing two or more powders, and thus adjusting the optimal additive material composition over the deposit. For cost-effective building of 3D geometries, a major section of part can be manufactured of relatively

affordable material, and to enhance their functionality, deposit inexpensive base material with e.g. durable, high-performance surfaces, for example metal matrix ceramic composites. DED is particularly suitable for manufacturing larger components than PBF, and parts up to 6 meters can be manufactured in electron beam DED manufacturing chamber. Since the laser-based DED processes can be mounted on an industrial robot, the maximum dimensions for the processed parts are theoretically boundless. (Ding et al. 2015, p. 13-15; Gibson, Rosen & Strucer 2015, p. 258, 266-267)

Typical characteristics of process-specific metal additive manufactured parts are explained in figure 13 below.

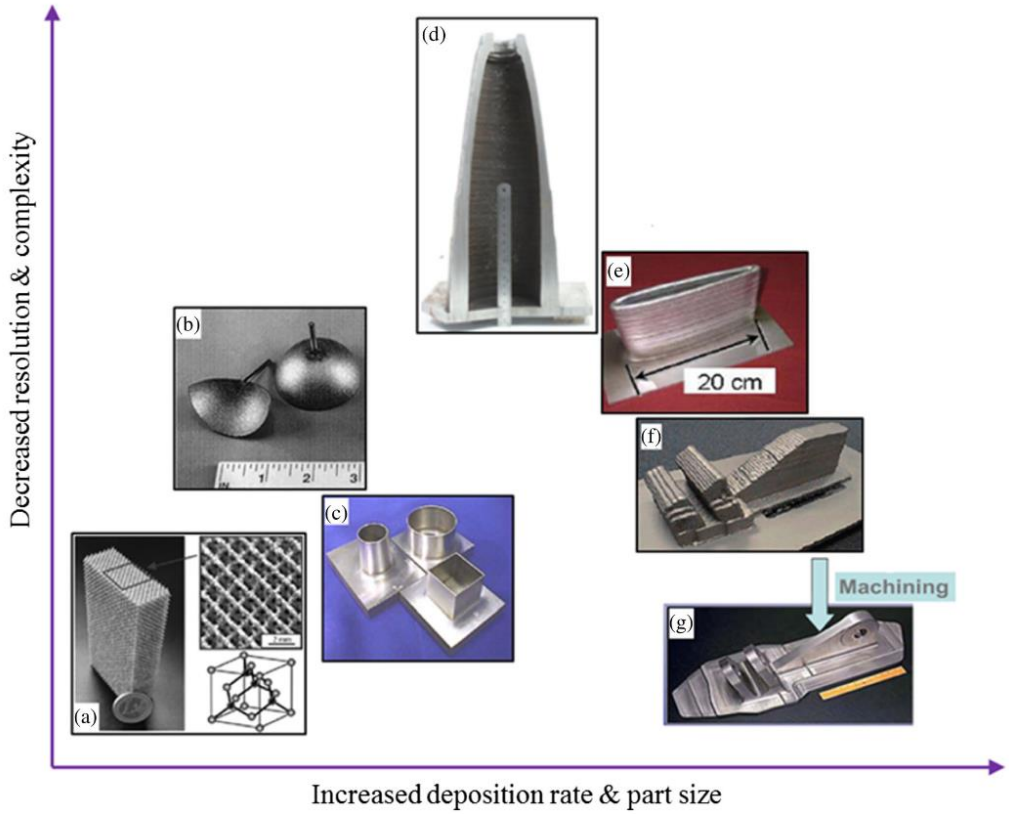

Figure 13. Comparison of surface finish and building speed of different MAM processes; a) Electron beam PBF-process fabricated titanium diamond lattice structure. b) Powder-feed laser-DED manufactured hemispherical shapes of 316L stainless steel. c) Powder-feed laser-DED as-consolidated INCONEL-625 geometries with the surface roughness of 1-2 µm. d) Wire-arc additive manufactured (WAAM) large titanium sample piece. e) Wire-feed EB-DED joined aluminum 2219 airfoil. f) Wire-feed laser-DED as-deposited bracket and g) the same piece after the post-machining process (material not specified)
(Ding et al. 2014, p. 3)

Wire-fed DED processes are mostly utilized only for coarse preform manufacturing, and extensive machining of workpieces is always require, whereas the electron beam-DED is currently dedicated only for large titanium part manufacturing. For Wärtsilä purposes, desired MAM method would provide end-use parts with minimal post-processing and machining need with moderate stock material pricing, thus the wire-fed and titanium-focused processes are excluded from the investigation. Thereinafter, this study is focused on powder-based AM processes only.

3.2 Process chain characteristics

Process chain in AM of metallic materials typically consists of eight consecutive steps which are shown in the figure 14.

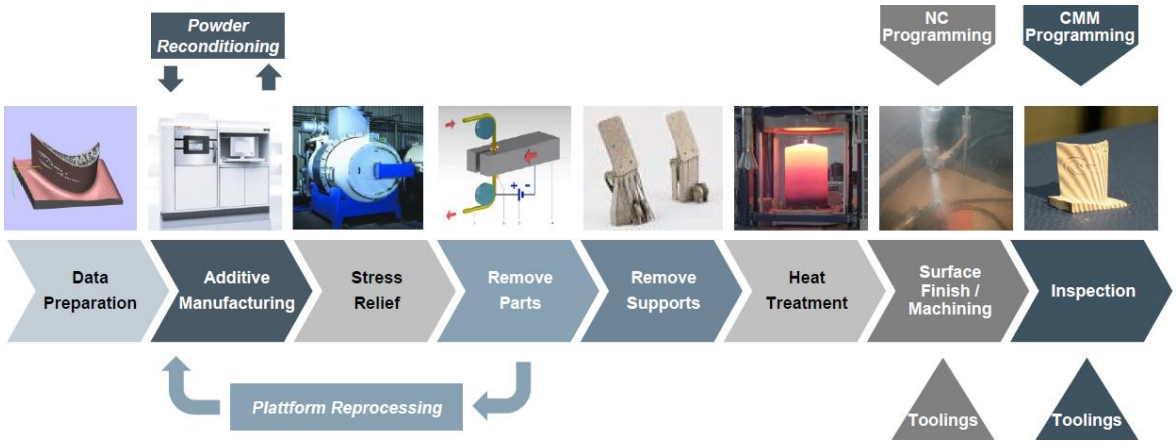

Figure 14. Typical additive manufacturing process chain for turbine blade using metal PBF as the main method. (Dusel 2014)

The first stage in chain is CAD design, which determines the manufacturability, profitability and performance of a component. Hence, it should always be done with great care and knowledge over the desired AM process and considering the limitations of it. After the design, geometry is converted to machine compatible form, necessary support structures are generated and manufacturing parameters are defined by operator before manufacturing phase is executed. Due to large amount of process heat in both PBF and DED, residual stresses are always present in as-manufactured parts, and must be relieved by annealing the whole batch in oven before cutting. Afterwards, the components are detached from substrate plate with wire cutter or band saw, and the support structures are removed. Currently,

especially with complex parts, significant amounts of manual removing work of supports is needed in post-processing, and thus minimizing the supports by part design should be a great concern. After the supports are removed, different heat treatments, e.g. hot isostatic pressing, could be applied to optimize the internal microstructures and reducing porosity of part. This is generally carried out to enhance fatigue strength and ductility, and to reduce porosity in parts. If the component contains strict tolerances, or requires better surface quality than in as-build condition, surface finishing with shot peening, sandblasting or polishing can be done after heat treatment. Final inspection is the last phase in metal AM process before end use of the component. Depending on the requirements, the phase contains several inspections with laser or computed tomography (CT) scanning. The surface of substrate is rough after the detaching of the parts and contains remains of the detached support structures. Additionally, the build platform must be machined smooth after every manufacturing cycle of PBF processing, and also if the substrate is used with DED processing. (Moylan et al. 2013, p. 23-27; Gibson, Rosen & Stucker 2015, p. 44-49)

Due to manifold nature of the metal additive manufacturing process chain, in addition to AM machine, multiple process equipment must be included into the production cycle. Figure 15 is indicating a minimum space recommendation of manufacturing cell for medium class PBF machine, EOS M290, and the ancillary machinery demands for holistic AM fabrication facilities. (EOS 2017) Ancillary equipment comprises, inter alia, furnace for stress relieving, inspection systems, and a post-processing bench with manual tools for support removal. Also is notable that the space in the immediate vicinity of the PBF must be ESD (electrostatic discharge) protected area, hence the feedstock powders are highly reactive and in worst case, can ignite from small spark. (Moylan et al. 2013, p. 2; 7)

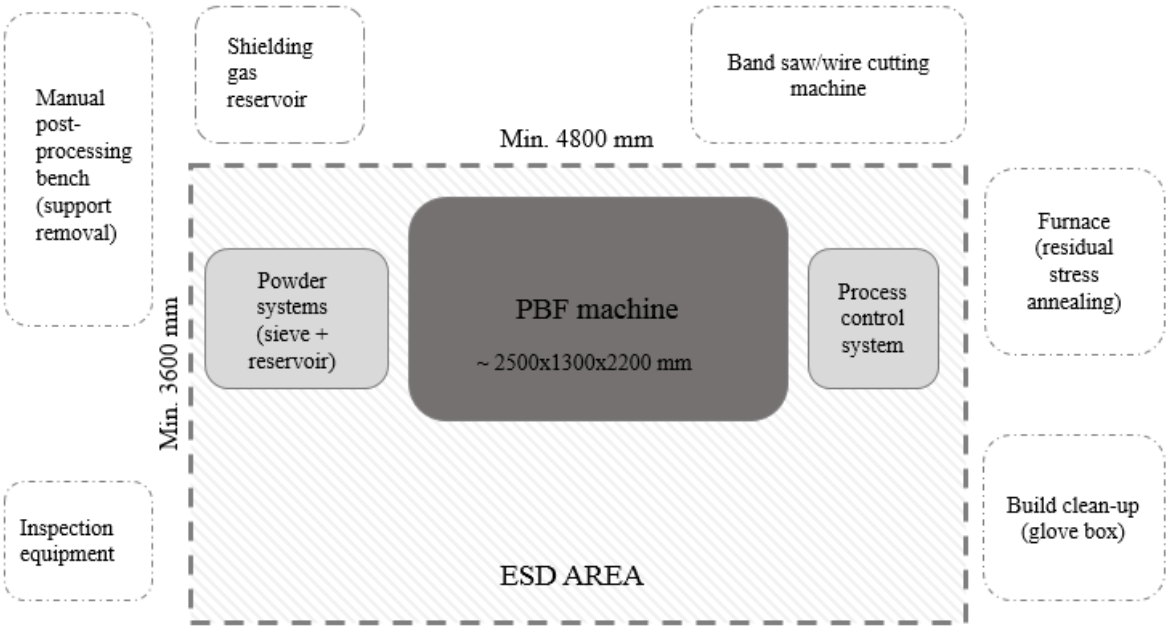

Figure 15. Layout demonstration of a metal additive manufacturing cell. (Moulan et al. 2013, p. 2; 7; EOS 2017; Gibson, Rosen & Stucker 2015, p. 44-49)

3.3 Building speed of PBF

Build rate defines the amount of solidified metal material over time and is usually given in form of mm^3/s or cm^3/h. The maximum building speed in PBF strongly depends on the volumetric energy density required for certain powder material, as well as manufactured geometry and the layer thickness (resolution) of the build. Thus, the supplier-given peak building values are measured with solid, plate-like structures that can be manufactured with minimal auxiliary time, which mostly consists of recoater cycle times. However, the realistic build rates in real-life part production are usually significantly lower than the theoretical values, practically being around 1/3 – 2/3 of the ultimate maximum value of the system. (SLM 2017)

When comparing different PBF systems by performance, laser power and laser beam quantity are the most important factors in PBF machine productivity, since the scanner and recoater systems are almost identical. However, by almost quadrupling the laser power from 100 W to 380 W resulted in only 72 % increase in total build rate with sample cubes manufactured of 316L. This is caused by the large share auxiliary times per layer, which can vary much, taking 30-80 % of total layer cycle time. If the geometry is tall and thin, relatively more time is spent for recoating, instead of melting the material. With dense and low parts the increase in laser power is the most effective in terms of building speed. (Sun et al. 2016, p. 201)

Also, as VED has the material specific maximum limits for decent manufacturability, and the melt pool stability requires scan speed to stay at a certain level, the highest laser beam power of 1kW is generally used only with aluminum and other materials with high thermal conductivity. Practically every other metallic materials are manufactured with lower beam power compared to aluminum, due to slower heat dissipation and greater laser absorption rates of the materials (Buchbinder et al. 2011, p. 1-3).

The surge development in deposition rates in 1997-2017 is represented in figure 16 below. In the early days of PBF, build speed was limited to poor beam quality and lack of laser power in machines. Since the system suppliers started to utilize fiber laser technology and multiple laser beams in their machines in a larger scale, maximum building speed of 100 cm^3/h on a decent resolution were obtained first time with PBF in the 2010's. However, the laser beam-wise VED limits have already been reached with the current processes, and the

next leap in PBF build rates could be achieved only by increasing the number of the beams in systems. The defect phenomena steering the process parameters for scan speed and laser power are addressed later more broadly in chapter 6.3.

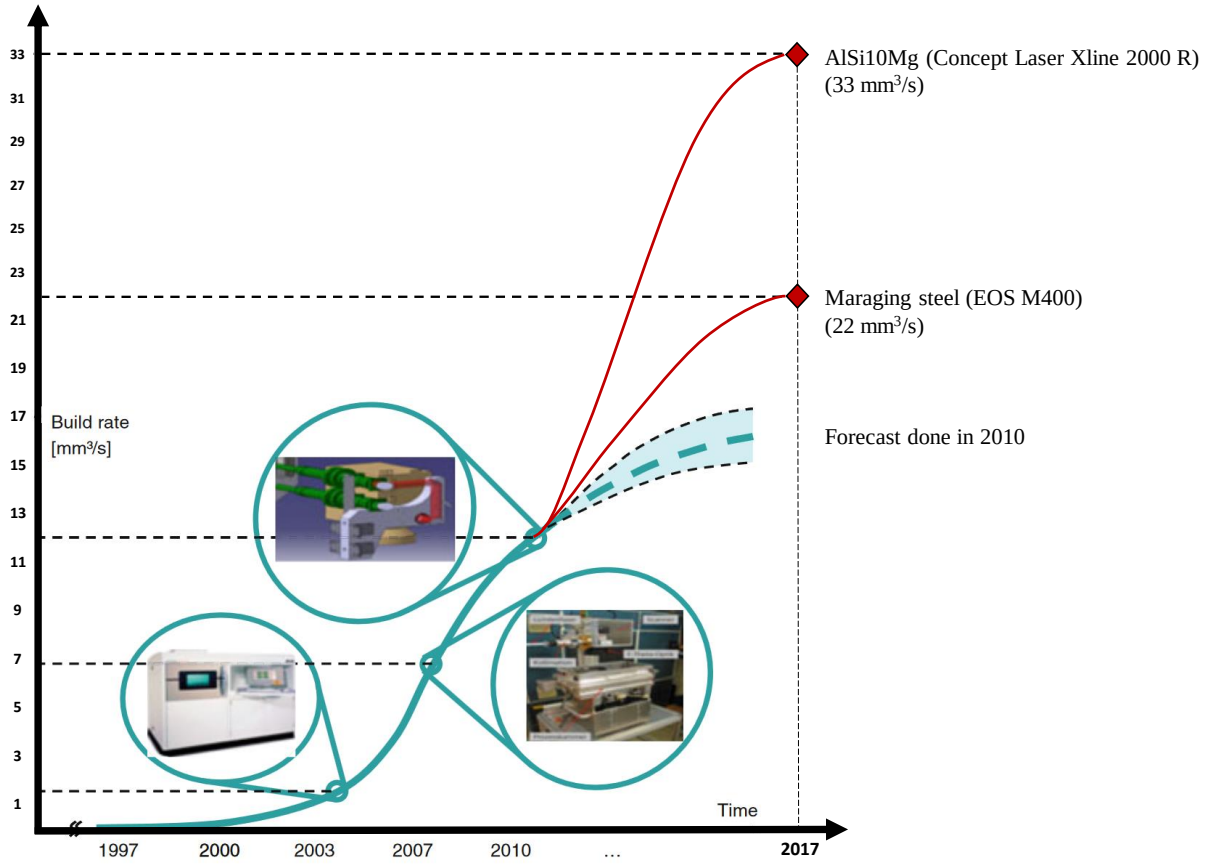

Figure 16. Development of laser-PBF machine volume build rates in 1997-2017. A major development in machine productivity rates has been achieved since the build speeds have 3-4 folded in a decade. (Modified: Schuh et al. 2012, p.144; EOS 2017; Concept Laser 2017)

3.4 Powder feedstock materials

Wide range of metallic materials are utilized in MAM, including stainless steels, tools steels, titanium, aluminum, INCONEL and other nickel alloys, and cobalt chromium. Since the powder bed fusion (PBF) and directed energy deposition (DED) processes are mainly welding, one the most important property of metallic materials for additive manufacturing is weldability, or in other words, printability (Gibson, Rosen, Stucker 2015, p. 258). It can be defined as a material's ability to resist distortions, lack of fusion, and changes in chemical

composition during the repeated melting and solidification cycles present in MAM (Mukherjee, Zuback & Debroy 2016, p. 1).

Powders used as a feedstock for metal additive manufacturing processes are mainly manufactured by gas-atomization (GA), where a jet of inert gas is blown to the molten metal droplets, and fine powder particles are formed. This way, the powder grains are spherical, regular shaped and are produced with great purity level with minimal oxidation, which all favor good flowability of powder. Furthermore, this is profitable for use in metal additive manufacturing processes to maximal solid density and melt pool stability in manufactured material. (Herzog et al. 2016, p. 373-374; Erasteel 2017; Zhong et al. 2015, p. 87-88)

Powders manufactured by water atomization (WA) are more affordable and could also be used for certain applications. They are manufactured mostly the same way as the gas atomized powders, but by utilizing a jet of water instead of inert gas. The grains produced by water atomization are more irregular and non-spherical, and thus are less optimal for MAM processes than gas atomized materials. (Herzog et al. 2016, p. 373-374; Hoeges, Zwiren & Schade 2017, p. 112-114) However, comparable results in manufactured test specimen have been realized between materials manufactured by gas or water atomization when the powders were solidified using PBF. No significant differences in mechanical properties were not observed, despite that chemical composition of water atomized powder was altered slightly from original raw material, which is typical to WA. (Hoeges, Zwiren & Schade 2017, p. 113-114)

Powder particle size distribution is supplier-dependent, but the mean grain size of MAM materials is around 20-150 µm. Laser-powered powder bed fusion machines are using the finest powders (20-70 µm), the electron beam PBF machines a little coarser (45-100 µm) and the directed energy deposition (DED) systems the biggest grain sizes (50-200 µm) of additive metal processes. (Gibson, Roser & Stucker 2015, p. 258)

Table 3 shows the characteristic prices for PBF-grade materials distributed by EOS, which, compared to conventional material pricing, are generally one or two orders of magnitude more expensive. However, in contrast with subtractive manufacturing materials, where significant amount of material is removed from billet and then scrapped, additive materials

are utilized usually almost entirely. This is profitable especially with highly valuable materials such as titanium, and complex geometries, where the portion of subtracted material from billet using conventional methods would be high. Also, instead of particular AM-grade powders, gas atomized powder thermal spraying materials could be utilized in most cases of MAM since the chemical composition, shape (spherical), and grain size distribution of the powder is similar among these two grades. The price of the AM-labeled materials is usually 2-5-fold higher than the comparable powders for thermal spraying. For instance, EOS 316L powder intended specifically for AM, and Höganäs 316L powder for thermal spraying applications, are practically identical for their characteristics. However, they differ greatly in their retail price, since the Höganäs powder is provided by supplier for around 45 €/kg, while EOS powder's pricing is being around 180 €/kg. (EOS 2017; Höganäs 2016; Slotwinski et al. 2014, p. 465-469). This can be explained by the dissimilar qualification and validation levels of the powder materials among suppliers. The provided warranty for raw material quality is the main reason for purchasing the feedstock from companies like EOS, instead of inexpensive yet practically similar powders from other suppliers. Also the intensifying competition in the powder metal industry is decreasing the prices in the coming years. (Ampower Insights 2017, p. 18)

Table 3. Material price ranges for powders supplied by EOS in North America for metal additive manufacturing using PBF. Welding wire feedstock prices are presented for reference. (EOS 2014)

Material	**Feedstock type**	**Price [€/kg]**	**Price [€/cm^3]**
316L SS	Powder	180	1,4
AlSi10Mg	Powder	152	0,4
Ti64	Powder	617	2,7
IN718	Powder	192	1,5
Steel	Wire	5	0,05
Titanium	Wire	170	0,8

4 METAL ADDITIVE MANUFACTURING SYSTEMS

Since the launching of the first commercial PBF systems in 1992, the process has grown by far the most common metal AM method in the industry. In 2016, PBF systems comprised 90 % of total metal additive manufacturing (MAM) system market in value, and had seven times higher unit sales than the systems exploiting DED technologies. (Caffrey, Wohlers, Campbell 2016, p. 61; Context 2016) As these two processes are currently dominating the MAM market, both PBF (powder bed fusion) and DED (directed energy deposition) systems are presented by the key factors of the different systems in this chapter. Both type of systems are divided into categories, and a typical example machine in every class is introduced more in detail. Complete list of system manufacturers, publicly available attributes, and manufacturing values of systems are represented in appendices I, II & III.

4.1 PBF systems

The field of laser powered, metal powder bed machine manufacturing companies has been growing strongly in recent years, but still, the sales proportions are somewhat concentrated in companies started right after invention of the technology in the 1990's. The largest three PBF suppliers by units sold are EOS GmbH, Concept Laser GmbH and SLM Solutions GmbH, respectively. They are all based in Germany, yet their competitors are mostly located outside Germany, e.g. 3D Systems in the United States, Renishaw in the United Kingdom and the numerous new rivals from China, like Syndaya and Huake 3D. In total, there are at least 15 laser-based PBF machine manufacturers and different machine models well over 30 in global market, and the amount is rising continually. (FIRPA 2016; Total Optics 2017) The market shares of metal additive manufacturing companies are represented in figure 17.

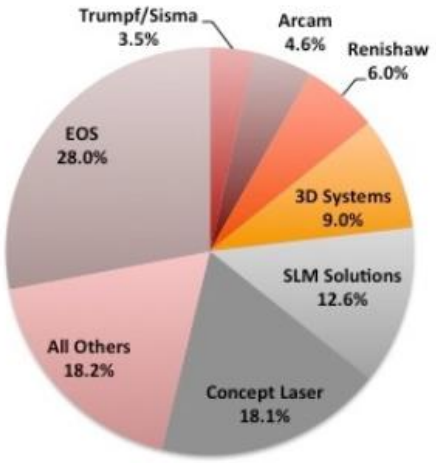

Figure 17. Market shares of MAM systems manufacturers globally in 2016. (Total Optics 2017)

4.1.1 Small class machines

Machine portfolio of the leading companies in general consists of systems in three categories. The smallest machine build chamber is usually around 100 mm per side, equipped with laser powers ranging from 200 W to 400 W, and these machines are mostly targeted for dental industry needs. System cost of these light machines is usually between 200 000-350 000 €. (FIRPA 2016) An overview of values of a small-class machine by EOS is presented in table 4.

Table 4. Small class PBF machine (EOS M100) general attributes. (EOS 2017; FIRPA 2016)

Company	**Model**	**Building chamber [mm** x **mm** x **mm]**	**Power [W]**	**Build rate [cm³/h]**	**Price [M€]**
EOS	M100	Ø 100 x 95	200	< 10	0,3

4.1.2 Medium class machines

Medium size machinery is the most common category in industry, owing to competitive productivity rate in relation to total system costs. Building volume of this class is generally around 300 mm x 300 mm x 300 mm and laser powers varying from 200 W to 1 kW, though the most common laser power being 400 W. To enhance productivity, multiple lasers are utilized for melting the material simultaneously in different parts of the chamber, although the system cost are rising correspondingly, as the laser is one the most expensive components

in the machines (Gibson, Rosen & Stucker 2015, p. 54). Price range for medium class machinery starts from 350 000 € for the most affordable single-laser configurations, ending in dual-laser systems such as SLM 250 2.0 (represented in table 5) for around 700 000 €. (FIRPA 2016)

Table 5. Medium class PBF machine (SLM 250 2.0) general attributes. (SLM Solutions 2017)

Company	**Model**	**Building chamber [mm** x **mm** x **mm]**	**Power [W]**	**Build rate AlSi10Mg [cm^3/h]**	**Price [M€]**
SLM Solutions	SLM 250 2.0	280 x 280 x 365	2x400	55	0,7

4.1.3 Large class machines

The most productive systems are almost without exception large multiple laser systems. The systems are often utilizing four 400-700 W lasers operating their own square in powder bed with small overlap to each other. High power lasers up to 1 kW are also available, and they are generally coupled with lower output lasers for skin-core-processes, where the part borderlines are melted with low power beam and the inside cores are produced with higher output. Thus, the surface quality can be optimized while the productivity rate is enhanced considerably. (EOS 2013, p. 9)

A large-class machine by Concept Laser is represented by its main operational values in table 6. The system manufacturers' flagships are also the most expensive PBF machines in market, pricing from 800 000 € to around 1,5 million €.(FIRPA 2016) Dimensions of the building chamber in the large class machines are generally around 300-400 mm per side, while the largest chamber in the market is 800 x 400 x 500 mm by Concept Laser X line 2000 R (table 6). Concept Laser also claims that the machine is the most productive in the means of building speed with 120 cm^3/h of solidified metal. (Concept Laser 2017) However, besides machine attributes alone, building speed strongly depends on the external factors such as part geometry, material and the manufacturing resolution, hereby any unambiguous conclusions over the figures provided by the system manufacturers cannot be done. (Sun et al. 2016, p. 201)

On the contrary to challenges with big machining centers' lack of ability to produce constant accuracy quality, the larger powder bed machines are usually as precise as the smaller models, since the process parameters and conditions are almost identical to smaller models (EOS 2017). As the act of manufacturing in PBF machines is operating without any physical tool contact, vibrations and large moving masses are absenting in work piece, unlike the situation with the traditional machining methods.

Table 6. Large class PBF machine (Concept Laser Xline 2000R) general attributes. (Concept Laser 2017; FIRPA 2016)

Company	**Model**	**Building chamber [mm** x **mm** x **mm]**	**Power [W]**	**Build rate AlSi10Mg [cm^3/h]**	**Price [M€]**
Concept Laser	Xline 2000R	800 x 400 x 425	2x1000	120	1,5

4.1.4 Hybrid-PBF machines

In recent years, alongside the machines operating with mere powder bed process, a few hybrid-PBF system manufacturers have emerged to the market. Combined in single machine, the process utilizes both laser-PBF and CNC machining technologies. Powder bed fusion is used for building material, and subtractive methods, such as high-speed milling, for surface smoothening of melted layers between the melting cycles. Surface quality of the as-build parts of hybrid-PBF machines is superior to normal powder bed systems, but the build rate, even at its best, is 2-3 lower since the milling and PBF processes cannot operate simultaneously. Hybrid-PBF systems are mainly utilized for mold manufacturing in polymer industry. (Matsuura 2016) The main attributes of the flagship model of Matsuura hybrid-PBF machine are presented in table 7 below.

Table 7. Hybrid-PBF machine (Matsuura LUMEX Avance-60) general attributes. (Matsuura 2016; FIRPA 2016)

Company	**Model**	**Building chamber [mm** x **mm** x **mm]**	**Power [W]**	**Build rate [cm³/h]**	**Price [M€]**
Matsuura	LUMEX Avance-60	600 x 600 x 500	1000	35	> 1

4.1.5 Electron beam melting systems

Electron beam melting (EBM) is an approach to powder bed fusion process where an electron beam is utilized as a heat source to induce fusion between powder particles. The process principle is similar to laser-based PBF machines, however, hence the strong negative discharging nature of the electron beam, the spot size, layer thickness, and mean size of powder particles must be greater than in the laser systems. Furthermore, the achievable surface quality is rougher, and minimum feature size is slightly greater in EBM manufactured parts. In turn, the need for support structures is an order of magnitude less than in laser-PBF, and due to process chamber temperature kept constantly elevated through the build, the parts suffer minimal residual stresses. (Gibson, Roser & Stucker 2015, p. 137-139)

At present, a Swedish system manufacturer Arcam is the only operator providing EBM systems in market. Their machinery is mostly utilized in medical implant production and aerospace industry using titanium as a feedstock material, yet other electrically conductive materials could be applied as well. The table 8 below shows the basic specifications of the medium-sized Arcam Q20plus EBM machine, which is the medium-sized of the three models provided the manufacturer. (Arcam 2017)

Table 8. Arcam Q20plus electron beam melting machine represented in system characteristic values. (Arcam 2017; FIRPA 2016)

Company	**Model**	**Building chamber [mm** x **mm** x **mm]**	**Power [W]**	**Build rate [cm³/h]**	**Price [M€]**
Arcam	Q20plus	Ø 350 x 380	3000	120	> 0,8

4.1.6 Ancillary systems

During the printing process, powder bed fusion systems are fully automatic and need only minor inspection. However, setting up, loading material, and unpacking the finished machine is extensively carried out manually, let alone the post processing, and is raising the production costs of AM. For this reason, approximately half of the systems manufacturers is also providing ancillary systems for their printing machines to increase their degree of automation. These systems include powder sieving stations and centralized powder feeding systems, removable build chambers, automated unpacking and excess powder removal stations, and systems facilitating the part removal phase. The optional auxiliary systems are listed in the appendix I.

If a critical failure in the part stays unrecognized until the very last phase of the MAM workflow, and the component is subsequently scrapped, the whole manufacturing process must be started from the beginning. This is why the importance of real-time, in situ process monitoring should be emphasized in feasible AM production. (Ray 2016) The need is well recognized by the system suppliers, and almost every manufacturer has their own melt pool- and layer imaging, and real-time process controlling solution sold as an additional service.

4.2 Directed energy deposition (DED) systems

Currently, directed energy deposition systems in industry are mostly used for three purposes. Repairing and rebuilding the worn out parts, adding new features, such as wear-resistant surfaces or external surfaces to existing components, or producing near-net shape billets of sophisticated materials, are the main utilization objectives for the state-in-the-art systems. (Gibson, Rosen, Stucker 2015, p. 267)

Commercially available directed energy deposition (DED) systems can be divided in three main categories: systems which only add material, hybrid additive-subtractive DED machines which combines a build-in printing head with subtractive machining center, and detached printing engines, which can be retrofitted with almost any machining center and thus add only the additive feature to them.

The number of powder fed-DED machine manufacturers is about ten, of which almost every one of them is also producing hybrid additive-subtractive systems, yet detached printing heads are provided by only a few manufacturers. DED systems are equipped with laser powers varying from 0.5 kW (LENS MR-7) up to 8 kW of Trumpf's TruLaser-machines. Maximum building speed is dependent on laser power, and as a rule of thumb, for 0.5 kW, 2 kW and 3 kW the supreme deposition rates accordingly are 0.1 kg/h, 0.5 kg/h and 1.0 kg/h, yet build rates over 3.5 kg/h with IN718 has been reported when using modified research machinery. (Zhong et al. 2015, p. 88). However, the above-mentioned peak rates are obtainable only for thick deposited material sections with optimal materials, geometries and parameters, and cannot be attained with complex shapes nor strict surface quality requirement.

Deposition heads of the systems are generally equipped with single nozzle, coaxial nozzle or 4-nozzle technology. Single nozzle configurations are delivering the powder to the melt pool from external tubing outside the laser process head, which is simplifying the apparatus and enabling good accessibility into tight locations. In the other hand, it is making the melt pool geometry direction specific, so the motion in relation with the workpiece must be same through the deposition. (Gibson, Rosen & Stucker 2015, p. 251)

Coaxial feeding provides a good shielding gas protection to the melt pool, and a better powder capture efficiency than single nozzle or 4-nozzle feeding. Coaxial nozzle technology is utilized e.g. in Hybrid Manufacturing Technologies' AMBIT-process head. (Hybrid Manufacturing Technologies 2017)
The most precise powder delivery composition is 4-nozzle configuration, where the powder is fed to the melt pool with four equally spaced nozzles around the process head. The powder flow is consistent and allows the accurate manufacturing of complex 3D geometries, especially where thicker and thinner regions are involved. (Gibson, Rosen & Stucker 2015, p. 251) 4-nozzle process head is employed in LENS manufacturing machines and external printing engines by Optomec. (Optomec 2017)

In the following sections, the three types of powder-fed DED systems are introduced more in depth.

4.2.1 Additive DED systems

In matter of surface quality, systems specialized only on additive manufacturing are usually the most accurate systems among DED systems. They consist of integrated, CNC-controlled printing head, shielding gas environment enclosed in a process chamber, and a powder feeder systems. For enhanced process stability and quality, printing head is mounted perpendicularly to building plate, and is operating horizontally layer by layer. Due to the nature of the process, additive DED machines cannot be compared to PBF machines in surface quality nor accuracy, and they are mostly capable of order of magnitude lower part complexity than PBF machines. However, the build rates are superior and the material diversity is greater than the powder bed fusion machines'. Also, the DED's ability to simply add functionalities and geometries to ready made parts is unrivaled in MAM processes. (Gibson, Rosen & Stucker 2015, p. 254-255)

In table 9, InssTec, a South Korean directed energy deposition system manufacturer, additive DED machine is introduced.

Table 9. General specifications of InssTec MX-1000 directed energy deposition (DED) AM machine. (InssTec 2017; FIRPA 2016)

Company	**Model**	**Building chamber [mm** x **mm** x **mm]**	**Power [kW]**	**Build rate [kg/h]**	**Price [M€]**
InssTec	MX-1000	1000x800x650	2	0,5	> 1

4.2.2 Hybrid additive-subtractive DED systems

Hybrid DED machines comprise a CNC machining center and an integrated AM process head within a single machine environment, which is enabling the utilization of the distinct advantages of both technologies. Near-net shape geometries can be produced using DED processing and the surfaces can be machined to their final geometry in the same machine. 5-axis milling tables are often employed, which is ensuring that any additively manufactured surfaces are able to be machined. Hybrid machines are operating on a standard G-code, which is used for controlling both additive and subtractive processing. However, as the hybrid technologies are using two fundamentally different approaches to produce the geometry, numerous complex considerations have to be taken into account in manufacturing. For instance, certain features could be produced either with additive method or machining them from billet material, nevertheless, depending on the chosen method, material properties and process suitability might be inconsistent for end use. (Maxey 2015) The fine powder materials are also contaminating the manufacturing shell, and can cause complications inside the machine, since the utilization rate of powder in process can be under 50 % (Lorentz et al. 2015, p. 98). The issues relating in additive and hybrid processes are discussed more in detail later in chapter 6.2. In table 10, a typical hybrid additive-subtractive machine by DMG is introduced by the main values of the system.

Table 10. Technical data of DMG Mori's Lasertec 65 3D, a hybrid DED system launched in 2014. (DMG Mori 2017; FIRPA 2016)

Company	**Model**	**Building chamber [mm** x **mm** x **mm]**	**Power [kW]**	**Build rate [kg/h]**	**Price [M€]**
DMG Mori	Lasertec 65 3D	Ø600 x 400	2	0,5-1	> 0,8

4.2.3 External printing engines

A modern CNC machining center can be converted to a hybrid additive manufacturing system by installing a printing engine technology to pre-owned machinery. Alternatively, an industrial robot arm could be employed with printing head, yet the manufacturing accuracy of this pathway is inferior to machining center option. The retrofitted DED-printing systems consist of a process head with a universal connector surface, powder feeder units, laser unit, safety equipment and optional closed-loop process controlling units.

Manufacturers specialized on external additive manufacturing engines of 3D geometry are, based on the supplier review, only a handful in the market: OR Laser, Optomec, Trumpf and Hybrid Manufacturing Technologies (FIRPA 2016). The last-mentioned engine is also implemented in Mazak's hybrid machines (3D Printing Industry 2014)

LENS external print engine's main values are represented in table 11 below.

Table 11. LENS printing engine technical preferences. (Optomec 2017)

Company	**Model**	**Installation**	**Power [kW]**	**Build rate [kg/h]**	**Price [M€]**
Optomec	LENS	CNC machining center/robot arm	0.5-3.0	0.5-1	0.2

5 DFAM – DESIGN FOR ADDITIVE MANUFACTURING

Additive manufacturing is a roof concept for numerous technologies utilizing the tool-less, layer-by-layer manufacturing principle, where in contrast to conventional subtractive methods, material is only added. It enables a great degree of freedom in design and materials and has gained great attention for its value-adding potential in industry, however the method is far from the absolute design freedom it is commonly considered. Multiple constrains, both in design and the manufacturing process must be respected in order to bring the virtual CAD design into physical form utilizing the AM processes.

The design principles for AM components are fundamentally different to conventional methods and constrains. Manufacturing process chain has to be optimized for additive manufacturing from the very beginning of the design to utilize the massive potential in manufacturing and functional means together with good manufacturability and feasibility. (Chekurov et al. 2017, p. 7) However, despite the evident strengths, design engineers in mechanical industry are in general reluctant to implement additive methods to their companies' products. They can find their knowledge over characteristics and boundaries of the methods, and the MAM technology itself, insufficient. Thus, the test specimen considered for AM can be designed to be manufactured using traditional methods, or the AM-adapted component is poorly following the constraints of the process. This could lead to costly building errors, inefficient material use, and laborious post processing of the build parts. These defects can only be avoided by observing the prevailing design values for additive manufacturing with PBF, collecting them in an unambiguous form, and carefully following them in design and manufacturing process. (VTT 2017, p. 6-8) In addition to design instructions, computational design tools such as topologic optimization, heat input simulation, and support generating software, are in key role in manufacturing feasibility enhancing and enabling the design of both high performance and cost-effective parts exploiting the strengths of AM.

In the following chapters, process-specific limiting values for manufactured geometry are presented for both powder bed fusion (PBF) and directed energy deposition (DED) processes, and based on the given values, effective design principles for AM parts are defined.

5.1 Manufacturing constraints in PBF

One of the main reasons for the need of DFAM instructions is to avoid the manufacturing defects typical to PBF methods, which are originating mainly from characteristics of powder material and the melt pool. A risk for these costly, un-wanted errors can be reduced drastically by following the design limit values. Furthermore, avoiding the addressed risk factors for defects, the components quality and manufacturability, along with operational reliability, can be significantly improved by following process specific design rules for PBF manufactured parts. (Bossuyt & Fournier 2016)

5.1.1 Overhangs

Overhang is a condition where a sliced geometry is widening too fast between consecutive manufactured layers and the geometry is intended to build on “empty”, as illustrated in figure 18. It occurs with shapes that contain wide ledges parallel to substrate, or steep horizontal changes in geometry with small angles to base plate.

As the powder works as insulator for the great amount of gas it holds, the melt pool in overhanging sectors will likely to be overheated when the heat cannot be properly conducted through previously solidified structure. Since powder bed is not providing support for molten material and supporting material is absent, the melt pool starts to sink into a powder bed during the scanning process and enclose the un-melted powder particles into it through partial sintering. This is visibly hindering the surface quality and distorts the part geometry. (Cheng & Chou 2014, p. 1076-1078) Further, the process becomes unstable, leading to excessive dross formation on underneath the structure (figure 19), suffer from curling defects (figure 21) and, at worst, can cause the whole build to fail. (VTT 2016, p. 10-12; Bossuyt & Fournier 2016)

a) 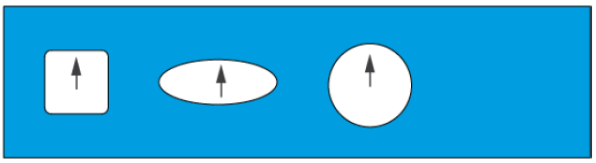 b) 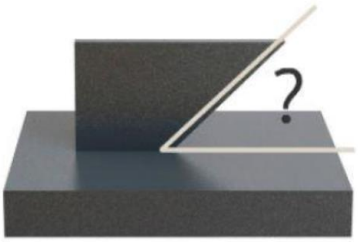

Figure 18. a) Overhanging geometries where some external supports are needed to points expressed with an arrow. (VTT 2016, p. 28) b) Minimum slope angle represented between part borderline and building plate. (Crucible 2015)

As denoted in figure 19, round and rectangular horizontal holes must be supported due to their overhanging nature, to achieve even moderate surface quality to the down facing section. Round holes are self-supportive from diameters 1-2 mm to 7 mm. Above that they must be supported or designed self-supportive, and under 1 mm diameter the holes are usually closed by the process. (VTT 2016, p. 38-39) Even within the self-supportive range, round holes are rather burry and especially with wider dimensions require machining for more precise result (figure 19). For all holes manufactured with PBF a general tolerance of ± 0,5 mm is defined by Thomas (2009, p. 178).

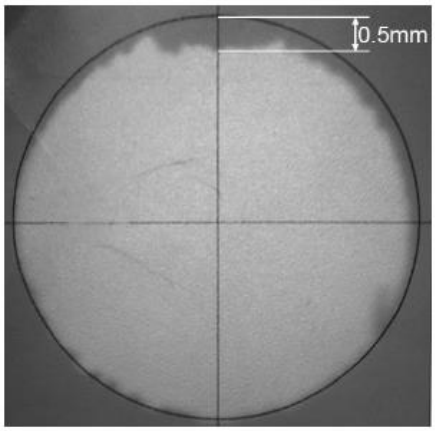

Figure 19. A shadowgraph illustration of 7 mm diameter hole with sagging defect in the down facing section. (Thomas 2009, p. 178)

Local minima is a distinctive case of overhanging, and it occurs in any areas which are not connected to the layer below. They can be obvious discontinuities in parts, such as the bottom of the ledge on the left in the figure 20, or be more concealed as seen on the right in the figure 20. Latter is caused at the top of the angled hole when the flange is tilted and it intersects the edge of the part, which can be a result of re-orientating the part from the initial building direction.

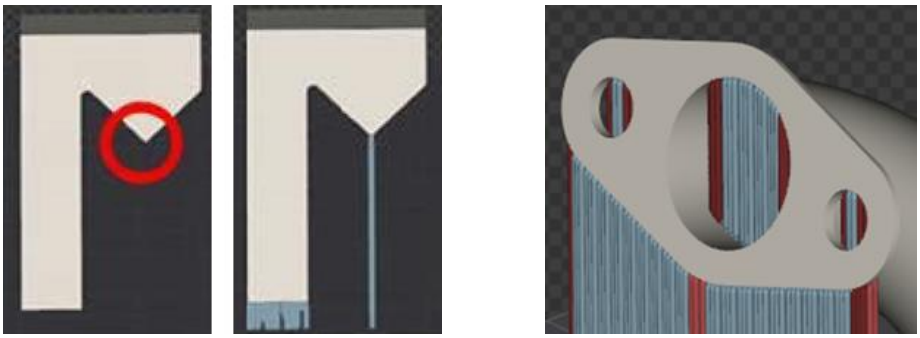

Figure 20. Examples of local minima, where the material is not connected to the previously melted layer in the build direction and thus need to be supported or designed out. (Modified: Saunders 2017e)

Maximum length for fully horizontal overhanging structures in PBF is generally under 1 mm with the material specific limit for vertical overhanging angle according to the table 12. The values in table are strongly dependent on the heat conductivity of the powder material, but also the process controlling of the certain machine. When the lower-conductivity powders are melted and surrounded by insulating grains the process heat cannot be conducted away from the melt pool and leads to overheating, and the defects are like those caused by overhanging situation. (Cheng & Chou 2014, p. 1076-1078; Saunders 2017e)

Table 12. Material specific minimum manufacturing angles in optimal conditions PBF processing with small layer thickness, defined in degrees between substrate plate and borderline of part cross-section perpendicular to z-axis. In general, PBF manufacturing especially with higher building rates, the 45-degree rule must be followed. (Altair 2014)

Material	**Minimum angle [degrees]**
Titanium	20-30^{o}
Aluminium	45^{o}
Stainless steel	30^{o}
CoCr	30^{o}
Inconel	45^{o}
Universal design limit for all materials	**45^{o}**

If either limit is exceeded, external, removable support structures must be included in sintered geometry to ensure proper part stability, thus extending the processing time and material waste. If the overhanging ledges are not supported, curling due to overheating, and dross formation defects are strongly affecting the geometry as represented in figure 21. This is caused by the residual stresses trapped inside the material caused by steep thermal gradient, and rapid solidification of molten metal. These affect the part by first bending it away from laser and by curling it towards the laser source hence the contraction forces as the molten metal solidifies, respectively. The forces affecting as a residual stress must be considered, since they can exceed the tensile strength of the material and thus crack the component. (Mercelis & Kruth 2006, p. 255) The residual stress mechanism is illustrated in figure 22.

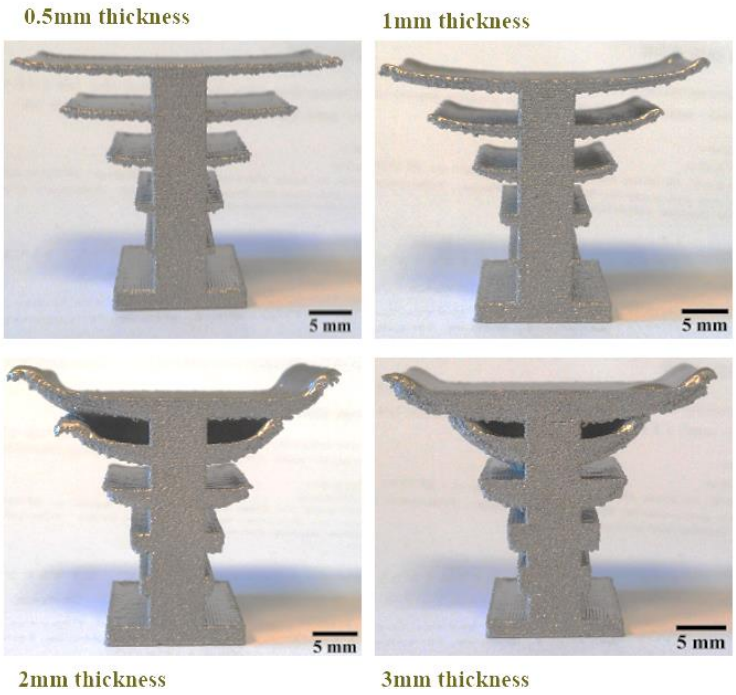

Figure 21. Typical overhanging part warping and dross formation on PBF manufactured AlSi12 test piece with variable ledge lengths and thicknesses. Better geometrical accuracy in achieved on wider overhangs with thinner ledges, due to fewer heat related stresses within solidified layers. (Vora 2012)

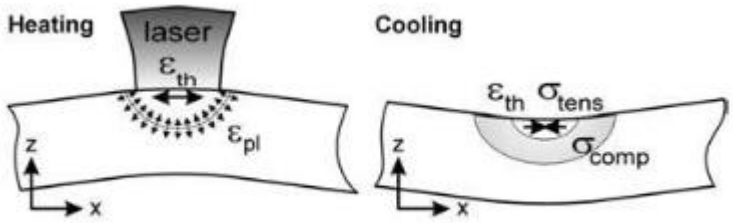

Figure 22. The two main mechanisms generating residual stresses inside PBF-manufactured parts. Heat input of laser induces heat expansion in material which bends the heat-affected layer away from beam. After the laser is moved away, the melt pool rapidly cools down, generating a tensile stress concentration. This phenomenon is a root cause to typical curling defect in PBF-manufactured parts. (Mercelis & Kruth 2006, p. 255)

Nonetheless, these values are only valid with certain process parameters. When the layer thickness is increased, the smallest manufacturable angle is also increasing and vice versa, as the overhanging length limit per layer stays constant. Satisfactory results have been achieved using maximum layer-specific overhang length of 75 μm, which was the same as

the used layer thickness. (Thomas 2009, p. 88-89; Kruth & Vandenbroucke 2007, p. 198-200) A general limit for slope angle a 45^{o} angle should be preferred as it is the most general value in typical material and parameter settings. (Thomas 2009, p. 192-194)
If possible, overhangs should always be avoided since their tendency to crack formation and excessive need for external supports are obstructing the manufacturing process (Thomas 2009, p. 157).

5.1.2 Supporting structures

Support structures are needed in PBF for several reasons. They attach the part to a substrate to minimize cracking and distortions, conduct the process heat away the workpiece and support the overhanging sections. After all, they are still unnecessary constructions for the end use parts, are increasing the manufacturing costs and are very laborious to remove. Hereby the need for supports should always be optimized by designing so called self-supportive shapes when possible, and by choosing the optimal orientation for manufacturing. (Calignano 2014, p.1-2; Bossuyt & Fournier, 2016) Self-supportive shapes can be manufactured without or with minimal external supports, and are not exceeding the steepness limit of 45 degrees.

For removable supports, good accessibility is a necessity which must be taken into account when aligning parts in different angles for manufacturing, and designing support structures. Supports are generated with sophisticated software, such as Materialise Magics, which usually combines rod-like (cone) supports for anchoring and heat dissipation and lattice-like (block) structures for supporting and preventing heat-related distortions. Likewise, with overhanging and overheating-prone structures, the process heat must be conducted away the workpiece through part material or support structures properly to achieve good surface quality and material strength consistency. (VTT 2016, p. 18-19) A case in point of golden principles in supports designing by Materialise is expressed in figure 23, wherein example a) expresses minimizing the supporting structures by vertical aligning, yet leading into higher heat input per layer and thus hindering manufacturability. In turn, case b) is utilizing much more supporting material and together by increasing the printing height, increasing the manufacturing and post-processing costs as well. However, by reducing heat-related stresses by lowering heat input per layer with slight re-aligning, manufacturability and feasibility increases substantially, and the chance for build failure lessens.

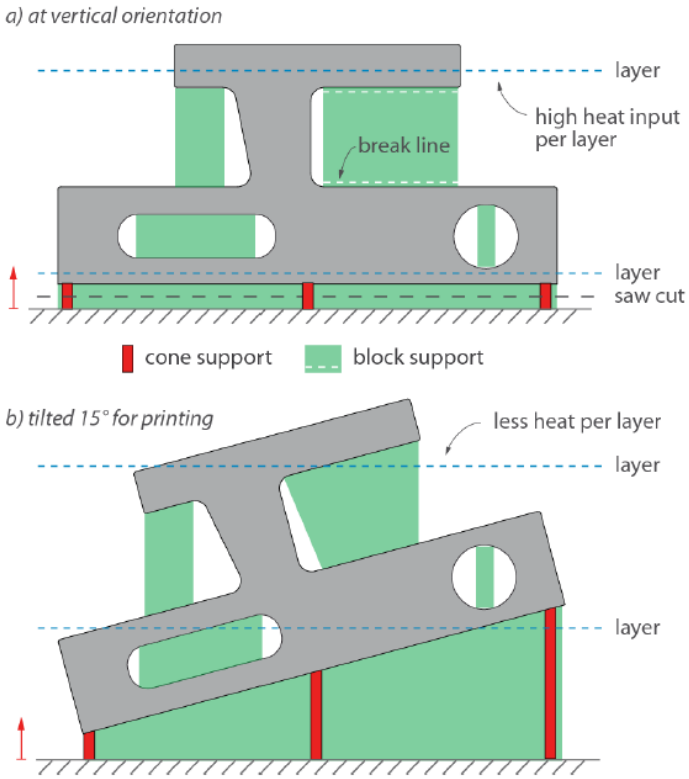

Figure 23. Aligning's effect on the manufacturability and to the need of support material**.** Option b) is using almost twice as much support material but overcomes case a) in feasibility due to smaller heat input per layer. (VTT 2016, p. 19)

5.1.3 Geometrical limitations

Powder bed fusion has many geometrical limitations, however, compared to conventional methods such as machining, turning and casting, the design freedom advantage is eminent. On the contrary to traditional methods, sharp edges and angles (including 90º corners) are hard to manufacture and are acting as a stress-raisers in structure as the heat conduction is limited in the thin sections leading to overheating, and thus should be avoided. Sharp-edged are recommended to be eliminated in design by filleting and using radii's 0.5 mm at minimum. (Crucible 2017) Convex radius fillets are recommended instead of straight 90º corners for their self-supporting tendency, and good results in sag-prevention and avoiding dross-formation were achieved with a tangent angle of 30º with relatively small ledges (< 15 mm) (Thomas 2009, p. 100-102) Tangent edge effect on overhang width is represented in figure 24 below.

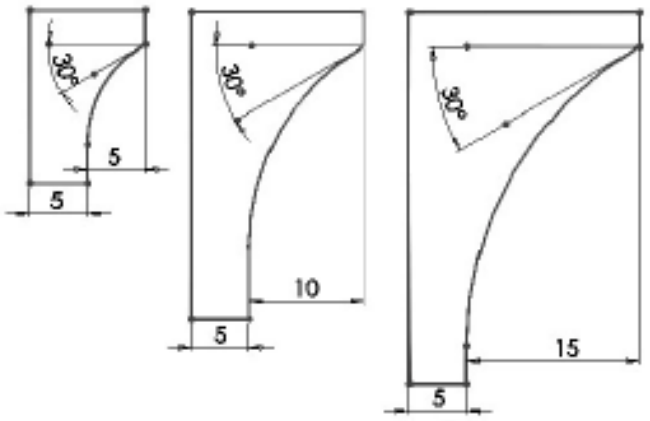

Figure 24. Convex radius fillet's tangent angle effect on overhang width of the ledge. (Thomas 2009, p. 102)

Powder bed fusion enables even complex internal shape manufacturing, yet the cavities has to be self-supportive due to low accessibility for removable supports, and have a draining outlet for un-melted process powder since the whole part is filled and buried under it. Minimum wall thickness for PBF-manufactured components is somewhat dependent on material and parameters used, but generally the limit for relatively low walls is reported to be 0.2-0.4 mm. However, structures thinner than 0.5 mm are not recommended to be manufactured for their potential porosity, and vulnerability to break in the case of recoater blade collision. (Thomas 2009, p. 165; VTT 2016, p. 133; Crucible 2017).
As a rule of thumb, geometrical part accuracy is reported to be around 40-60 μm with small (< 50mm) parts, and with larger parts a general tolerance of ±0.2 % applies. (EOS 2017)
In addition to minimum wall thickness, the commonly considered minimum gap between parallel structures is 0.5 mm. (Thomas 2009, p. 113)

Since the outer walls of PBF-manufactured parts are grainy, and slightly porous as represented in figure 25, the surfaces are needed to be machined if the functionality of the final part demands smooth surface. Thus, the CAD model must contain the oversize dimension in order to obtain the dimensional demand in final product. The layer thicknesses for additional material for machining are measured in table 13.

Table 13. The layer thickness which is required to machine for the respective material demand after Thomas (2009, p. 125).

Requirement	Up-facing [mm]	Down-facing [mm]	Vertical [mm]
Smooth surface (slightly porous)	0.3	0.8	0.1
Fully dense surface	0.7	0.8	0.1

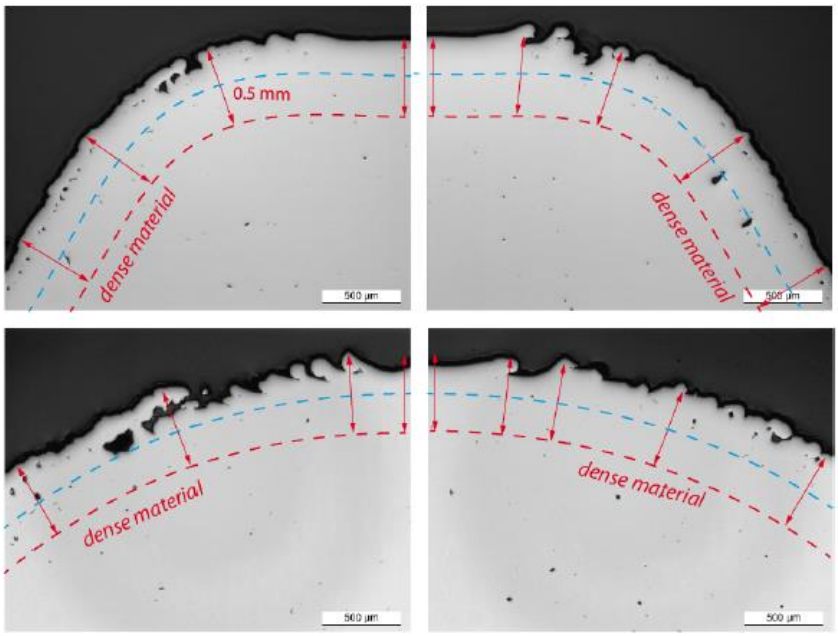

Figure 25. If the surface of the part must be fully dense, a layer of material must be machined off it. Blue line represents the smooth but porous surface, and lower dotted red line the borderline of fully dense area. (VTT 2016, p. 81)

5.1.4 Surface quality

According to Thomas (2009, p.160), surface quality of parts strongly depends on the orientation and angle of the slope. The smoothest surfaces are in the vertical walls and up facing geometries leaning in slight angle. The worst surface quality is formed to down facing walls when the overhanging problem starts to affect the grains of metal.

Layer's location in the Z-direction affects the surface quality also, as layers located at the bottom side of the part will be produced with better surface quality than the upper side layers. This was reckoned to ensue from repeated heat cycles the lower layer are undergoing, thus promoting the smoothening diffusion. (Abd-Elghany & Bourell 2012, p. 422)

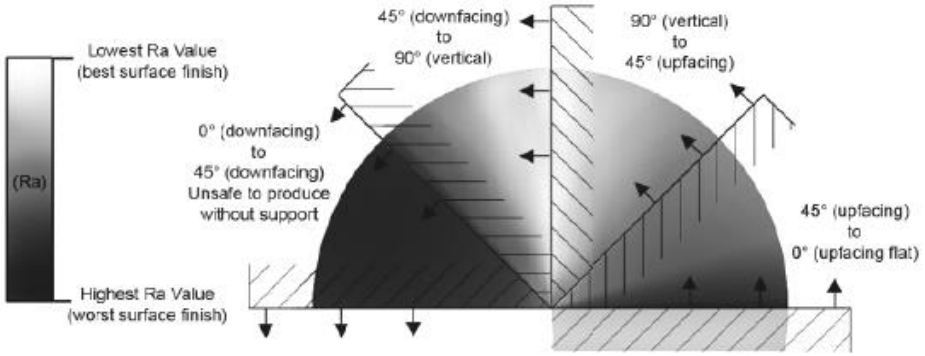

Figure 26. Illustration of the effect of orientation on the surface quality of parts in PBF systems. (Thomas 2009, p. 160)

Surface quality by arithmetical scale is usually between 5-25 µm in parts manufactured by PBF. It strongly depends on powder material and grain size, layer thickness, manufacturing parameters and part aligning. According to VTT (2014, p.38) surfaces which are built vertically are produced with smoother surfaces, and the geometries build horizontally will suffer worse Ra-values. As the smoothness of surface is subject to various factors, achieving good surface quality (below Ra 10 µm) requires overall optimization of the manufacturing parameters and choices in design process. (VTT 37-39; Townsend et al. 2016, p. 42; 34-35)

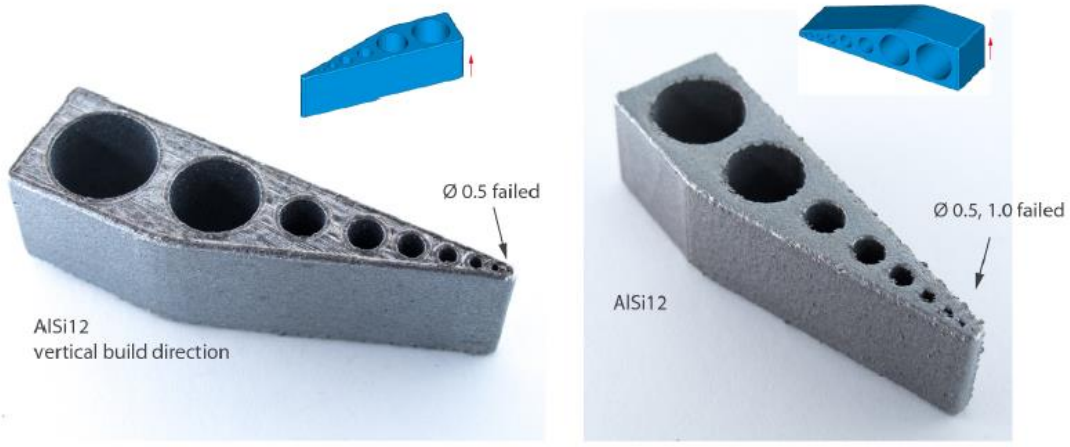

Figure 27. Part orientation, and building direction effect on the as-built surface quality and dimensional accuracy of round holes**.** Sagging and dross formation are coarsening surface quality of the horizontally built part. (VTT 2016, p. 38)

5.2 Manufacturing constraints in DED

Similar design rules apply for both metallic additive manufacturing processes, PBF and DED. Design ruling especially concerning powder and solidified material properties are much like the same, since the powder feedstocks the both processes are utilizing are analogous. Still, parts manufactured by DED are evidently simpler and less complex than the ones PBF systems are capable of, due to coarser resolution, fewer design freedom, and higher build-rate characteristic to DED manufacturing. Thus, constrains and considerations outlined in the latter chapters are more process-related than the design rules for powder bed fusion introduced in the previous section 5.1.

5.2.1 Geometric limitations

Process head in DED manufacturing must always work in normal to workpiece surface, yet the nozzle can be operated in nonvertical positions as well. Thus, the production capability for overhanging structures depends on the process head multiaxis motion ability and system's equipment for turning the workpiece. (Gibson, Rosen & Stucker 2015, p. 248) For machines with horizontally moving substrate only, a general overhanging angle of 30^{o} to z-axis cannot be exceeded without manufacturing additional support structures. However, by pulsed laser process developed explicitly for research purposes, walls with overhanging angles up to 60^{o} have been successfully build. (Nassar & Reutzel 2015, p. 273-280)

Systems equipped with tilting rotation table, overhanging geometries can be manufactured self-supportively, since the workpiece rotation axis can be tilted. This enables the material to be deposited in a way which would be impossible for 3-axis machines without supports. (Ding, Dwivedi & Kovacevic 2017, p. 67-68)

Dimensions of a deposit layer in DED manufacturing is intensely defined by the material feed rate in nozzle, and the nozzle speed relative to the substrate. Consequently, as the feed rate stays constant in process, the nozzle speed determines the layer thickness of deposit. Sharp corners require accelerations and decelerations in the process head movement, and thus are leading to unequal thickness within the layer. As a result, this can lead to unwanted nozzle collisions to deposited geometry and set the whole process unstable. Consequently, sharp corners should always be avoided and replaced with a curve or another smooth transition in geometry. (Leandri 2015) Process head dimensions and trajectories has to be carefully taken into account especially in repair functions, since the already existing material can limit the working area accessibility.

Similarly, to manufacturing with powder bed fusion (PBF), parts produced using directed energy deposition (DED) undergo a series of rapid heating and cooling cycles. This is inducing considerable amounts of residual stress inside the part, which can lead to total failure of the component. (Zhang et al. 2014, p. 839-840) Reducing material thickness in deposit bead, and consequently making more accurate geometries, also reduces the material's resistance to thermal cracking, which has to be taken into account especially when manufacturing thin-walled structures. This can be managed by increasing the nozzle speed and laser power, since the heat input per length decreases, which is having a diminishing effect over residual stresses. (Güpner, Patschger & Bliedtner 2016, p. 657) Minimum wall thickness for the most accurate systems utilizing 4-nozzle-technology is 0,3 mm, which is claimed to be manufacturable by Optomec. (Optomec 2017)

5.2.2 Material-related advantages and limitations

One of the most promising approach in DED manufacturing is the process' ability to produce functionally graded materials (FGM). The principle of FGM is to gradually mix two materials with different material properties, and thus achieve cost-effective yet highly functional materials. In figure 28, an experiment of graded 304L stainless steel/Inconel 625 deposit is presented. The root of the deposited geometry was able to be manufactured of more ductile and cost-effective stainless steel, and the other end with greater wear-resistivity Inconel 625, thanks to the material selection, and increasing hardness profile upon the deposit.

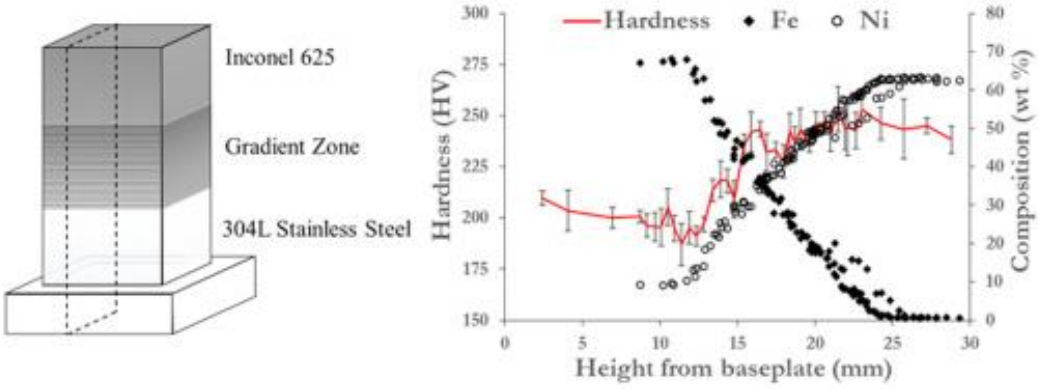

Figure 28. Schematic of a functionally graded 304L/Inconel 625 test spexiemen and the variable hardness deviation of the deposited part. (Modified: Carroll et al. 2016, p. 48; 53)

However, 3D-manufacturing by DED has its own limitations. Materials manufactured by directed energy deposition have a very fine grain structure due to extremely high cooling rates (typically 10^3-10^5 $^oC/s$) of melt pool during solidification. Unique and non-equilibrium grain structures, which cannot be created using conventional methods, are characteristic to laser deposition, but sometimes is leading to unwanted phases in metal's microstructure. These forms include exceptionally hard but brittle phases, which can aggravate cracking under fatigue loading, or cause a sudden fracturing of the structure after a sharp impact. (Gibson, Rosen & Stucker 2015, p. 248; Park et al. 2016, p. 143-144) Additionally, defining the risk for the undesirable phases is difficult, and in spite of the eminent advantages of this approach, currently no commercially available software exist for designing functionally graded materials in CAD environment, which is constraining its implementation in industrial applications. (Tammas-Williams & Todd 2017, p. 109; Leandri 2015)

The properties of the deposited material can be balanced more suitable for certain applications by increasing the grain size in deposited material. The phenomenon can be induced in material's micro structure with heat treatments, or by decreasing the cooling rate of the deposit. This can be done by lowering the traversing speed of process head or increasing the laser power. For instance, Vickers 500-hardness of experimental H13 tools steel deposits were 630 in as-build state, and after heat treatments, the value was decreased to HV 535, while the microstructure was similar to wrought material. (Park et al. 2016, p. 144-145)

5.2.3 Surface quality

Surface quality of DED manufactured materials is largely determined by two main factors. First, the strength of the stair-stepping effect which more present in DED than in PBF, is dependent on layer thickness, which typically vary from 0,2 mm to 0,75 mm in DED manufacturing. The degree of stair-stepping is directly proportional to the layer-thickness, which can be seen in figure 29. Secondly, the partially melted powder particle sticking to deposit surfaces are deteriorating the quality of solidified bead, and the effect is strongly connected to the process parameters. (Rombouts et al. 2013, p. 810) For example, with OPTOMEC's LENS machinery, vertical wall surface roughness are claimed to be in range R_a 12-25 µm, however the stair-stepping effect (figure 29) is not taken into account in this value. (Optomec 2017)

Figure 29. Schematic cross-section of the layer-by-layer DED manufactured wall with the characteristic stair-stepping effect in both sides. (Optomec 2017)

Surface quality and feature precision on directed energy deposited parts is always a trade-off between building speed and accuracy. With wider deposition beads and thicker layers, along with high laser power, the productivity is maximized at the expense of dimensional accuracy, and vice versa. A strong stair-stepping defect and other surface quality related issues of DED are the main drivers for commercialization of the hybrid systems. By combining the subtractive machining to the additive manufacturing process, even the demanding geometric tolerances of the required features could be met and machined to part in the same phase. For hybrid systems, tool accessibility issues must be avoided right in the design to ensure the manufacturability of desired geometries and tolerances.

Surface quality of the deposited parts can be enhanced in different process-related means, such as using substrate heating. Building platform temperatures up to 600 °C could be applied. (Zhang et al. 2014, p. 842-843) This is, however, substantially hindering the total manufacturing process chain particularly with large work pieces, hence the part handling, manufacturing equipment and process controlling becomes more complex.

Re-melting the topmost deposit layer with relatively high laser power has also been noted to reduce surface roughness. In an experiment, the R_a value of DED manufactured 316L surface was enhanced from 15 µm to values under R_a 2 µm. (Rombouts et al. 2013, p. 813) However, it is unclear, whether or not this kind of process amendments are possible to execute in relatively closed process controlling interfaces of commercial DED systems.

5.3 Effective design philosophy for AM parts

Following the design rules defined in the previous chapter, a designer is only ensuring the viability of the desired geometry. However, in addition to manufacturability, the feasibility of additive manufacturing is intensely relying on the designer's creativity and ability to utilize the geometrical freedom which is provided by the method. Along with AM-oriented thinking of possible solutions, computational optimization tools such as topological optimization, have a great contribution to successful design for additive methods. They also help to overcome the psychological barrier by creating optimal, yet highly complex geometries, which using just conventional CAD tools are not obvious, or are very laborious to form. In other words, the parts intended to be manufactured using additive manufacturing of metals must be specifically designed for AM in order to be profitable, and intensive integration of design, computing, manufacturing and qualification is required. (Kow 2017; Quinlan et al. 2017, p. 3). In this chapter, the DFAM-based guidelines for cutting-edge design for additive manufacturing are defined.

5.3.1 Functional design and part integration

The main principle of additive manufacturing is that the material is placed only where it is needed. This means extracting only the essential features and functions of the component to the final design, and nothing more. Since the method offers significant freedom of action in design means, the focus should always be on the functionality, instead of old customs and principles of how the things are done. For instance, if the component's main function is to transmit force, only the necessary features, and adequate volume of material should be added to the design for required strength properties. The concept of function-concentrated design is demonstrated in figure 30, where a metallic clamp is analyzed regarding its functional features, which are critical for the part operation. Furthermore, the main body is re-designed to comprise the isolated shapes, and could be hereafter used as a design space for topologic optimization.

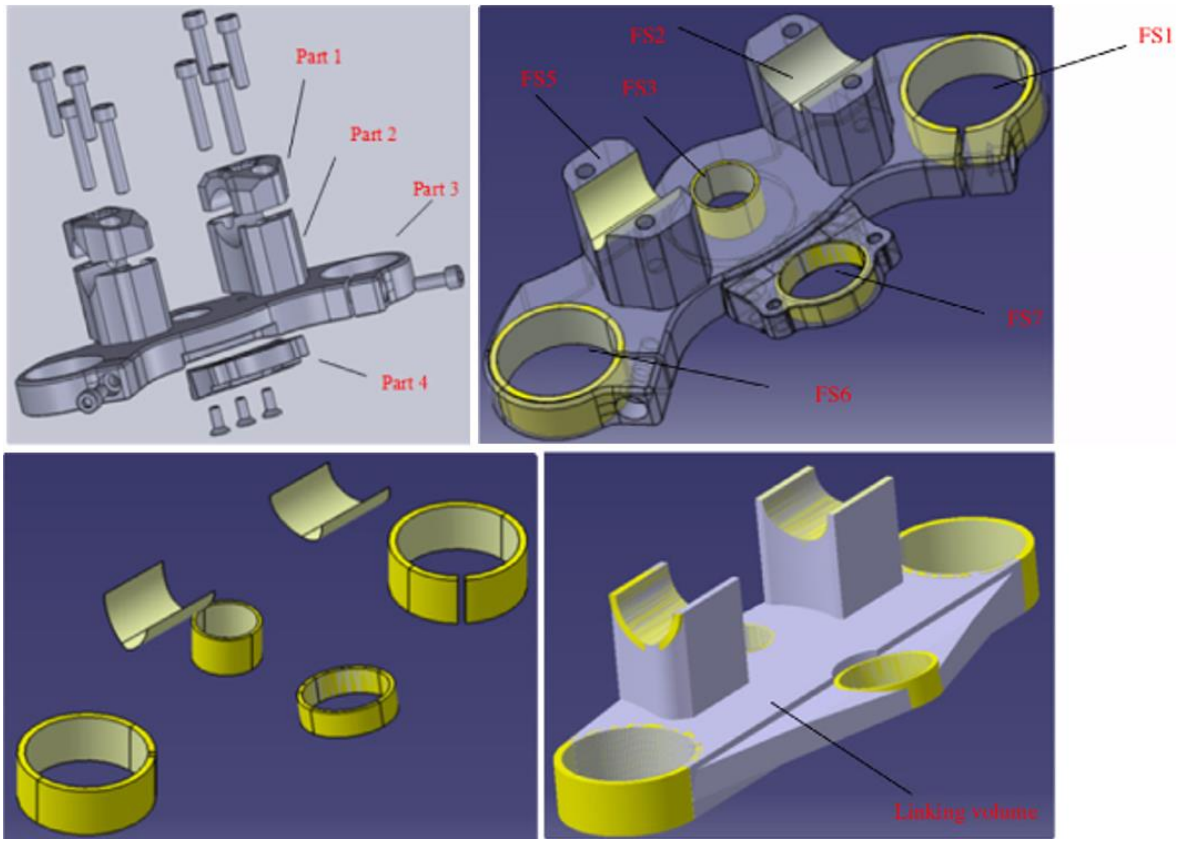

Figure 30. A re-design process of a clamp for additive manufacturing by identifying the functional shapes and the volume required only for cohesion. The linking volume expressed in the lower right corner can be later exploited as a design space for topological optimization for further weight reduction and increasing manufacturing efficiency. (Modified: Yang, Tang & Zhao 2015, p. 448)

Part consolidation into fewer, but relatively complex parts is utilizing the freedom of AM in numerous ways. First, the need for assembly work can be eliminated, which also reduces the amount of tooling and fixtures necessary in production. The single part can also be designed to be easily installable and the ergonomic aspects could also be considered in new level. Supply chain for the components also simplifies while the number of parts reduces. Critical flaws in assemblies could be eliminated hence the integration of parts reduces joining interfaces, gaskets, and fixtures. Furthermore, this is leading to decreased need for maintenance, and enables higher performance of the product. (Gibson, Rosen & Stucker 2015, p. 414)

5.3.2 Topologic optimization

Topologic optimization is considered as the most important optimization instrument for additive manufacturing. It is a computational tool that optimizes material deviation within a given design space to endure the stresses caused by pre-measured load sets. The workflow of topologic optimization process is presented in the figure 31. With finite element analysis (FEA), the algorithm defines the contribution of every element within the design space, and removes all material which is not critical to part load bearing properties or functionality, thus generating the optimal geometry for the certain set of loading conditions. Furthermore, these constrains can be weighted for certain goals, which can be e.g. minimized mass or maximized stiffness of the structure. Also, unwanted stress concentrations inside the structure can be eliminated, as the optimized structures are usually equally strained. Calculation generates a geometry, which is a slightly disconnected mesh of voxels and thus cannot be utilized without smoothening or rendering it first. Traditionally the results has been used only as an initial template for final shape of the part, hence the result geometries are often impossible to be manufactured by casting or machining. However, the design freedom provided by layer-wise production of geometry enables the utilization of optimal geometry almost directly to the final design. Still, manufacturability analysis and DFAM inspections and modifications are needed to execute by designer. (Gibson, Rosen & Stucker 2015, p. 428-432; Saunders 2017b; VTT 2016, p. 116-118)

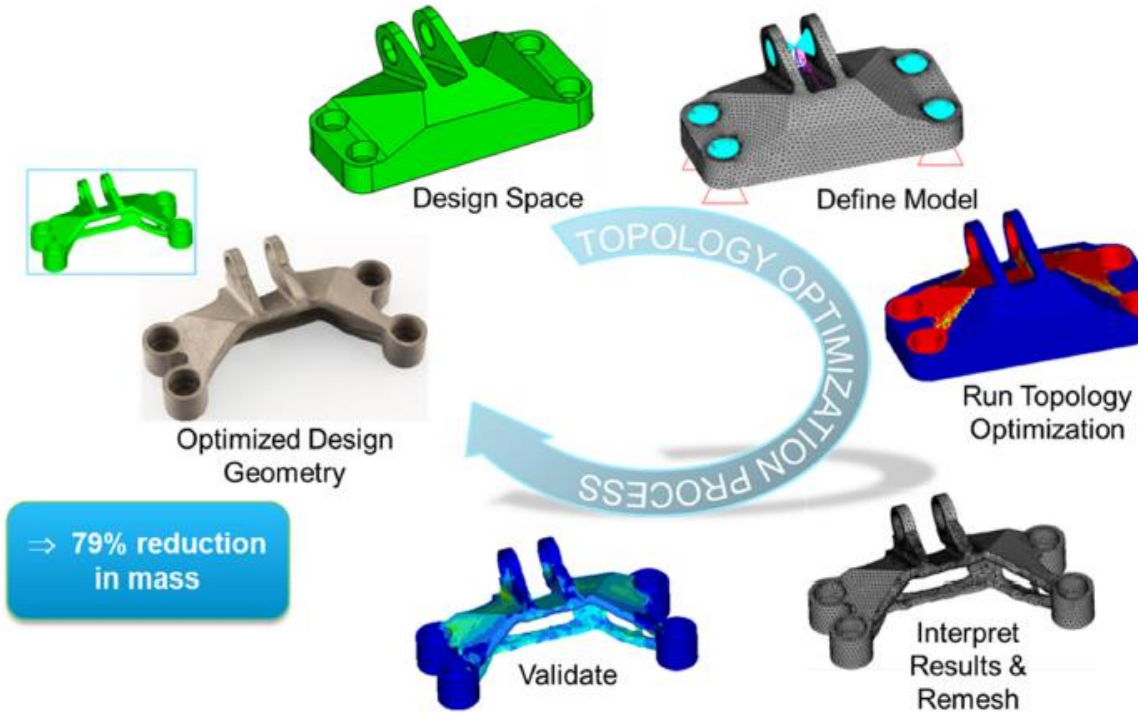

Figure 31. Workflow of topologic optimization for additive manufacturing. A significant weight reduction of 79 %, along with equal strain conditions inside the formed structure were achieved in comparison with conventionally manufactured bracket. (VTT 2016, p. 117)

5.3.3 Self-supportiveness and part orientation

Support generation software enables the manufacturing of almost any kind of geometries by generating auxiliary support structures into build geometry. Since the supports are always physically joined into the part, the support-affected surfaces are mostly requiring smoothening by machining or grinding after removal of anchoring lattices. For their costly and time-consuming removal effort, the amount of any redundant structures in additively manufactured components should always be minimized by design. (Kow 2017)

A demonstrating example of self-supportive design is presented in figure 32, where an additively manufactured hydraulic block is illustrated. Only critical features, such as flow channels and pipe interfaces are needed for the main function, and only minor structures, such as the supporting frames, are added to ensure the fixing of the flow channels, and the manufacturability of the design.

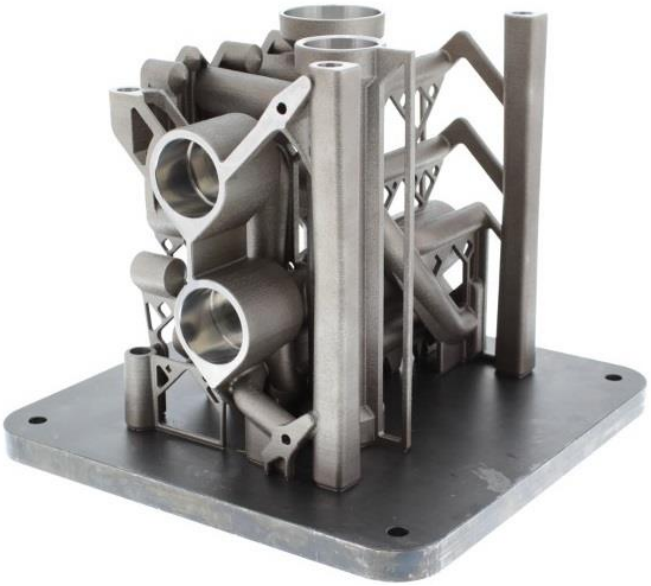

Figure 32. Hydraulic block with integrated self-supportive structures which are also functional parts of the component. Overhanging is avoided by designing drop-shaped pipe interfaces, 45-degree flow channels, and rectangular lattice supports in part. (Simufact 2017)

5.3.4 Design case example

As a case example of the effective design viewpoint, a sophisticated development process of bicycle frame for powder bed fusion manufacturing is shown. The design is started by defining the constraints and loading conditions of the frame structure, and the topologic optimization is executed to pre-defined design space (on the left in figure 33). The software removes excess material wi1thin the given safety factor for strain conditions, and generates an approximation where the material should be. Yet the optimization results were employed only as a guidance for design, the effect of topologic optimization results on the subsequent CAD geometry on the right side is clearly visible. Notable amounts of supports, which are represented in yellow on the right in figure 33, are needed in this configuration. (Saunders 2017c)

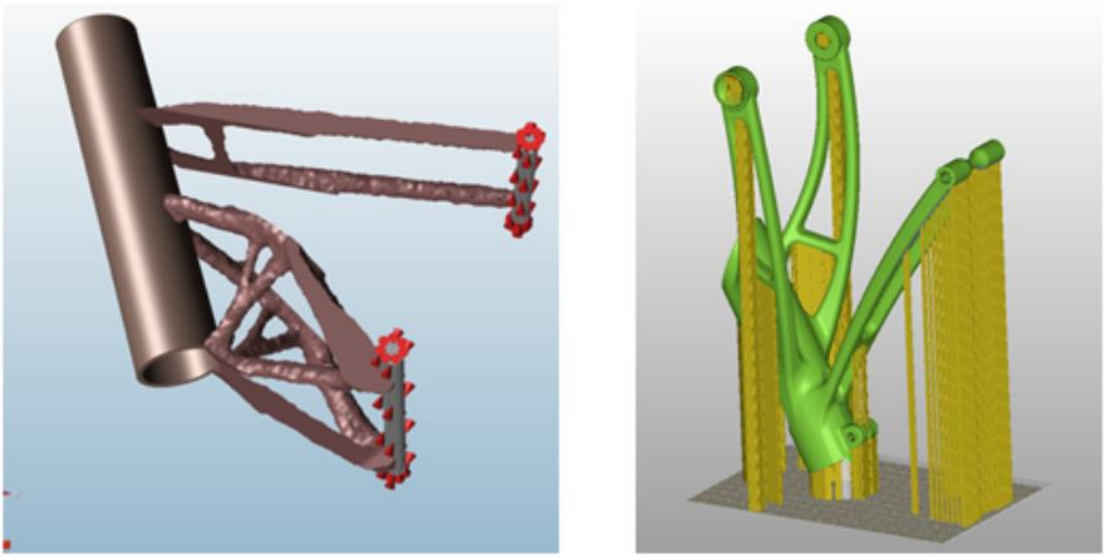

Figure 33. Initial geometry of bicycle frame based on topologic optimization calculation (left), and the CAD geometry's first manufacturability evaluation in support generation software (right). (Saunders 2017b)

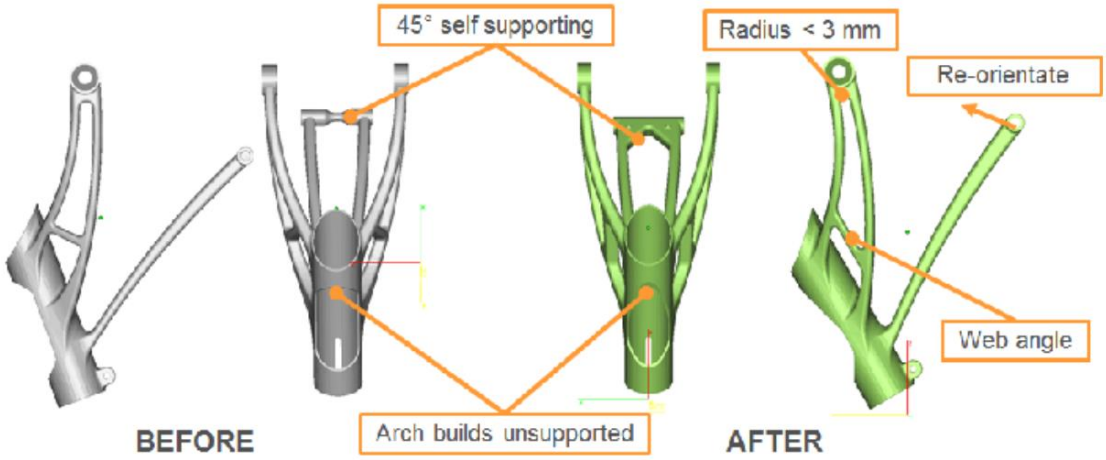

Figure 34. DFAM iterations of AM bicycle frame. (Saunders 2017c)

Changes needed to execute in part design for minimized support structures can be minor, whilst they enhance the part's manufacturability and feasibility prominently for additive manufacturing. In figure 34, details denoted in orange are the features which causes the need for external support structures. By slightly editing those after the DFAM ruling, auxiliary support structures and post processing could be eliminated almost entirely (figure 34). Ultimately, the hollowed frame was printed successfully. (Saunders 2017c)

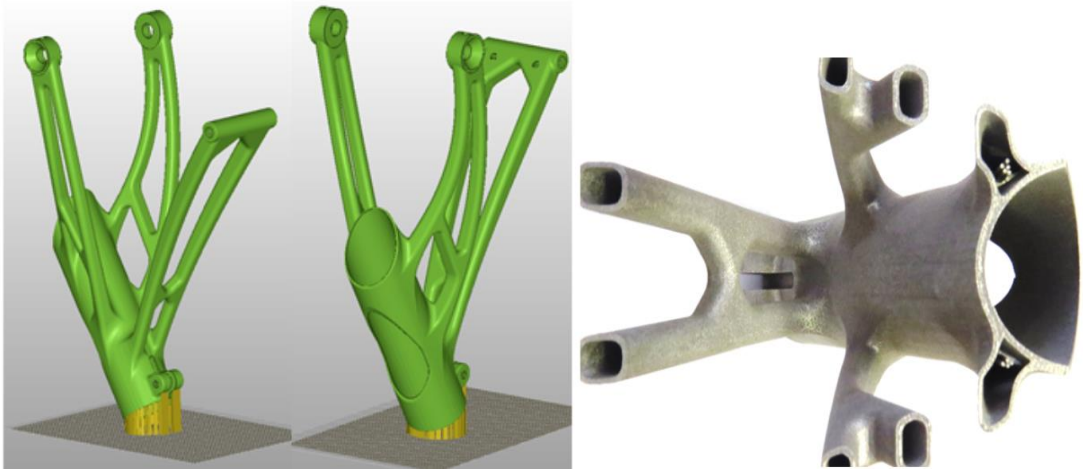

Figure 34. The optimized supports of the same bicycle frame after the iterations (left), and the final as-build frame after the DFAM process (right) (Saunders 2017c)

6 COST STRUCTURE OF MAM

Since the methods of metal additive manufacturing are still rather expensive, the objective of utilization of MAM should either be to minimize components' manufacturing cycle cost, or to maximize their performance. Cost savings go hand in hand with decreasing amount of manufactured material, since the machine time decreases accordingly, and the effect is demonstrated in the figure 36. Using this strategy, the costs can be directly compared with conventionally manufactured, such as machined and casted, parts, since the operational requirements are the same. On the other hand, increasing the part's end-use performance aims to overcome the increased price of the production in the long run. This strategy is, in turn, utilized in intricate objects which cannot be manufactured using orthodox materials or methods, and the cost savings are generated by the enhanced end-use efficiency of the parts. Successful utilization of MAM is typically a specific combination of these two approaches. (Hällgren, Pejryd & Ekengren 2016, p. 247-248)

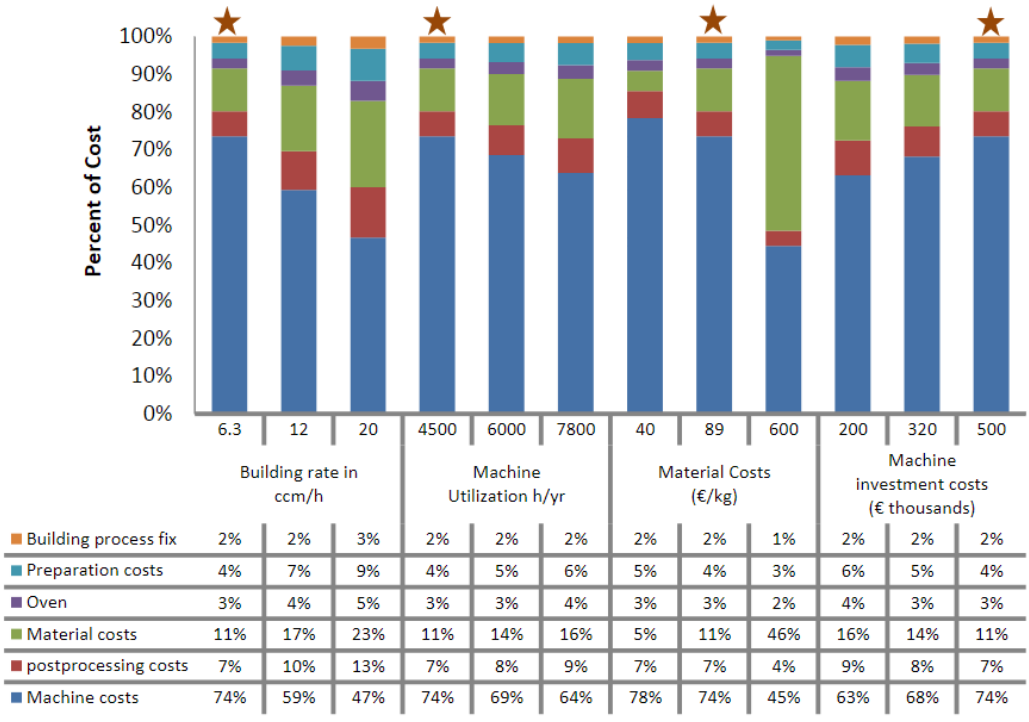

	6.3	12	20	4500	6000	7800	40	89	600	200	320	500
Building process fix	2%	2%	3%	2%	2%	2%	2%	2%	1%	2%	2%	2%
Preparation costs	4%	7%	9%	4%	5%	6%	5%	4%	3%	6%	5%	4%
Oven	3%	4%	5%	3%	3%	4%	3%	3%	2%	4%	3%	3%
Material costs	11%	17%	23%	11%	14%	16%	5%	11%	46%	16%	14%	11%
postprocessing costs	7%	10%	13%	7%	8%	9%	7%	7%	4%	9%	8%	7%
Machine costs	74%	59%	47%	74%	69%	64%	78%	74%	45%	63%	68%	74%

Figure 36. Cost distribution chart of powder bed fusion, which is visualizing the role of decreasing the processing time of the machine as the main driver in cost reduction. The red star is indicating the base model in the figure. (Lindemann et al. 2012, p. 177–188; Thomas & Gilbert 2014, p. 16)

6.1 Manufacturing lot size effect

In general, metal additive manufacturing is cost-effective especially in small lot sizes or even individual items. In production of small series, AM can be directly compared with casted parts, where the great initial investment of molds is directly increasing the unit costs in small lots sizes. Due to process characteristics, the unit price in DED manufacturing are not so heavily affected by the lot size, as the manufacturing time consist almost entirely of the deposition time. In powder bed fusion, the unit costs are decreasing significantly when the unit quantity in a single batch is increasing, as the auxiliary process costs are divided among many parts. Recoating process of powder material in the PBF machine is the most important auxiliary factor, and is taking a noteworthy time in manufacturing cycle of layers. The quantity of required layer cycles is dependent only on the height of the build, thus single parts should be always oriented as horizontally as possible. By manufacturing full substrates of parts in a time, the amount of spread, but un-used powder in chamber can be optimized, and the waste in manufacturing time minimized. (Piili et al. 2015, p. 391-393)

In figure 37, the effect of increased manufacturing batch size on the unit costs is demonstrated with round ø16x90 mm bars, which were evaluated to be manufactured of 50 µm layers of Inconel 718 by a Finnish supplier's PBF machine. Stress-relief was contained in additive manufacturing costs, as residual stresses could induce distortion if the samples were sawed off the plate without annealing them first. The heat treatments in the quotation included precipitation hardening and solution annealing. The unit prices for the test bars were over 4-fold larger with the batch size of four specimen, compared to unit price for part in a batch of 30. However, if only couple of pieces are needed, the overall cost for manufacturing would be naturally lower for the smaller lot sizes, being 1830 € for 4 parts, and 2280 € for 8 pieces, whilst the price for 30 specimens was 3500 €. The phenomenon is due to fairly large share of powder recoating cycle from the total manufacturing time of one layer of metal by PBF. Recoating time is always constant, apart from the scanned volume per layer.

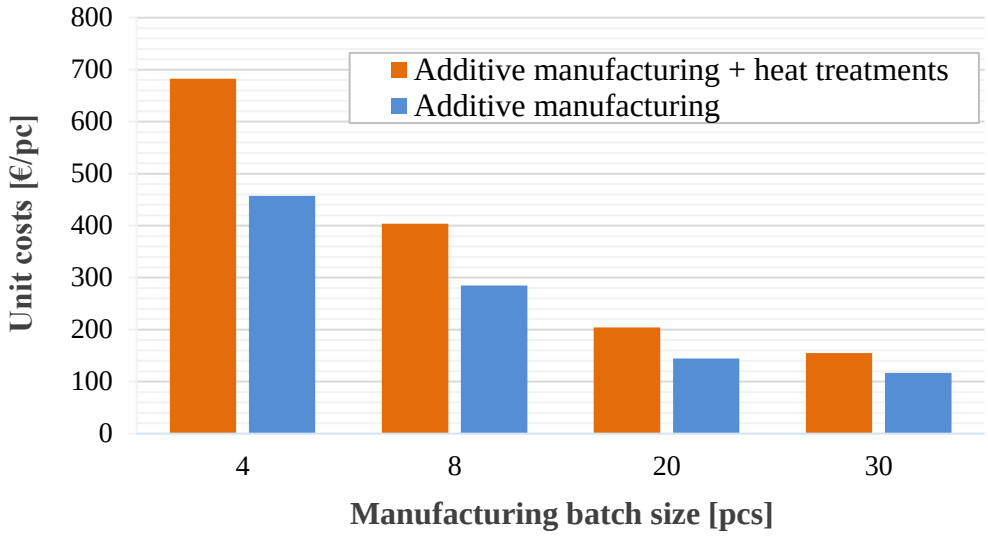

Figure 37. The relationship between unit cost and batch size in a single manufacturing cycle of Inconel 718 test specimen from a supplier. 30 pieces was the maximum number of specimens the machine could manufacture in a single run, and the increments in batch size were specified in the supplier's offer. (Supplier 2017)

6.2 Volumetric costs of AM production

Defining a precise yet simple rule of thumb for volumetric price for additively manufactured parts is challenging, which is clearly visible in the figure 38. For a group of four test specimens, the overall cost divided by the manufactured material volume results in over 3-fold higher volumetric price compared to parts made in a set of 30. In conjunction with batch size planning, build height's influence over the build time by increased recoating cycles has to be carefully taken into account in cost evaluating.

The findings concerning cost structure and the effect of batch size are in line with experimental studies found in literature, e.g. the works of Rickenbacker, Spierings & Wegener (2013, p. 214)

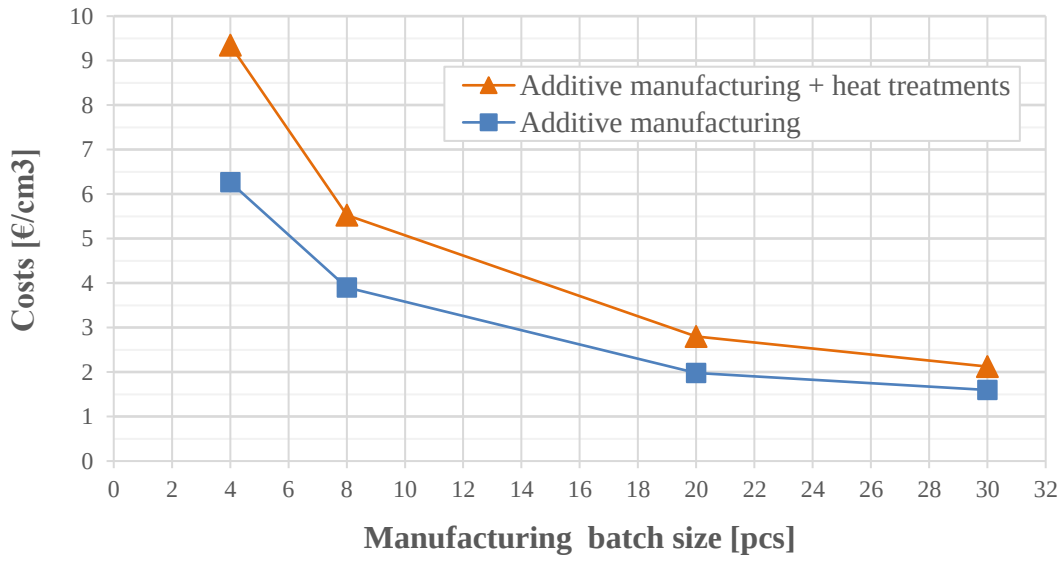

Figure 38. The effect of manufacturing batch size on the volumetric unit price of the IN718 test specimens, represented in costs per 1 cm^3 of manufactured metal by PBF. The connecting lines are only for visual guidance. (Supplier 2017)

6.3 Cost estimation models

For measuring the true costs ensuing from in-house metal AM production, comprehensive cost estimation models must be utilized. Since additive manufacturing is intensely upfront-concentrated, and only a minor share of costs is caused by labour, machine hourly rate is a good instrument for defining the price tag for processing. Machine hourly rate of AM machines consist of summed up system investment costs, capital interest costs, maintenance costs and labour costs, divided by the hours the machine is utilized over the payback period. Using this formula, the residual value of the system is presumed zero. Example calculations for a rough estimation of medium-class PBF machine's hourly rate is demonstrated in the table 14. Since the metal AM systems are developing intensively, payback period for the systems was set to 3 years, after which the machine should be renewed. Utilization of 80 % is near the full operational capability, when accounting for maintenance and turnaround times (Ray 2016). Utilization percentage has a strong effect over machine hourly rate, and decreasing it from 80 % to 60 %, the hourly rate raises from 62 €/h to 83 €/h. The cost evaluation model represented below contains only the major factors comprising the price, and a more precise model could be formed by applying case-specific circumstances. Thus the model should be used only for getting an idea of the scale of costs. By entering the

characteristic values of DED machine, the tools could also be utilized for manufacturing cost estimations of other MAM systems.

Table 14. A rough estimation and the constituting factors of machine hourly rate of powder bed fusion (PBF) machine for metal additive manufacturing. Characteristic values for medium-class machine in industrial scale production were utilized in forming of hourly cost of in-house manufacturing. (Ray 2016)

Factor	**Value**	**Unit**
Machine system costs	800 000	€
Payback period	3	A
Interest rate	5%	%
Total investment costs	926 100	€
Employee + overhead costs	117 000	€/a
Employee cost per period	351 000	€
Maintenance costs per period	30 000	€
Utilization rate	80%	%
Machine hours	7000	h/a
Machine hours per payback period	21000	h
Machine hourly rate	**62**	**€/h**

Highly specialized metal printing companies can operate their machines with high utilization (> 70%), and hereby offer competitive prices especially for small series and prototyping purposes. However, when the demand for AM parts is largely increased for e.g. as a result of successful part implementation into serial production, internal AM production becomes more profitable.

The phenomena and the feasibility break-even point in in-house AM production is illustrated in figure 39. It demonstrates the total production costs as a function of utilization rate of a medium-sized PBF machine are compared to the corresponding costs of an outsourced production. For in-house production costs, the values expressed in table 15 were utilized, and the total fixed cost of 1,2 M€ for a 3-year AM production period was determined, which excludes materials, energy and rents. Contracted, highly specialized production is presumed to continuously operate on 80 % utilization rate, which is setting the outsourced AM processing hourly rate to 81 €/h which includes a humble 30 % margin estimated for the service. The total contracted production costs were then measured by multiplying the estimated hourly rate of 81 €/h by the total machine hours of the 3-year period with four increments in utilization percentages: 50 %, 60 %, 70 %, and 80 %. Furthermore, these utilization percentages were converted into machine hours, which were 12140 h, 15768 h, 18396 h, and 23652 h, respectively. Hereby, as the amount of AM processing was defined by operational hours of machine, the overall prices of in-house and outsourced production could be compared. The break-even point for in-house machine utilization rate was defined to be around 60-65 %, which means that the in-house machine must be almost completely employed for cost-effective and feasible part production. However, this is relevant only for prototype or end-use part production, and when the value is measured only by the straight manufacturing costs, and not for instance shortened iteration time between designs. Also, the used business margin of 30 % for the outsourced production could be underestimated, and thus increasing the break-even point for in-house manufacturing. Moreover, real-world AM suppliers can include additional costs such as fail rate costs to the total quotation price, which can constitute 20 % of the total price (Ray 2016).

Furthermore, in-house production can be a strategic choice. For instance, Airbus is using their medium-class Concept Laser machine in Hamburg site only for prototyping purposes, and to define the optimal process parameters for achieving consistent manufacturing quality and defect-free material with specific geometries. After the careful process validation, the serial production of actual end-use parts is outsourced using the already investigated parameter settings. (Sanders 2017)

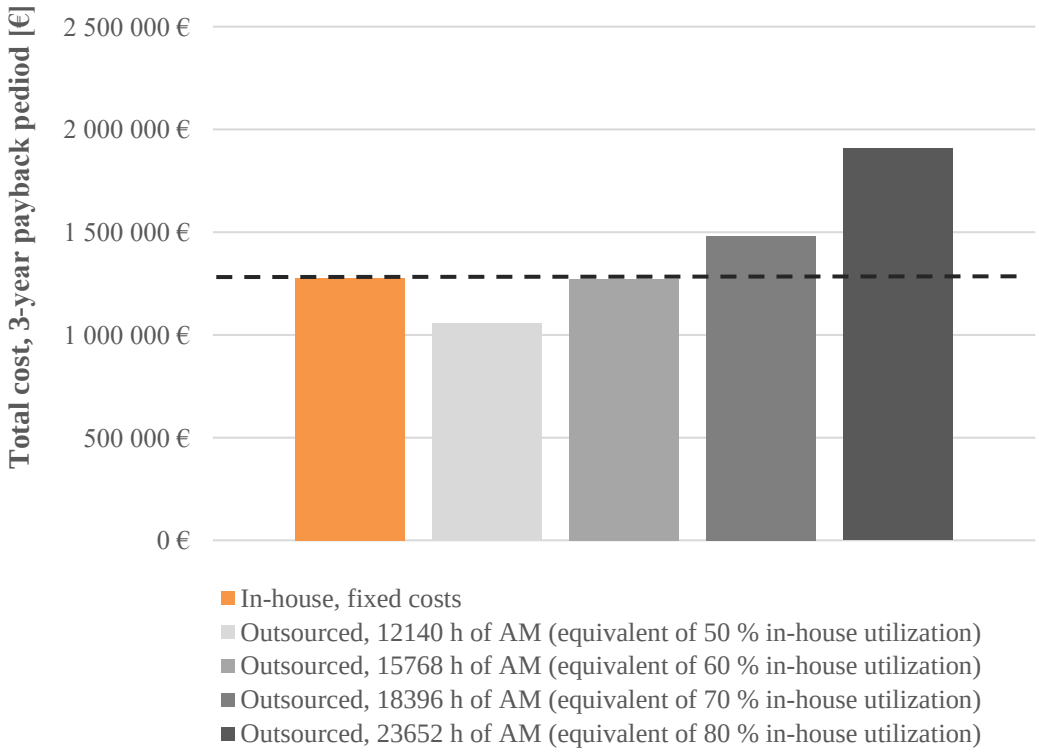

Figure 39. The utilization rate's effect on the in-house manufacturing feasibility compared to outsourced production in 3-year payback period. Break-even point in the utilization rate for feasible in-house production by total costs is estimated to be around 60-65 %.

Estimated hourly rate of a medium-sized PBF machine can be utilized in constructing a volume-based cost model for in-house PBF manufacturing. An example cost estimation of 300 cm^3 aluminium part manufactured by PBF is presented in table 15. Powder materials have their own material-specific drop-down menus in the spreadsheet model in Excel, since the material properties are strongly influencing build rates and building times, which are further affecting the manufacturing cost. However, since the model is utilizing only build volume to describe the true geometry of the measured model, the calculated build time can be inaccurate.

Table 15. A rough volume-based manufacturing cost estimation of a 300 cm^3 AlSi10Mg part(s) by PBF.

Factor	**Value**	**Unit**
Part volume	300	cm^3
Support volume	15	cm^3
Total building volume	315	cm^3
Material density	2,7	g/cm^3
Material cost	0,4	€/cm^3
Mass of part	810	g
Build rate	25	cm^3/h
Build time	12,6	h
Machine hourly rate	62	€/h
Total manufacturing cost	**907**	**€**

For more precise build time calculations for PBF, using the more sophisticated model demonstrated in table 16 is recommended. It utilizes the most essential manufacturing process parameters, and mean geometric dimensions of the constructed geometry, thus taking the build height and its effects on the building time into account. Also, the material distribution over the built height is considered with the simple input for mean area per cross-section of part, which can be easily exported from a CAD software. For example, if the height of a 300 cm^3 part in build chamber is doubled along with mean area by layer, the build time is roughly elevated by 50 %. With volume-based model only, the increase in building time, and consequently in costs, would not have been exposed. In conclusion, orientation of the part is strongly affecting the build time, and consequently the manufacturing costs.

Table 16. Process parameter-based approach for part manufacturing cost estimation of PBF.

Factor	**Value**	**Unit**
Quantity of lasers	2	pcs
Part volume	300	cm^3
Build height	150	mm
Mean area by layer	2000	mm^2
Layer thickness	50	µm
Scan velocity	1000	mm/s
Hatch distance	0,1	mm
Scan area per second	200	mm^2/s
Scan volume per second	10	mm^3/s
Scan time per layer	10	s
Layer cycles	3000	pcs
Scan time total	8,3	h
Build rate	18,9	cm^3/h
Recoating time per cycle	9	s
Auxiliary time total	7,5	h
Total manufacturing time	15,8	h
Total manufacturing costs	**901**	**€**

Both of the previously presented cost models are based on the hourly rate of the AM system, which is heavily dependent on the utilization rate of the machine. In AM service companies, build planning softwares are utilized in process time calculations, and by multiplying the time with hourly rate, the costs could be accurately defined.

7 MECHANICAL PROPERTIES & INDUSTRIAL USE OF MAM PARTS

7.1 Mechanical properties

Additively manufactured metals are typically comparable to wrought materials by mechanical properties, and usually even exceed them by tensile strength and yield strength. AM metals have a unique elongation behavior, which is usually significantly different to comparable casted or wrought material. These distinctive properties are originated by the repeated, fast heating-cooling cycles of material during the process, which are causing a fine grain structure in material, which is characteristic to MAM. Therefore, different heat treatments and e.g. hot isostatic pressing (HIP) are widely used to adjust the as-built material properties into more suitable for desired application. In this chapter, material properties of both PBF (powder bed fusion) and DED (directed energy deposition) processed materials are discussed.

7.1.1 Yield & tensile strength

In most cases, MAM materials are virtually fully dense (> 99,5 %), and are exceeding the mechanical properties of wrought reference materials in static loading cases. However, since the solidification procedure of the powder is always an intricate combination of process parameters and environmental factors, eventual material properties of certain material and geometry can fluctuate notably from the expected. For example, applied laser power, scanning/nozzle speed, cooling rate, and material composition all have their distinctive effect on the defect formation, and further on the resulting material properties. Therefore, defining the prevailing material properties which are prevalent in a certain geometry beforehand is highly challenging. (Hu & Mahadevan 2016, p. 135-136)

Also, while surrounding geometry is defining the thermal history of a specific sample, it is altering the metallurgical composition of the part unevenly depending on the sample location. Thus, the outcome of the additive manufacturing should always be designed and inspected by the most critical geometry and its location in the part. For instance, both yield and tensile strength have been observed to be slightly decreased in the upper sections of the DED manufactured geometry. In an experiment with 306L stainless steel, a decrease of 8-23 % in tensile strength, and 17-24 % decrease in yield strength were measured in the 60

mm distance from base plate. Specimens manufactured with lower laser power were found to have higher strength, and suffer smaller reduction in strength as-built than the parts processed with higher energy input. The phenomenon was concluded to proceed from decreased cooling rate and consequently coarser grain structure in samples which were located in greater distance from the substrate. The highest tensile strength measured for the test specimens was 609 MPa for low-power and 581 MPa for high-power walls, while the peak values for yield strengths were 337 MPa and 277 MPa, respectively. Nonetheless, despite the decrease in strength, all of the values were still greater compared to wrought reference material. (Wang, Palmera & Beese 2016, p. 230-234)

Additively manufactured material is usually weaker to some extent in Z-axis (building direction) in comparison with the mechanical properties in x-y-plane (table 17). This anisotropy is caused by the uneven distribution of defects inside the structure, and layer-wise fusing of the weld beads, which forms more consistent bond with adjacent than overlapping beads. By directed energy deposition, the strength difference in XY and Z-planes can be even 25 % with fully dense, as-built condition stainless steels (Ma et al. 2013, p. 213).
Also tensile deformation of AM materials differs significantly from the wrought equivalents and among manufacturing orientations, yet the stress-strain behavior can be effectively optimized with heat treatments and hot isostatic pressing (HIP), which can be seen in the figure 40 below. (Mover & Long 2016, p. 205)

Table 17. Material properties of additively manufactured 316L austenitic stainless steel by PBF and DED. Wrought, solution annealed material is presented for reference. (EOS 2014b; Ma et al. 2013, p. 213; Makeitfrom 2017)

Material	**Process**	**Direction**	**Yield strength [MPa]**	**Tensile strength [MPa]**	**Elastic modulus [GPa]**	**Elongation to break [%]**
316L	PBF	X-Y	530 ± 60	640 ± 50	185	40 ± 15
		Z	470 ± 90	540 ± 55	180	50 ± 20
316L	DED	X-Y	490	685	200	20-51
		Z	280	580	-	20-62
316L	Wrought	-	190	540	200	43

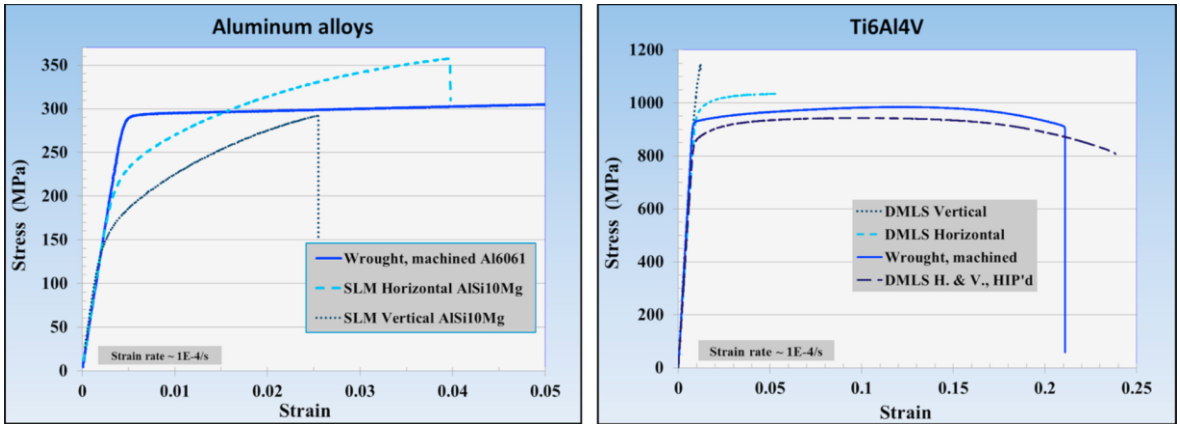

Figure 40. Stress-strain curves of PBF-manufactured aluminium alloy (AlSi10Mg), and titanium alloy (Ti6Al4V) compared to their corresponding wrought material sample. (Mover & Long 2016, p. 205)

It is also worth noticing that the Young's modulus of AM materials can be altered by heat treatments and HIP'ing, which is unusual for conventional materials. For instance, elastic moduli of IN718 samples manufactured with PBF were observed to be significantly different than in as-build state after the applied heat treatments or hot isostatic pressing. In as-build condition, elastic moduli of the specimen were measured to be 173 GPa. After the samples were HIPped in 1180 ^{o}C and 150 MPa pressure, and thereafter homogenized and aged by heat treating, the value was increased into 190 GPa. While the Young's modulus was increased by 10 %, porosity of the material was reduced upon the same time by 64 %, from 0.11 % to only 0.04 %. With heat treatment (HT) and hot isostatic pressing (HIP) the material properties of AM materials can be strongly affected, and porosity reduction together with changes in microstructure have been linked to altering of mechanical properties. The phenomenon is demonstrated in figure 41, where relative changes in mechanical properties of PBF-IN718 are presented. Highest values by far in yield strength, tensile strength, and hardness were obtained by treating the material by combined heat treatment (HT) and hot isostatic pressing (HIP). (Popovich et al. 2017, p. 16)

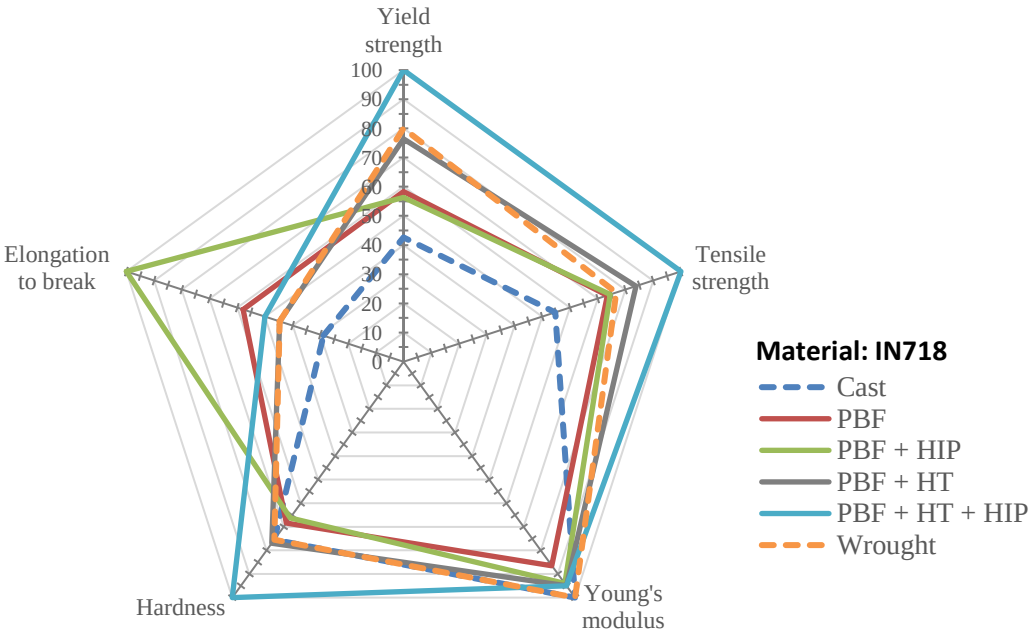

Figure 41. Relative evaluation of mechanical properties of IN718 manufactured by powder bed fusion, and conventional methods. The highest value of each property is given the value 100 %, and the inferior materials are presented as a proportion of it. (Data from: Popovich et al. 2017, p. 16)

7.1.2 Fatigue strength

Due to presence of internal voids and defects in the additively manufactured structure, the material's resistance to crack propagation under dynamic loading is often decreased. Thus the fatigue strength of MAM objects is often inferior to wrought materials.

Compared to A356, a similar alloy than AM-grade aluminum, additively manufactured AlSi10Mg's strength properties are superior both in static and dynamic means. (Beretta & Romano 2017, p. 181). However, as AlSi10Mg is currently the only commercially available aluminium alloy which is suitable for AM, the wide spectrum of conventional aluminium materials can be utilized to meet the application-specific requirements for e.g. fatigue properties more effectively. For instance, in as-build state, PBF-manufactured AlSi10Mg endures 30 % lower cyclic stress compared to wrought Al6061 for any prescribed lifetime. (Mower & Long 2016, p. 206)

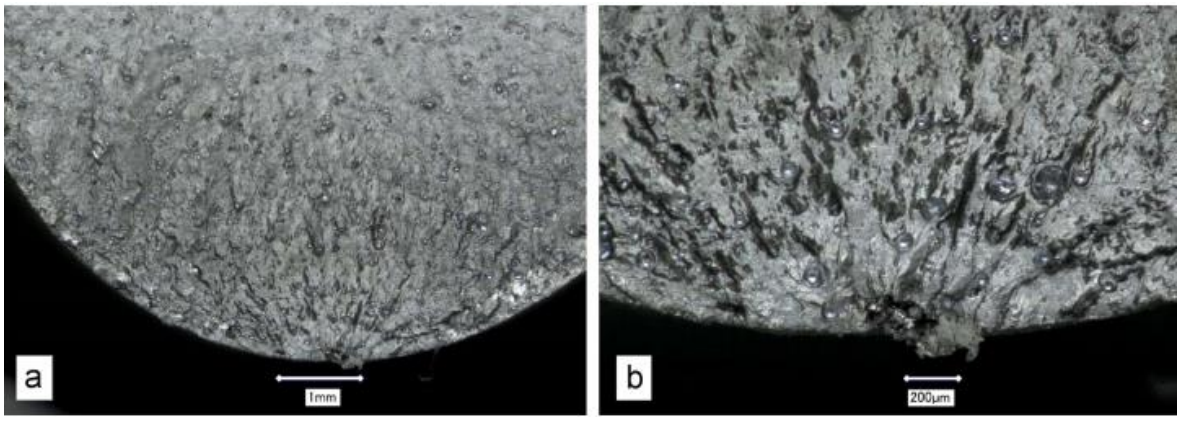

Figure 42. Fracture surface of an AlSi10Mg fatigue test specimen. The failure is initiated from the surface defect (a), and the mechanism is defined to quasi-brittle cracking originated from the linked cavities and balling defects in the sample. (b) (Mower & Long 2016, p. 207)

However, the crack propagation resistance, and furthermore the fatigue strength can be enhanced by several post-processing means. Surface polishing, machining and hot isostatic pressing (HIP) has been noted to decrease the aggravating effect of manufacturing flaws on fatigue strength, which can be clearly seen in figure 43. (Mover & Long 2016, p. 207)

Hot isostatic pressing suppresses internal voids in the material, and fuses any un-melted powder particles together with combined heat and pressure. It homogenizes the material and alters the material's microstructure. For example, Airbus is HIP-treating each one of the PBF-manufactured parts which are intended to be used in flying planes to ensure the consistency of the material. (Sanders 2017) However "HIPping" has been showed to be extremely effective when employed on AM-titanium parts, but can actually decrease the fatigue performance of AM-316L parts. This is caused by the HIP-affected balance of dominant failure mechanisms and material properties, which are all material and process-specific. Also, even despite the inclusive set of heat treatments and HIPping, AM metals are still slightly anisotropic hence the characteristic internal defects they always contain. (Yadollahi & Shamsaei 2017, p. 17-20)

Several surface treatments can also be applied to AM materials to reduce its tendency to crack initiation. Improving the surface roughness can almost triple the ultimate fatigue strength of titanium manufactured by PBF. For the benefit of conventional methods, milling the surface has been found to be the most effective surface treatment for increasing fatigue strength. (Bagehorn, Wehr & Maier 2017, p. 140)

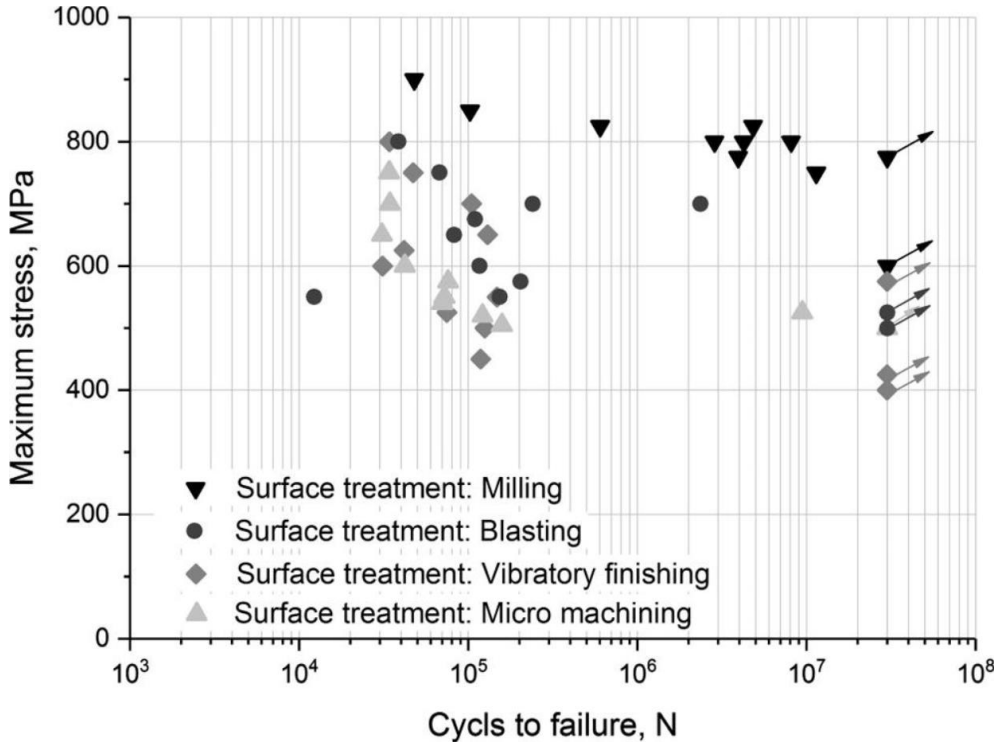

Figure 43. The effect of surface treatments over fatigue strength of hot isostaticly pressed PBF-Ti6Al4V samples. For reference, the endurance limit for similar specimens in as-build condition were 300 MPa. (Bagehorn, Wehr & Maier 2017, p. 140)

7.2 Industrial case examples

One of the most well-known industrial applications of metal additive manufacturing is a fuel nozzle, which was developed for General Electric's revolutionary LEAP jet engine. The part is brilliantly representing the effective utilization of DFAM guidelines and design principles. It is also a great example how the functionality of part has been optimized simultaneously in multiple areas, such as durability, weight reduction and operational efficiency, by design. The part is manufactured using PBF, and it comprises a number of internal flow channels, cooling the casing with fuel in the combustion chamber. This ensures a staggering 5-fold increase in lifetime for the AM nozzle compared to the previously used, conventionally produced model. Also, the AM nozzle is reducing the weight by 25 %, and the number of parts in a nozzle component from 20 to only one, although there are still multiple parts in the final assembly of the whole nozzle. Due to its unconventional design and by utilizing 19 nozzles per engine, the fuel consumption of an aeroplane is be decreased by 15 percent. (3dprint.com 2016; Industrial Laser Solutions 2013) The AM nozzle has been a standard

part in commercial A320neo planes since 2016, and by summer 2017, 12.200 LEAP engines has been ordered. (GE 2017a)

Figure 44. GE's fuel nozzle for the LEAP jet engine is manufactured by powder bed fusion, and is about 30 cm tall. (3dprint.com 2016)

After the successful implementation of additive manufacturing in the fuel nozzle, General Electric has been focusing their AM development efforts from part level to system level. Started in 2015, their ATP (Advanced TurboProp) program has already led into manufacturing of a prototype engine in only two years (figure 45). Hence the extensive utilizing of AM in the engine, 855 conventionally manufactured parts has been replaced with only 12 AM components in the assembly, including a novel gear box casing made with PBF. Due to innovative design, the new engine concept consumes 20 % less fuel, is providing 10 % more shaft power, and weights 5 % less than the other comparable turboprop engines in the same class. These enhancements were achieved by utilizing the design freedom of AM in e.g. flow optimization of the combustion chamber, and part consolidation, which is demonstrated in right in the figure 45. (GE 2017b; 3ders 2017)

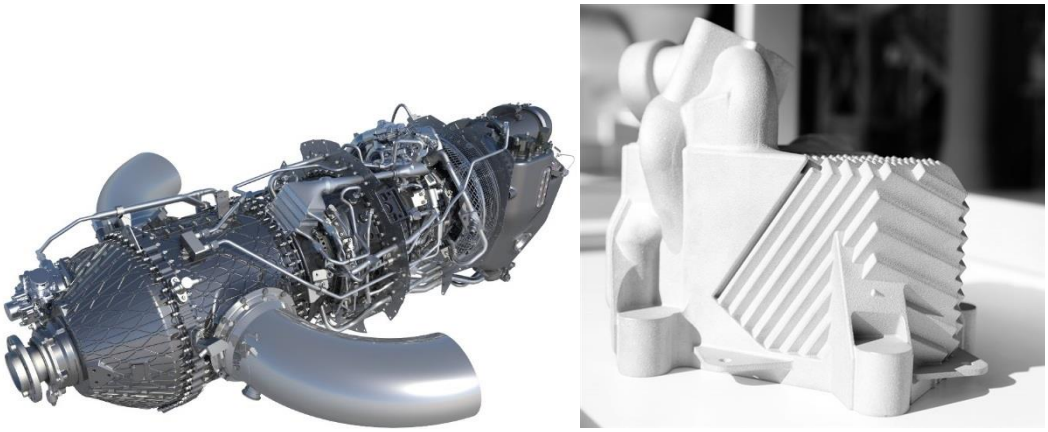

Figure 45. GE's Advanced TurboProp (ATP) engine (left), and a consolidated AM fuel heating casing of the engine (right). (GE 2017a; 3ders 2017)

Another example of successful implementation of MAM processing have been obtained by Caterpillar. It is an American corporation which manufactures industrial machinery and engines, such as bulldozers and power generating solutions. Its subsidiary, Solar Turbines, has implemented PBF manufactured parts into their gas turbine production models, and used DED processing for repairing the worn out parts. For instance, the company replaced a casted gas swirler, which delivers air/fuel mixture to the combustion chamber of gas turbine, with a PBF manufactured part, thus reducing annual capital and operating expenses by 350 000 €. Solar Turbines has also utilized DED approaches to reconstruct the features of damaged labyrinth seals (figure 46), and other critical gas turbine components, thus dodging 10 tonnes of precious INCONEL 901 material from being scrapped as un-usable parts. Less material is used in deposition, and also the machining need for the excessive material in deposit decreased. Employing lased-based DED also reduces the safety issues concerning the previously used arc-welding repair methods. (Caterpillar 2017)

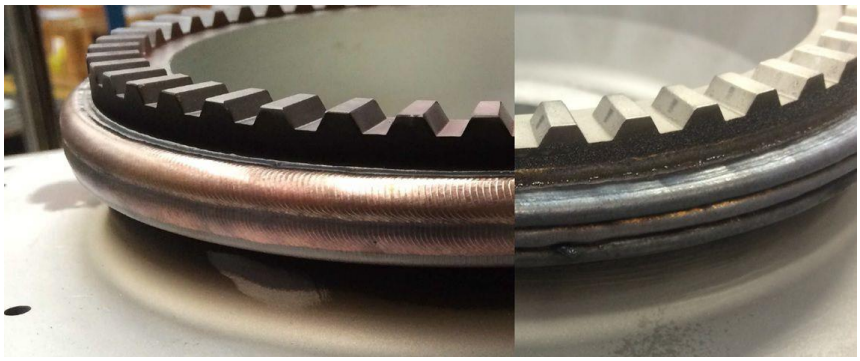

Figure 46. Repaired labyrinth seal of a gear wheel using gas tungsten arc welding (left), and directed energy deposition (right). The build operation carried out by DED processing is reducing repair time by 70 %, uses a lesser amount of material, and costs 120 $ less per piece than the previously used arc welding method. (Caterpillar 2017, p. 35)

One of the most advanced utilizer of production scale AM in Europe is Airbus, a multinational aircraft manufacturer. It started its Future by Airbus-program in 2011, and ever since, it has been working intensively on metal additive manufacturing to achieve weight savings and functional increases in company's aircrafts, since the field aerospace engineering is intensively driven by the mass optimization. Along with numerous topologically optimized bracket and support concepts, Airbus, together with their subsidiary APWorks specialized on AM technologies, have also developed their own AM powder metal alloy to effectively meet the serious requirements set for their products. The material, Scalmalloy, is utilized in the company's most sophisticated wall concept (figure 47) manufactured by PBF. Every branch of the 2-meter structure is unique, and has a different thickness distribution and geometry in its truss beams. Manufacturing of the wall trusses involves seven manufacturing batches in medium-class PBF machine, and every build is different.

With the design optimization enabled by additive manufacturing, the AM wall is 15 kilograms lighter than the current riveted aluminium sheet metal design, which means a significant 45 % saving in mass per wall. The biomimicking wall concept is planned to reach serial production phase in A320 commercial aeroplane in 2018. (Wired 2015; Autodesk 2017; Sander 2017)

Figure 47. A batch of topologically optimized, interlocking aircraft interior wall components (left), and an illustration of the ready assembled wall structure (right). (Autodesk 2017; 3D Printing Industry 2016)

8 EXPERIMENTS

Directed energy deposition (DED) of nickel-based alloys on cast iron was studied in the experimental part of the thesis, and the objective was to investigate the technological requirements for industrial scale DED manufacturing. Also, the demands for additive process parameters and conditions to produce high performance, defect-free & fully dense material on nodular cast iron were elaborated.

8.1 Background

Wärtsilä is interested in hard-facing nodular cast iron, which is vastly used in its products. IN 718 was selected for its high resistance against wearing and corrosion, however the desired properties could be ruined due to dilution to base material. Therefore, a layer of buffering material is needed to persist the residual stresses originated from rapid solidification, along with the dilution's effect on material properties of deposit. No corresponding studies on producing 3D geometry with the same specific materials were found, however, several articles about laser cladding/DED processing of nickel alloys on cast iron have been utilized in the planning of the experiments. Arias-Gonzales et al. (2016) build single NiCrBSi beads on nodular cast iron, which were succesfully obtained with slight micro porosity, yet relatively high dilution levels of around 15 %. Liu et al. (2016) predicted that the graphite in the cast iron would induce some cracking problems due to microstructural changes, namely brittle martensitic phases in the dilution zone, and that preheating would mitigate it. They deposited NiCrCo on cast iron, which resulted in micro cracking in bonding zone, since the dilution was extraordinary high (36-73 %).

8.2 Experimental procedure and materials

The manufacturing tests were carried out in the welding laboratory of Lappeenranta University of Technology using the research equipment of the lab. The system comprised a 10 kW IPG fiber laser as a heat source, a Precitech laser deposition process head with a 6x4 mm rectangular spot, a tilting turntable by Finnrobot, NC-controlled Siemens gantry system for moving the processing head, and a Plasma-Technik PZ Twin-10 disc-operated powder feeder unit with an lateral feeding nozzle made of copper tube.

The studied base material was EN-GJS-500 nodular cast iron, which was casted into 35cm x 18 cm x 8 cm blocks, and then the 80-millimeter-wide, circular deposition geometries were machined into the material (figure 48). Before tests, one block was cleaned with acetone and retained in room temperature, and the other was heated in furnace at 150 ^{o}C for four hours to remove any residual water, which could be permeated in the pores of cast iron. For laser deposition of the topmost layers, Inconel 718 powder was used, with grain size range of 53-150 µm. Höganäs 1315-00 powder was selected for the buffer material to be situated between the base material and the wear- and heat resistant IN718. It contained approximately 76 % Ni, 20 % Cu, 2 % Si, 1 % of Boron, and 1 % Iron with grain size distribution between 36-125 µm (Höganäs 2017). The carrier/shielding gas used was Argon.

Figure 48. Pre-machined cast iron block, and the portal-mounted laser deposition head with external powder feeding nozzle, and tilting turntable utilized in the experiments.

Manufacturing parameters were tested with structured test patterns to find the optimal combination of laser power, deposition speed, and powder feed rate. Satisfactory results were obtained using the parameters presented in table 18, with deposit beads approximately 6,0 mm in width, and 1,0 mm in height. Material samples were manufactured on 20-

millimeters-thick plates of base material using parameter set 1, and were prepared for macro/micragraph analyzes displayed in the result section. The first round deposition test were conducted with parameter set 1, and thereafter with increased heat input using parameter set 2, in accordance to the table 18. In the experiment, two different tilting angles, 45^{o} and 65^{o}, were utilized, according to the chamfer angles of the designed geometry, and the deposition was carried out sequentially from bottom to top.

The powder adhesion efficiency value was measured by laying deposit beads using the parameter set 2 on a cast iron plate, and by comparing the mass of the workpiece before and after the test, and by calculating the overall powder feeding from the processing time.

Table 18. Deposition parameters of the tests.

Set	**Power [kW]**	**Speed [mm/min]**	**Spot size [mm]**	**Powder feed [g/min]**	**Focal point [mm]**	**Gas flow [l/min]**	**Hatch spacing [mm]**
1	3,15	800	6x4	26	+50	8	2
2	3,15	600	6x4	26	+50	8	2

8.3 Results

The desired amount of deposited material embodied approximately 8 mm of buffer, and couple of millimetres of IN718 on top of it. Results of the deposition tests are reviewed in this chapter, and they consist of examination of the material samples, and further, analysis of the actual circular deposition geometries.

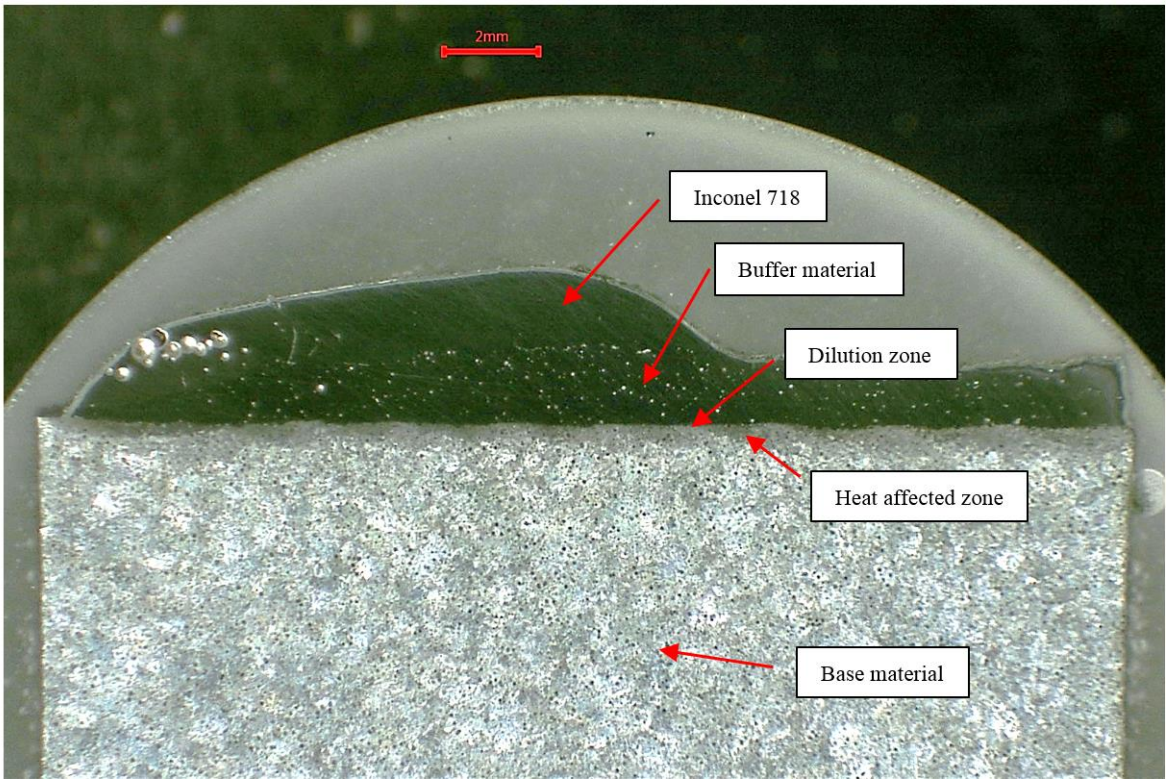

Figure 49. Macrograph of a polished DED material test sample with its characteristic areas. Base material (nodular cast iron) was first deposited with buffer material (Ni-based alloy), followed by a bead of IN718 upon. **(**Scale bar: 2 mm**)**

In avoidance of brittle microstructures in dilution zone often leading to cracking, minimizing the zone's thickness is crucial. Furthermore, this helps dodging the entrainment of graphite's carbon atoms in deposit, which would otherwise increase its hardenability. Thin dilution zone, approximately 0.5 mm thick, was obtained in first deposit bead, however gas formation/entrapping was still induced, resulting in pores inside the buffer material. This is clearly visible in figures 50 and 51, where polished micrographs of material samples are shown.

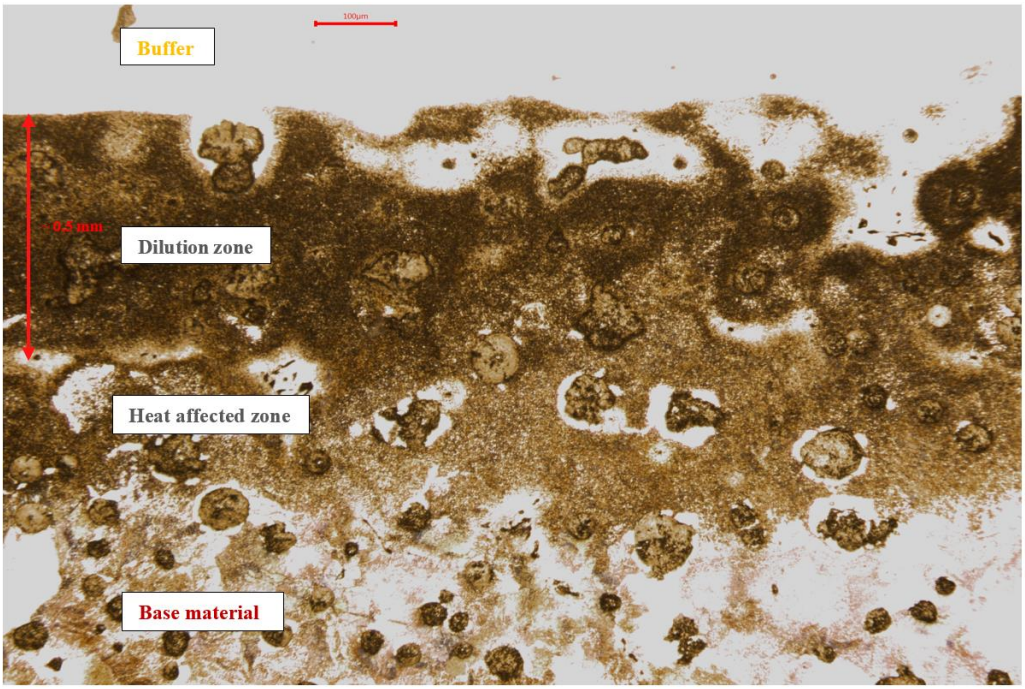

Figure 50. HAZ and the dilution zone between the base material and buffer. Scale bar: 100 µm.

The defects in the buffer material in figure 51 were recognized as gas pores, which are formed due to trapped gas in the melt pool. No such porosities were observed in the IN718 sample, which was deposited onto bead of buffer material.

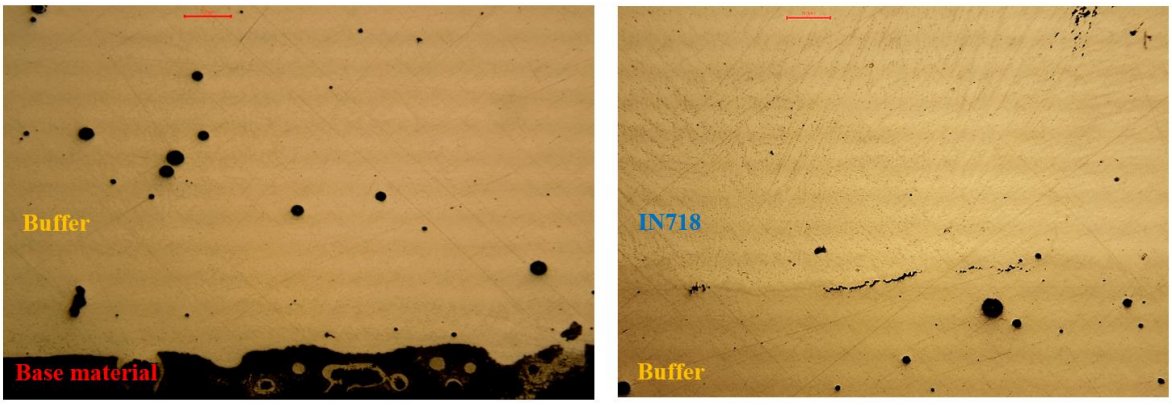

Figure 51. Micrographs of deposited materials: buffer material with internal porosities (left), and almost fully dense IN718 (right). Scale bar: 100 µm**.**

The first deposits crakced right after the first set of beads were laid onto un-preheated, room temperature block. Increasing the heat input by lowering the deposition speed from 800

mm/s to 600 mm/s (switched to parameter set 2 defined in table 18), cold cracking was reduced. The first half of deposition was built succesful, however, the first “clinking” sounds originated from cold cracking were heard after the second half of deposition layer. Hereafter, preheating the blocks with blowtorch to 60-85 ^{o}C before deposition succesfully postponed the cracking to emerge after two sets (two complete layers consisting of 9 beads each) of buffer beads, and the result is presented in figure 52 below. The preheating increased also the temperature of block after processing, and with residual heat from process, it reached 145 ^{o}C right after the deposition.

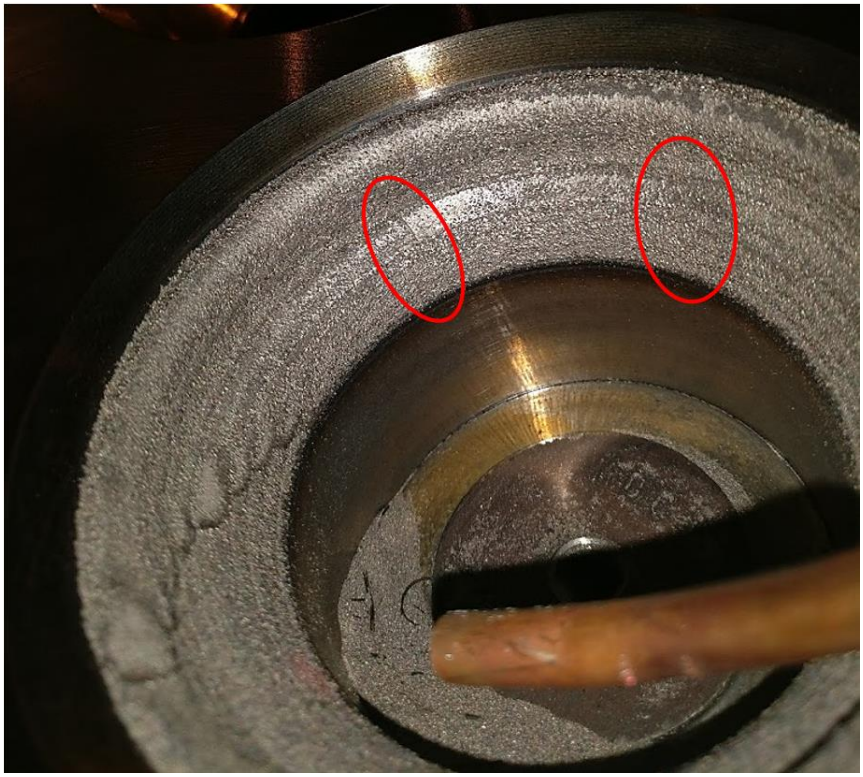

Figure 52. Circular buffer geometry after two deposited layers. Surface cracks (circled in red) and a few cold cracks were formed in the cooling phase of NiCu-based buffer, even with increased heat input.

As a countermeasure for observed cold cracking in each of previously deposited round geometries, two additional strategies for pre-heating were tried out. As the block temperature of 80-90 ^{o}C seemed to mitigate the cracking earlier, the workpiece temperature was first increased to 85 ^{o}C, deposited with buffer material in 3-bead sets, and between the sets the block was cooled down to the starting temperature. Thus, the temperature after processing was able to been kept under 100 ^{o}C, which was expected to reduce tensions in the deposited

material. However, this turned out to not be the case, since the clinking sounds of severe cold cracking were again observed after the second set of beads. Parallel cracking phenomenon was occurring also similarly when the beads of IN718 were welded straight upon the base material, instead of buffer material layer.

Additionally, more intense pre-heating of 200 ^{o}C was applied to the block with furnace to address its effect on the residual stresses in deposited metal. One layer of deposited buffer material which consisted of 9 beads was melted onto circular cup of the heated block, which resulted in the most severe surface cracking of the all deposits; the more forceful pre-heating seemed to only worsen the problem. However, the flaws in the buffer were reckoned as hot cracks, since no cold cracking sounds were heard in the cooling phase of the block, nor the appearance of the weld surface was similar to previously manufactured sets. All of the test above were carried out using parameter set 2.

8.4 Discussion

Even though each of the circular geometries cracked in some phase of the solidification, successful and crack-free deposition section is likely to be achieved by the means of process development. Possible solutions to be further evaluated and studied in order eliminate cracking:

- Different, more resilient buffer material selection
- Increased heat input by decreasing speed, or increasing laser power
- More intense (> 300 ^{o}C), yet more regional preheating with induction heater
- Powder feeding unit must produce more consistent powder flow
- Coaxial process head for more controlled process atmosphere
- Radially welded, or split beads instead of continuous tangential deposits

The rotationally symmetrical deposition is very challenging geometry, since the thermal expansions of the base material, and the deposits occur in the opposite directions. First, the deposited material is melted and solidified, which is heating the base material. As the block and the deposited ring are cooling down, the hole in the block is expanding, unlike the deposit ring, which is shrinking towards the center of the hole. This induces massive amounts of stress in the deposit, causing it to shatter. Moreover, the assumption of geometry's strong effect on the cracking is further confirmed, since absolutely no cracking occurred in the parameter testing phase. Both materials, base and buffer, were the same, only the path of the welding was straight, instead of circular.

The buffer material, which was intended to be ductile and easy to be manufactured on cast iron, proved to be brittle, vulnerable to cracking and inclined to internal porosities. Together with brittle phases in deposited material, internal cracks and defects are providing an unfortunately good environment for crack initiation and growth in buffer material. Each one of the round deposit geometries suffered from (cold) cracking in some point of the process. The origin of the pores cannot be thoroughly traced, but it was proposed that they were either vaporized residuals of cutting fluid used in the machining, bubbles of shielding gas, or carbon dioxide formatted from the base material's graphite. Either way, this has to be taken into consideration when the manufacturing process is further improved and tuned up to be able to produce crack-free deposits with minimal internal porosities. Furthermore, the crack initiation is much more severe problem than the porosity, hence the effect of another buffer material on crack initiation should be investigated by conducting similar experiments to find more suitable material pair, and parameters.

Processing head must always be aligned perpendicularly to the deposited surface. Therefore, the machined geometry in cast iron block should be designed so that the need for changing the tilting angle of turntable is minimized, and the accessibility of process head is assured. Moreover, the welding process is easier to handle and keep stable if the tilting motions of the table (or trajectories of robot arm if employed) are simplified. By the manufacturability means, the deposited circular geometry could be enhanced even more by utilizing only one chamfer angle, instead of two (45^{o} & 65^{o}).

As the powder metals are in the core of the process, several observations are related into it. The powder is fed into melt pool in the process with carrier gas, and despite the optimal nozzle position, only around 40 % of the fed powder was melted into deposit. Rest of the powder is blown away, and is spreading around the manufacturing cell during the processing. Moreover, the major share of un-used powder is impairing the cost-effectiveness of deposition, since the material feedstocks are costly. With coaxial process head, adhesion of the raw material could be greatly enhanced, together with better process stability and melt pool shielding. For this reason, commercially available hybrid-DED machines, along with AM-dedicated systems, are almost without exception utilizing the coaxial nozzles.

Also, quite surprisingly, issues with consistent powder feeding were often hampering the deposition. Powder feeder unit suffered from feeding jams during processing, and if sufficient amount of powder was not delivered into melt pool, the overheated bead cracked right away. Since the occasional discontinuities in the powder feeding lasting only couple of seconds were occurring all the way during the deposition process, and resulted immediately in cracking in the most severe jamming situations, this was also considered as the potential root cause for the cracking problem. Therefore, constant flow of powder is extremely important, and must be ensured by high-quality feeder unit equipped with proper process monitoring system in industrial-scale manufacturing.

The powder used in the deposition process is especially harmful for lungs and electro-mechanical systems, therefore the equipment and personnel must be protected properly from the fine metal dust. However, for operators, a simple respirator and cell ventilation are adequate safety procedures, and the machinery could be encapsulated and sealed during the processing. Machines which are dedicated only on AM, and Hybrid-DED systems are usually operating behind sealed casing, which could easily solve the health issues of floating powder in the cell.

Another process-related thing to protect from is the laser radiation. The manufacturing cell must be isolated behind protective shades, and personnel inside the cell must be equipped with special, laser-absorbing glasses. However, this is only needed with open systems, since encapsulated DED-machines (either AM-only, or hybrid-DED-machines) are usually fortified with semipermeable windows similar to laser goggles, and thus eliminating the need for personal protection from laser.

The studied block geometries necessitate sequential engagement of both subtractive, and additive processing. As the industrial production with these technologies is entirely numerically controlled, and mere additive processing is utilizing numerous of different subsystems simultaneously, the programming using several user interfaces and controls is complicated. A hybrid-DED machine could be effectively utilized in manufacturing of the entire experiment parts, hence the integrated control system of all subsystems, provided by OEM's of the machines. Since both subtractive, and additive operations could be performed in the same machine, the machined initial shape for the rotationally symmetric "cups" could be deposited in the same machine, and later machined again to its final form, with only a single fixture. However, since the hybrid systems can run only one operation at a time, subtractive or additive, the utilization rate of the subsystems is inferior to separated, two machine approach. On the other hand, the required floor area, as well as protective measures against powder spreading, must be higher than the order of magnitude.

9 CONCLUSIONS

This thesis was carried out to fill the gap in knowledge concerning metal additive manufacturing, its possibilities in industrial applications, and to provide sufficient understanding of manufacturability and DFAM for the design and manufacturing personnel of Wärtsilä. However, as this work is among the very first trials of the company in the area of AM, and the main areas have just been defined, a lot of detailed and well-structured research is needed to be done by the company before any tangible AM solutions could be implemented in the engine. Although the key findings of the study can be used directly for training purposes, their main value is to work as the backbone of Wärtsilä's future AM strategy.

The results from the literature research are strongly indicating that the metal additive manufacturing have just recently achieved the necessary maturity level for shifting from rapid prototyping and small series production, to serial production of end-use parts. Based on the market analysis, and industrial benchmarks, the implementation rate of AM parts is increasing continuously. Also, the AM machinery is becoming more and more autonomous and adaptive, thus increasing the quality of parts, and productivity and cost-effectiveness of the production.

The initial guiding hypothesis for the study was, that feasible utilization of AM requires simply good understanding of the limitations and characteristics of the used methods (PBF, and DED) and materials, together with some optimization of the designed structures. It was assumed that simply by surveying difficult parts to manufacture, it is possible to find ideal objects to be produced via additive means, such as fuel injection equipment. However, during the research, it gradually became more and more apparent that this was not even close to the whole nature of the matter, and this observation was strengthened throughout the experiments. Additive manufacturing is incredibly complex ensemble of tasks, since almost everything is different compared to the usual habits in mechanical part design, metallurgy, and manufacturing, and all these things must work together in a completely new way. The importance of intense teamwork between experts in various fields of technology and business cannot be over-emphasized.

In the transition phase from conventional manufacturing to AM, one of the greatest barriers to overcome will be the need to envision the whole design process in a completely way. Where the conventional manufacturing is not involved, all of the past constraints must be completely ignored, and the old customs have to be questioned. Only by doing so, the real functionalization leap is enabled. For example, all channels for cooling water are traditionally smooth-walled, yet much better solution would be to improve the heat conduction by i.e. filling the channel with cell structures. Previously, the manufacturing methods constrained the shape, but with AM all these new kinds of tactics are available.

Also, the immense application potential provided by AM still must be realized by the designers in a concrete way. This is where the human factor comes into effect – skillful professionals with years of experience and knowledge over laws of engine systems and manufacturing methods are used to do things in a certain manner, and favor ways they are already familiar with. On the contrary, more inexperienced in particular engine systems, yet highly AM-oriented designers, are more likely to think “outside the box” and to try innovative solutions, however, lacking the true understanding of the demands of specific components in the engine. Delicate balance should prevail between these two approaches both to understand the true operating environment of the target parts, and to expand the thinking patterns in utterly unorthodox ways.

9.1 Answering the research questions

In this chapter, the answers for guiding research questions of the thesis are elaborated.

1. *What is the status of metal additive manufacturing systems now and in the near future?*
    - In metal additive manufacturing, powder bed fusion is by far the most popular method, and is the industrial standard. The number of PBF machine suppliers were identified over 20, and the metal machines are sold at an accelerating pace. Over the last few years, the main focus in the development of the machine systems has strongly shifted from prototyping to increasingly automated serial production of end-use parts. Due to this, the number of lasers, and the maximum size of the manufacturing chamber has increased in PBF machines, and a quad-laser PBF machine with building volume of 1 m^3 was announced by Concept Laser in November 2017. However, the field is constantly developing, and in 2017, companies like Desktop Metal and Markforged have aggressively entered the market. The rivaling systems are resembling more extrusion-based polymer 3D printing or binder jetting methods, than any existing metal AM process. Their machines are utilizing metal injection molding (MIM) materials, which are sintered after the extrusion phase. Although they promise to be significantly faster and dramatically decrease the costs of parts, yet virtually no research data on actual material properties exists. In the short term, the most complex and demanding metal AM parts will still be produced by PBF, and DED is applicable for repairing, hard-facing surfaces, and building rib-on-plate structures from advanced materials.

2. *What are the design rules required to follow to optimize the component functionality and properties for metal additive manufacturing technologies?*
    - For the sole manufacturability of AM designs, comprehensive DFAM guidelines defined in chapter 5 must be utilized. Relatively simple geometric limitations, currently including 45-degree overhang angle, minimum wall thickness of 0.5 mm, and maximum self-supportive hole diameter of 6 mm, are essential in ensuring the successful forming of 3D geometry. However, in

addition to good manufacturability, the designs have to be much “smarter”, more complex, and thoroughly different than conventionally manufactured components, hence effective design guidelines must be, where appropriate, applied. These include, among other things, topological optimization, increased functionalization, part consolidation, and the most importantly, self-supportiveness. In other words, the parts intended for additive manufacturing need to be designed specifically for AM from the very beginning in order to minimize costs, and maximize functionality and manufacturing efficiency. Also, since the field is strongly developing, also the DFAM guidelines must be regularly updated. Due to enhanced real-time process control of PBF systems, the DFAM constrains will be loosened in future, and for instance, overhang angles of only 20 degrees can be already successfully manufactured using the most sophisticated machines.

3. *What are the characteristic costs and properties of metal additive manufactured parts and materials?*

- Manufacturing costs, both with PBF and DED, are mainly comprised by the machine’s hourly rate, which is again proportional to its utilization rate. Break-even point in utilization rate when considering between in-house AM and outsourcing, is around 60-65 %.

  Manufacturing lot size heavily affects the unit costs in PBF, and taking complete advantage of manufacturing chamber space by stacking it full is preferred. Also, the amount of post-processing, heat treatments, and inspections required after actual AM is increasing the total cost of parts. Thus, volumetric price of additively manufactured metal may vary from 1-2 €/cm^3 up to 10 €/cm^3, depending on the above-mentioned points.

  Additively manufactured metal is generally slightly anisotropic, hard, and has higher yield and tensile strength than wrought equivalent, yet the fatigue properties are inferior to conventional references. However, the mechanical properties can be greatly enhanced with post-processing means, such as hot isostatic pressing, heat treating, and smoothening the surface with i.a. milling or blasting. By cooperation of the design, metallurgy, manufacturing, and post-processing, the inferiorities in material properties could be overcome.

4. *How the metal additive manufacturing technologies should be utilized to add value to Wärtsilä's engine design and manufacturing process?*
    - Additive manufacturing could be utilized in high-performance parts, and in tools used in manufacturing and assembling phase of the engines. However, AM is still rather expensive technology, and usually cannot compete with conventional methods in manufacturing cost-effectiveness. Thus, in the design and manufacturing of AM components, the aim should be on the increased functionality and efficiency of the part, so the decreased life-cycle costs of the parts could outweigh the increased initial investment. In the engine point of view, these ultimate objectives for AM could be related in increased fuel-efficiency, extended lifetime of components, and improved reliability.

      Also, implementation of AM requires intensive teamwork between people with different expertise, otherwise the consequence would be only partial optimization of the process. For systematic approach for feasible AM, a utilization roadmap introduced in chapter 9.2 was produced to facilitate the defining of competence needs. Moreover, a question list was generated to simplify the cooperation work of different expertise to find potential applications of AM in engine part level.

9.2 Utilization roadmap

Additive manufacturing of metal materials is providing huge potential, and is enabling completely new opportunities in manufacturing, design, and materials. The benchmarked industrial example parts are confirming, that the great promises of MAM could be effectively actualized. However, since many fields in the whole process cycle of AM are fundamentally different to conventional methods and require a vast understanding of AM-specific phenomena, it creates a need for specialized team for additive manufacturing. Based on the identified skillset requirements for AM in the research, a teamwork concept for feasible utilization of additive manufacturing was generated, and is presented in the figure 53.

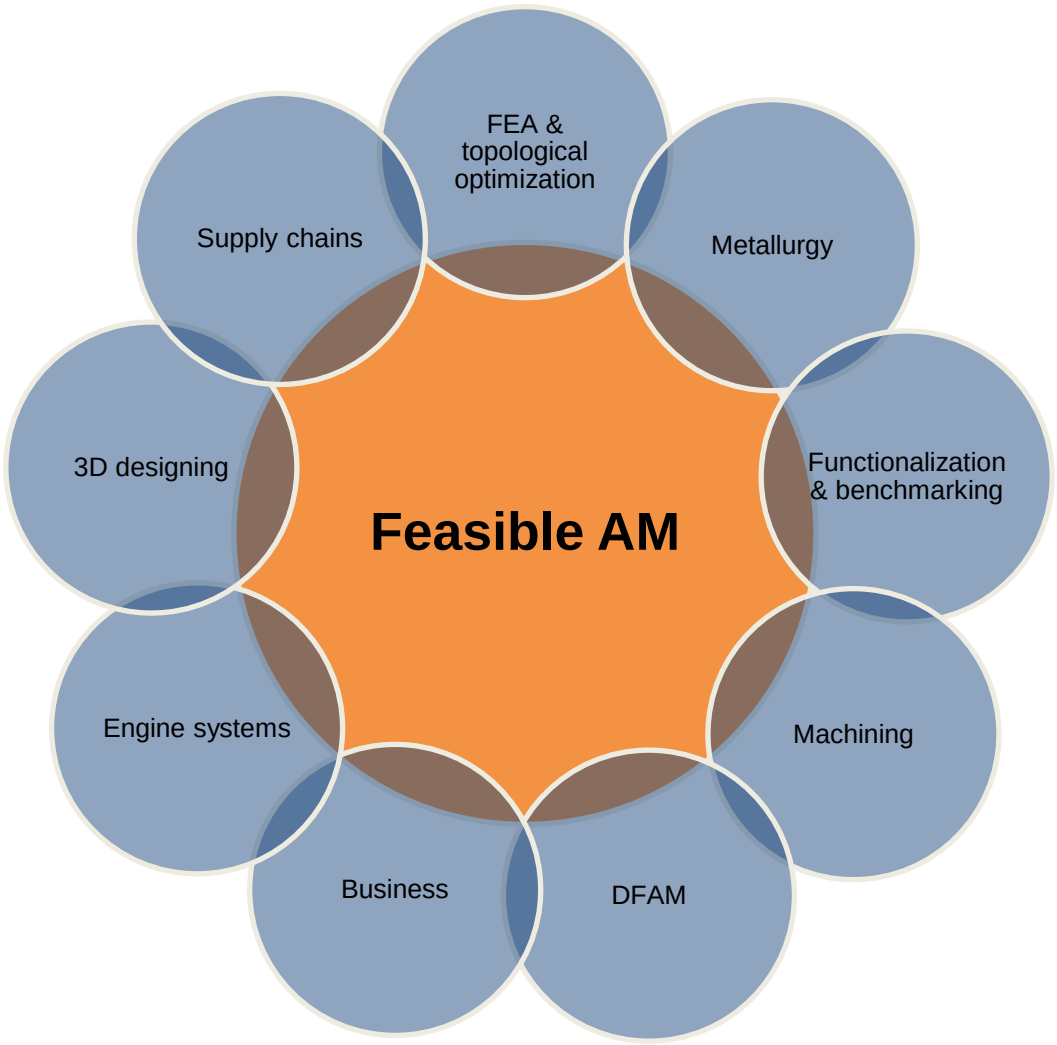

Figure 53. Different areas of expertise which comprise the holistic teamwork approach for feasible AM in Wärtsilä.

Each of the nine fields in the model must be covered and optimized to take full advantage of the AM in the industrial, serial production scale. For single piece manufacturing, or prototyping purposes, the model could be also used, yet the small scale manufacturing process is much more straight-forward and easier to handle. However, the highest potential and profits lies on the serial production of highly optimized, high performance components.

Based on the main advantages of the metal AM, a question list was formed to systematize the drafting process of potential applications, and is presented below.

Meta AM could be beneficial in manually lift-able component where/which

- Even a small reduction in mass is increasing the value (for example, where high accelerations are present)
- Is geometrically constrained by current manufacturing processes
- Is comprised of many small parts and sub-assemblies, and could be consolidated into few larger entities
- The utilization of poor machinability materials could be valuable
- Effective heat transfer, in as compact size as possible, is needed
- The internal flow losses must be minimized

9.3 Further studies

Currently, the real financial key figures of metal additive manufacturing case studies are carefully buried within the involved companies, and very little reliable information about the commercial feasibility of concept designs is available. In turn, the viability is also connected to the functional efficiency of the end-use part in certain application. Thus, learning by doing is practically the only way to gather trustworthy statistics on different applications.

During the thesis, the following areas were identified the most important for further investigation:

- Experimental design study, where the cooperation principle of holistic AM approach for PBF is utilized throughout the project
- The characteristics of large-scale hybrid-DED manufacturing, and different buffer materials of blocks studied in the experimental part of this thesis.
- Application potential and material properties of the new metal AM technologies, such as Desktop Metal's Single Pass Jetting, and similar Markforged's Atomic Diffusion Additive Manufacturing

Also, the impact of different software used in the designing, and process simulation should be studied, as they were outside the scope of this study. The synergy effect on the whole AM production should be examined, which is a result of consolidation of different software modules (such as 3D modeling, topological optimization, computational fluid dynamics, FEA, and AM process simulation and controlling) into a single design environment, where every operation is reversible. Currently, the modules do exist independently, but each operation is executed separately, and valuable data is lost in the workflow.

10 SUMMARY

In this thesis, characteristics and requirements in industrial scale utilization of additive manufacturing of metal materials were studied. In the literature part, the market and powder metal-based AM processes were reviewed, together with commercially available machine systems, and their characteristics. The DFAM design guidelines were defined based on the findings in the literature study. Furthermore, effective design principles of AM components were derived from the DFAM constraints. Also, cost-structures of MAM systems and parts, and the related phenomena were defined, and the characteristical material properties, and example parts from industrial applications of metal AM were elaborated. In the experimental part of the thesis, nickel-based alloy deposition on nodular cast iron was investigated.

Additive manufacturing process encompasses everything from the solidification of the raw material, and forming of certain microstructures in metal, to producing of 3D geometry with functional features. Almost every step of the conventional manufacturing process chain is compressed into a single stage. Hence, huge amounts of scientific and practical knowledge must be utilized, and attention be paid into process design. What was also found during the experiments, successful utilization of MAM in industrial scale is extremely demanding, and each one of the numerous parameters in the AM process cycle must be carefully optimized. It has a paradigm impact on the very fundamental members of engineering, for example 3D modeling softwares commonly used in the design, which are mostly feature-based. They are all tuned for conventional methods, and are operating through extrusion and cutting of geometry. For AM, generating the geometry can be profoundly more optimal and intricate, because the material could be added only where it is needed, in contrast with old style, where the material is removed where it is not needed. Learning by doing is practically the only way to gather trustworthy statistics on different applications of AM, and as the method will change the whole manufacturing industry in the long run, the work must be started now.

LIST OF REFERENCES

3D Systems 2014. Our story. Internet article. [Available: https://www.3dsystems.com/our-story][Accessed 12.3.2017]

3D Print Industry. 2014. Mazak adds hybrid metal 3d printer to machine tool lineup. Internet article. [Available: https://3dprintingindustry.com/news/mazak-hybrid-metal-3d-printer-35803/][Accessed 18.10.2017]

3ders. 2016. Gartner: 3D printing to accelerate in manufacturing industries in 2017. Internet article. [Available: http://www.3ders.org/articles/20161231-gartner-3d-printing-to-be-increasingly-adopted-by-manufacturing-industries-in-2017.html][Accessed 6.4.2017]

3ders. 2017. An inside look at GE's new 1,300-horsepower 3D printed ATP aircraft engine. Internet article. [Available: http://www.3ders.org/articles/20170727-an-inside-look-at-ge-new-1300-horsepower-3d-printed-atp-aircraft-engine.html][Accessed 18.10.2017]

3dprint.com. 2016. GE is Using 3D Printing and Their New Smart Factory to Revolutionize Large-Scale Manufacturing. Internet article. [Available: https://3dprint.com/127906/ge-smart-factory/][Accessed 13.10.2017]

Abd-Elghany, K. & Bourell, D.L. 2012. Property evaluation of 304L stainless steel fabricated by selective laser melting. Rapid Prototyping Journal, Vol. 18 Issue: 5. P.420-428.

Altair. 2014. Additive layer manufacturing. Internet article. [Available: http://www.llb.mw.tum.de/fileadmin/w00bqy/www/downloads/TUM_Leichtbauseminar_Kat

Aniwa. 2016. Internet source. [Available: http://www.aniwaa.com/3d-printing-technologies-and-the-3d-printing-process/][Accessed 16.3.2017]

Ampower Insights 2017. Additive Manufacturing Make or Buy? Vol 1. 34 p.

Arcam. 2017a. Arcam Q20plus. Internet article. Available: [http://www.arcam.com/technology/products/arcam-q20/] [Accessed 21.7.2017]

Arcam. 2017b. Internet source. [Available: http://www.arcam.com/wp-content/uploads/justaddbrochure-web.pdf][Accessed 27.3.2017]

Arias-Gonzales, F., del Val, J., Comesana, R., Penide, J., Lusquinos, F., Quitero, F., Riveiro, A., Boutinguiza, M. & Pou, J. 2016. Fiber laser cladding of nickel-based alloy on cast iron. Applied Surface Science, Vol 374, p. 197-205.

Autodesk. 2017. Reimagining the future of air travel. Internet source. [Available: https://www.autodesk.com/customer-stories/airbus][Accessed 27.9.2017]

Bagehorn, S., Wehr, J., Maier, H. 2017. Application of mechanical surface finishing processes for roughness reduction and fatigue improvement of additively manufactured Ti-6Al-4V parts. International Journal of Fatigue, Vol 102, p. 135-142.

BCG 2015.Industry 4.0: The Future of Productivity and Growth in Manufacturing Industries. Internet article. [Available: https://www.bcg.com/publications/2015/engineered_products_project_business_industry_4_future_productivity_growth_manufacturing_industries.aspx][Accessed 10.6.2017]

Beretta, S. & Romano, S. 2017. A comparison of fatigue strength sensitivity to defects for materials manufactured by AM or traditional processes. International Journal of Fatigue Vol 94, P.178-191.

Bloomberg. 2017. Internet article. [Available: https://www.bloomberg.com/news/articles/2017-01-12/ports-chase-natural-gas-boost-as-marine-emissions-rules-tighten][Accessed 14.9.2017]

Bossuyt, T. & Fournier, S. 2016. A Few Basic Design Rules for Metal 3D Printed Parts. Internet article. [Available: https://medium.com/@makernest/a-few-basic-design-rules-for-metal-3d-printed-parts-1eec4980bb24][Accessed 12.6.2017]

Buchbinder, D., Schleifenbaum, H., Heindrick, S, Meiners, W. & Bultmann, J. 2011. High Power Selective Laser Melting (HP SLM) of Aluminum Parts. Physics Procedia, Vol 12. P. 271-278.

Caffrey, T., Wohlers, T. & Campbell, I. 2016. Wohlers Report 2016 – 3D Printing and Additive Manufacturing State of the Industry – Annual Worldwide Progress Report. Fort Collins, Colorado, USA: Wohlers Associates. 335 p.

Calignano, F. 2014. Design optimization of supports for overhanging structures in aluminum and titanium alloys by selective laser melting. Materials & Design, Dec. 2014. P. 203-213.

Carroll, B., Otisa, R., Borgonia, J., Suh, J., Dillon, P., Shapiro, A., Hofmann, D., Liua, Z. & Beese, A. Functionally graded material of 304L stainless steel and inconel 625 fabricated by directed energy deposition: Characterization and thermodynamic modeling. Acta Materialia Vol 108, P. 46-54.

Caterpillar. 2017. 2016 Sustainability report. Internet source. [Available: http://reports.caterpillar.com/sr/_pdf/2016_cat_sr.pdf#page=19][Accessed 27.9.2017][Accessed 25.9.2017]

Chekurov, S., Eklund, P., Kujanpää, V., Pekkarinen, J., Syrjälä, K. & Vihinen, J. 2017. 3D-tulostuksen suunnittelu- ja päätöksenteko-opas yrityksille. DIMECC Oy. Tampere 2017. 42 p.

Cheng, B. & Chou, K. 2014. Thermal Stresses Associated with Part Overhang Geometry in Electron Beam Additive Manufacturing: Process Parameter Effects. Mechanical Engineering Department, The University of Alabama, Tuscaloosa, AL 35487. P. 1046-1087.

Ciurana, J., Hernandez, L. & Delgado, J. 2014. Energy density analysis on single tracks formed by selective laser melting with CoCrMo powder material. Int. J. Adv. Manuf. Technol., 68 (2013), pp. 1103–1110

Concept Laser. 2017. X line 2000R Metal laser sintering system. Product brochure. 4 p.

Crucible. 2015. Design guidelines for Direct Metal Laser Sintering (DMLS). Internet article. [Available: https://www.crucibledesign.co.uk/images/uploaded/guides/bs7000-part-2-a-management-guide-download-original.pdf] [Accessed 12.6.2017]

Custompartnet. 2017a. http://www.custompartnet.com/wu/laminated-object-manufacturing. Internet source. Internet source. [Accessed 15.3.2017]

Custompartnet. 2017b. Internet source. [Available: http://www.custompartnet.com/wu/fused-deposition-modeling] [Accessed 15.3.2017]

Davis, A. 2014. Layer-by-Layer: The Evolution of 3-D Printing. Internet article. [Available: http://theinstitute.ieee.org/tech-history/technology-history/layerbylayer-the-evolution-of-3d-printing][Accessed 1.4.2017]

Ding, D., Pan, X., Cuiuri, D. & Li, H. 2015. Wire-feed additive manufacturing of metal components: technologies, developments and future interests. The International Journal of Advanced Manufacturing Technology, Vol 81. P. 465-466.

Ding, Y., Dwivedi, R. & Kovacevic, R. 2017. Process planning for 8-axis robotized laser-based direct metal deposition system: A case on building revolved part. Robotics and Computer-Integrated Manufacturing, Vol 44, P. 67-76.

Dusel, K-H. 2014. Director of Rapid Technologies, MTU Aero Engines. Aachen, Laser applications of tomorrow congress 7.9.2017.

EOS 2014. EOS of North America, Inc. Internet product pricing leaflet. Available: [https://www.cmu.edu/ices/advanced-manufacturing-laboratory/eos-materials-price-list_06-19-14.pdf][Accessed 21.7.2017]

EOS. 2013. Open and Flexible: EOS Part Property Management Provides both Individualization and Standardization. Internet brochure. [Available: https://cdn3.scrvt.com/eos/public/7e99ba072eca9ad8/294354957693f78ddb4787d3959e7057/ppm_whitepaper.pdf][Accessed 17.10.2017]

EOS. 2014. EOS StainlessSteel 316L. Material data sheet. EOS München 2014. 5 p.

EOS. 2017a. EOS M 400-4 – The Ultra-Fast Quad-Laser System with a Large Building Volume. Internet source. [Available: https://www.eos.info/systems_solutions/eos-m-400-4][Accessed 6.6.2017]

EOS. 2017b. EOS stainless steel 316L. Material data sheet. PDF document. [Available: https://cdn1.scrvt.com/eos/77d285f20ed6ae89/dd6850c010d3/EOSStainlessSteel316L.pdf] [Accessed 31.8.2017]

Erasteel. 2017. Gas atomization. Internet article. [Available: http://www.erasteel.com/content/gas-atomization-0] [Accessed 19.7.2017]

Everton, S., Hirsch, M., Stravroulakis, P., Leach, R. & Clare, A. 2016. Review of in-situ process monitoring and in-situ metrology for metal additive manufacturing. Materials & Design, Vol 95, p. 431-445.

Fabricating & Metalworking 2016. Internet source. [Available: http://www.fabricatingandmetalworking.com/2016/02/metal-additive-manufacturing-meets-quality-assurance/][Accessed 12.4.2017]

FIRPA. 2016. AM konematriisi 14.3.2016. Internet source. [Available: http://www.firpa.fi/AM_konematriisi_viimeisin.pdf][Accessed 18.10.2017]

Flame Spray Technologies. 2017. Internet source. [Available: https://www.fst.nl/about/laser-cladding/][Accessed 15.3.2017]

Frazier, W. 2014. Metal additive manufacturing: A review. Journal of Materials Engineering and Performance. Vol 23, issue 6. P. 1917-1928.

Gartner 2012. Internet source. [Available: http://www.gartner.com/newsroom/id/2124315] [Accessed 24.3.2017]

Gartner. 2014. Internet source. [Available: http://www.gartner.com/newsroom/id/2825417] [Accessed 24.3.2017]

Gartner. 2015. Internet source. [Available: http://www.gartner.com/newsroom/id/3117917] [Accessed 24.3.2017]

GE. 2017a. A Treat For The AvGeeks: An Inside Look At GE's 3D-Printed Aircraft Engine. Internet article. [Available: https://www.ge.com/reports/treat-avgeeks-inside-look-ges-3d-printed-aircraft-engine/][Accessed 24.10.2017]

GE. 2017b. An Epiphany Of Disruption: GE Additive Chief Explains How 3D Printing Will Upend Manufacturing. Internet article. [Available: https://www.ge.com/reports/epiphany-disruption-ge-additive-chief-explains-3d-printing-will-upend-manufacturing/][Accessed 18.10.2017]

Gibson, I., Roser, D., Strucker, B., 2015. Additive manufacturing technologies. Springer New York, Heidelberg, Dordrecht & London. 509 s.

GKN 2017. Internet source. [Available: http://www.gkngroup.com/additive-manufacturing/our-expertise/Aerospace-Centre-of-Excellence/Pages/st-louis-large-scale-deposition.aspx] [Accessed 12.4.2017]

Gu, H., Gong, H., Dilip, J. J. S., Pal, D., Hicks, A., Doak, H. & Stucker, B. 2014. Effects of Powder Variation on the Microstructure and Tensile Strength of Ti6Al4V Parts Fabricated by

Selective Laser Melting. Proceedings of the 25th Annual International Solid Freeform Fabrication Symposium. Austin, Texas, USA. 4-6.8.2014. P. 470–483. [Available in PDF-file: http://sffsymposium.engr.utexas.edu/sites/default/files/2014-040-Gu.pdf]

Güpner, M., Patschger, A. & Bliedtner, J. 2016. Influence of Process Parameters on the Process Efficiency in Laser Metal Deposition Welding

Herzog, D., Seyda, V., Wycick, E. & Emmelmann, C. 2016. Additive manufacturing of metals..Acta Materialia 117. P. 371-392.

Hoeges, S., Zwiren, A. & Schade, C. 2017. Additive manufacturing using water atomized steel powders. Metal Powder Report, Vol 72, Iss 2, 2017, P. 111-117.

Hällgren, S., Pejryd, L. & Ekengren, J. 2016. Additive Manufacturing and High Speed Machining -Cost comparison of short lead time manufacturing methods. 2016. Procedia CIRP, Vol 50. P. 384-389.

Höganäs. 2016. Certificate of analysis 316L 20-53 µm. Material data sheet. PDF document.

Höganäs. 2017. Product specification 1315-00. Material data sheet.

Hu, Z. & Mahadevan, S. 2017. Uncertainty quantification in prediction of material properties during additive manufacturing. Scripta materialia, Vol 135, p. 135-140.

Hybrid Manufacturing Technologies. 2017. AMBIT Multi-task tools. Internet source. [Available: http://www.hybridmanutech.com/hybrid-manufacturing.html][Accessed 24.10.2017]

Industrial Laser Solutions. 2013. Additive manufacturing at GE Aviation. Internet article. [Available: http://www.industrial-lasers.com/articles/print/volume-28/issue-6/features/additive-manufacturing-at-ge-aviation.html][Accessed 18.10.2017]

Jamshidnia, M. Sadek, A. & Kelly, S. 2015.Additive manufacturing of steel alloys using laser powder-bed fusion. Advanced Materials and processes, January 2015. P. 20-24.

Koenig, B. 2017. Additive grow and has growing pains. Internet source. [Available: http://advancedmanufacturing.org/additive-grows-growing-pains/][Accessed 15.5.2017]

Kow, C. 2017. 3D Metal Printing: Tips, Trends, and Common Misconceptions. Internet article. [Available: http://www.machinedesign.com/3d-printing/3d-metal-printing-tips-trends-and-common-misconceptions][Accessed 7.8.2017]

Kruth, J. P. &. Vandenbroucke, B. 2007. Selective Laser Melting of Biocompatable Metals for Rapid Manufacturing of Medical Parts. Rapid Prototyping Journal , Vol. 13, no.4. P. 196-203.

Leandri, A. 2015. Key design considerations for metal additive manufacturing. Internet article. Available: [http://blog.grabcad.com/blog/2015/11/02/key-design-considerations-for-metal-additive-manufacturing/][Accessed 22.7.2017]

Lindemann, C., Jahnke, U., Moi, M. & Koch, R. 2012. Analyzing Product Lifecycle Costs for a Better Understanding of Cost Drivers in Additive Manufacturing. Proceedings of the 23th Annual International Solid Freeform Fabrication Symposium. Austin, Texas, USA. 6-8.8.2012. P. 177–188. Available in PDF-file: http://sffsymposium.engr.utexas.edu/Manuscripts/2012/2012-12-Lindemann.pdf

Liu, H., Hao, J., Han, Z., Yu, G., He, X. & Yang, H. 2016. Microstructural evolution and bonding characteristic in multi-layer laser cladding of NiCoCr alloy on compacted graphite cast iron. Journal of Materials Processing Technology, Vol 232, p. 153-164.

Lorentz, K., Jones, J., Wimpenny, D. & Jackson, M. 2015. A REVIEW OF HYBRID MANUFACTURING. Annual International Solid Freeform Fabrication Symposium 2015, Austin, TX.

Ma, M., Wang, Z., Wang, D. & Zeng, X. 2013. Control of shape and performance for direct laser fabrication of precision large-scale metal parts with 316L Stainless Steel. Optics & Laser Technology, Vol 45, p. 209-216.

Makeitfrom. 2017. Annealed 316L Stainless Steel. Internet page. [Available: https://www.makeitfrom.com/material-properties/Annealed-316L-Stainless-Steel][Accessed 6.10.2017]

Matsuura. 2016. LUMEX Avance-60. Internet source. [Available: http://www.matsuura.co.jp/english/pdf/2016/Matsuura_Press_Release_lumex60_20160614E.pdf][Accessed 6.6.2017]

Maxey, K. 2015. A Profile of Hybrid Additive Manufacturing Technology. Internet article. [Available: http://www.engineering.com/3DPrinting/3DPrintingArticles/ArticleID/10484/A-Profile-of-Hybrid-Additive-Manufacturing-Technology.aspx][Accessed 12.7.2017]

Mc Cue 2016. Wohlers Report 2016: 3D Printing Industry Surpassed $5.1 Billion. [Available: https://www.forbes.com/sites/tjmccue/2016/04/25/wohlers-report-2016-3d-printer-industry-surpassed-5-1-billion/#6b627f3c19a0][Accessed 12.7.2017]

Mercelis, P. & Kruth, J.P. 2006. Residual stresses in selective laser sintering and selective laser melting. Rapid Prototyping Journal, Vol. 12 Issue: 5. s. 254-265.

Mower, T. & Long, M. 2016. Mechanical behavior of additive manufactured, powder-bed laser-fused materials. Materials Science and Engineering: A, Volume 651, 2016. P. 198-213.

Moylan, S., Slotwinski, J., Cooke, A., Jurrens, K., M. & Donmez, M. 2013. Lessons Learned in Establishing the NIST Metal Additive Manufacturing Laboratory. Internet article. [Available: http://nvlpubs.nist.gov/nistpubs/TechnicalNotes/NIST.TN.1801.pdf][Accessed 21.10.2017]

Mudge, R. & Wald, N. 2007. Laser Engineered Net Shaping Advances Additive Manufacturing and Repair. RPM Innovations, January 2007. P. 44-48.

Mukherjee, T., Zuback, J. & Debroy, T. 2016. Printability of alloys for additive manufacturing. Scientific Reports 6.

Nassar, A. & Reutzel, E. 2015. Beyond layer-by-layer Additive Manufacturing – Voxel-wise Directed Energy Deposition. Applied Research Laboratory at the Pennsylvania State University, University Park, PA.

Optomec. 2017. LENS Materials FAQs. Internet brochure. Available: [https://www.optomec.com/wp-content/uploads/2014/02/LENS_MATERIALS_Datasheet_WEB2016.pdf][Accessed 26.7.2017]

Park, J., Park, J., Lee, M., Sung, J., Cha, K. & Kim, D. 2016. Effect of Energy Input on the Characteristic of AISI H13 and D2 Tool Steels Deposited by a Directed Energy Deposition Process. Metallurgical and Materials Transactions, Vol 47.

Piili, H., Happonen, A., Väistö, T., Venkataramanan, V., Partanen, J. & Salminen, A. 2015. Cost Estimation of Laser Additive Manufacturing of Stainless Steel. Physics Procedia, 78. P. 388–396.

Pocketnewsalert 2017. Internet source. [Available: http://www.pocketnewsalert.com/2017/01/audi-and-eos-development-partnership-focuses-on-holistic-approach-for-metal-based-additive-manufacturing.html][Accessed 15.5.2017]

Popovich, V., Borisovb, E.V., Popovich, A., Sufiiarovb, V., Masaylob, D. & Alzinac, L. 2017. Impact of heat treatment on mechanical behaviour of Inconel 718 processed with tailored microstructure by selective laser melting. Materials & Design 131, p. 12-22

Quinlan, H., Hasan, T., Jaddou, J. & Hart, J. 2017. Industrial and Consumer Uses of Additive Manufacturing: A Discussion of Capabilities, Trajectories, and Challenges. Special Issue:

Environmental Dimensions of Additive Manufacturing and 3D Printing, vol 21, Iss s1. P. 1-265.

Ray, J. 2016a. Calculating the Cost of Additive Manufacturing. Internet article. [Available: https://www.linkedin.com/pulse/calculating-cost-additive-manufacturing-jason-t-ray][Accessed 14.9.2017]

Rickenbacker, L., Spierings, A. & Wegener, K. 2013. An integrated cost-model for selective laser melting (SLM). Rapid prototyping journal, Vol 19, Iss: 3. P. 208-214.

Sander, P. 2017. Vice President of Emerging Technologies, Airbus Operations GmbH. Hamburg, Airbus factory visit on 10.5.2017.

Sanders, M. 2016a. DfAM essentials - print parts efficiently and effectively. Internet article. [Available: https://www.linkedin.com/pulse/dfam-essentials-print-parts-efficiently-effectively-marc-saunders][Accessed 12.6.2017]

Savini, A. & Savini, G. 2015. A short history of 3D printing, a technological revolution just started. Conference paper on History of High-Technologies and their Socio-Cultural Contexts Conference (HISTELCON), 2015 ICOHTEC/IEEE International, Tel Aviv.

Saunders, M. 2017a. X marks the spot - find ideal process parameters for your metal AM parts. Internet article. [Available: https://www.linkedin.com/pulse/x-marks-spot-find-ideal-process-parameters-your-metal-marc-saunders/][Accessed 11.9.2017]

Saunders, M. 2017b. Can you build AM parts without supports? Internet article. [Available: https://www.linkedin.com/pulse/can-you-build-am-parts-without-supports-marc-saunders][Accessed 7.6.2017]

Saunders, M. 2017c. Making the world's first 3D printed MTB. Internet article. [Available: https://www.linkedin.com/pulse/making-worlds-first-3d-printed-mtb-marc-saunders][Accessed 7.6.2017]

Saunders, M. 2017d. Is topological optimisation really optimal? Internet article. [Available: https://www.linkedin.com/pulse/topological-optimisation-really-optimal-marc-saunders][Accessed 7.6.2017]

Saunders, M. 2017e. Design for metal AM - a beginner's guide. Internet article. [Available: https://www.linkedin.com/pulse/design-metal-am-beginners-guide-marc-saunders][Accessed 3.8.2017]

SFS-ISO/ASTM 52900. 2016. Additive manufacturing. General principles. Terminology. Helsinki: Finnish Standards Association SFS. 22 p.

Schuh G, Behr M, Brecher C, Bührig-Polaczek A, Michaeli W, Schmitt R, Arnoscht J, Bohl A,Buchbinder D, Bültmann J, Diatlov A, Elgeti S, Herfs W, Hinke C, Karlberger A, Kupke D, Lenders M, Nußbaum C, Probst M, Queudeville Y, Quick J, Schleifenbaum H, Vorspel-Rüter M. & Windeck C. 2012.Individualised production. In: Brecher C (ed) Integrative production Technology for high-wage countries. Springer, Berlin Heidelberg, Berlin, Heidelberg. P. 77– 239.

Simufact. 2017. Additive Manufacturing Technology. Internet source. [Available: https://www.simufact.com/additive-manufacturing.html][Accessed 30.5.2017]

SLM Solutions 2017. Machnines. Internet page. [Available: https://slm-solutions.com/machines] [Accessed 30.5.2017]

Slotwinski J., Garboczi E., Stutzman P., Ferraris C., Watson S. & Peltz, M. 2014. Characterization of Metal Powders Used for Additive Manufacturing. J Res Natl Inst Stand Technol, 9/2014.

Solidworks. 2015. Preparing SOLIDWORKS Models for 3D Printing. Internet source. [Available: http://blogs.solidworks.com/tech/2015/05/preparing-solidworks-models-3d-printing.html [Accessed 10.3.2017]

Sun, Z., Tan, X., Beng, S., Wai, T. & Yeong, Y. 2016. Selective laser melting of stainless steel 316L with low porosity and high build rates. Materials & Design, Vol 104. P. 197-204.

Supplier. 2017. Confidential quote from a supplier.

Tammas-Williams, S. & Todd, I. 2016. Design for additive manufacturing with site-specific properties in metals and alloys. Scripta Materialia, Vol 135, P. 105-110.

Thomas, D. 2009. The Development of Design Rules for Selective Laser Melting. Doctoral thesis. University of Wales Institute, Cardiff. 318 p.

Thomas, D. S. & Gilbert, S. W. 2014. Cost and Cost-effectiveness of Additive Manufacturing – A Literature Review and Discussion. Gaithersburg, December 2014. NIST Special Publication 1176. National Institute of Standards and Technology, U. S. Department of Commerce. 77 p.

Total Optics. 2017. Internet source. Available: [http://optics.org/news/8/4/1/smartechApril2017] [Accessed 22.7.2017]

Townsend, A., Senin, N., Blunt, L., Leach, R.K. & Taylor, J. 2016. Surface texture metrology for metal additive manufacturing: a review. Precision Engineering 46, 2016. P. 34-47.

Vartanian, K & Mc Donald, T. 2016. Accelerating Industrial Adoption of Metal Additive Manufacturing Technology. [Available: https://advanceseng.com/general-engineering/accelerating-industrial-adoption-metal-additive-manufacturing-technology/][Accessed 3.3.2017]

Vora, P. 2012. Benchmarking capabilities of SLM and EBM to build overhangs without supports. Seminar presentation, Solid Freeform Fabrication Symposium 2012, 6.8.2012 Austin, Texas, USA.

VTT. 2016. Design guide for additive manufacturing of metal components by SLM process. Research report VTT-R-03160-16. VTT Technical Research Centre of Finland. 148 p.

Wang, Z., Palmera, T. & Beese, A. 2016. Effect of processing parameters on microstructure and tensile properties of austenitic stainless steel 304L made by directed energy deposition additive manufacturing. Acta Materialia, Vol 110, p. 226-235.

Wärtsilä 2017. Internal newsletter in Compass intranet. Login required.

Wired. 2015. Airbus' Newest Design Is Based on Bones and Slime Mold. Internet article. [Available: https://www.wired.com/2015/12/airbuss-newest-design-is-based-on-slime-mold-and-bones/][Accessed 27.9.2017]

Wohlers, T. & Gornet, T. 2014. History of Additive manufacturing. Section of Wohlers report 2014. 34 p.

Yadollahi, A. & Shamsaei, N. 2017. Additive manufacturing of fatigue resistant materials: Challenges and opportunities. International Journal of Fatigue, Vol 98, P. 14–31.

Yang, S., Tang, Y. & Zhao, Y. 2015. A new part consolidation method to embrace the design freedom of additive manufacturing. Journal of Manufacturing, Vol 20, p. 444-449.

Zhang, K., Wang, S., Liu, W. & Long, R. 2014. Effects of substrate preheating on the thin-wall part built by laser metal deposition shaping. Applied Surface Science, Vol 317, P. 839-855.

Zhong, C.,Gasser, A., Schopphoven, T. & Poprawe, R. 2015. Experimental study of porosity reduction in high deposition-rate Laser Material Deposition. Optics & Laser Technology, Volume 75. Pages 87-92.

Metal PBF machine suppliers by December 2017 Appendix I, 1/2

Company	*Country*	*Process*	*Machine*	*Building chamber [mm x mm x mm]*	*Power [W]*
Matsuura	Japan	Hybrid-PBF (Laser)	LUMEX Avance-60	600 x 600 x 500	1000/500
		Hybrid-PBF (Laser)	LUMEX Avance-25	256 x 256 x 185	400/500/1000
Arcam	Sweden	PBF (EB)	Q10plus	200 x 200 x 180	3000 (EB)
		PBF (EB)	Q20plus	Ø 350 x 380	3000 (EB)
		PBF (EB)	A2X	200 x 200 x 380	3000 (EB)
EOS Gmbh	Germany	PBF (Laser)	M100	Ø 100 x 95	200
		PBF (Laser)	M280	250 x 250 x 350	400
		PBF (Laser)	M290	250 x 250 x 350	400
		PBF (Laser)	M400	400 x 400 x400	1000 / 4x400
ConceptLaser	Germany	PBF (Laser)	M2 Cusing	250 x 250 x 280	200 / 400
		PBF (Laser)	M2 Cusing Multilaser	250 x 250 x 280	2x200 / 2x400
		PBF (Laser)	X line 2000 R	800 x 400 x 500	2x1000
		PBF (Laser)	ATLAS	1100 x 1100 x 300	1000
		PBF (Laser)	M Line Factory	400 x 400 x 425	1-4x400 / 1-4x1000
Renishaw	UK	PBF (Laser)	AM 250	250 x 250 x 300	200 / 400
		PBF (Laser)	AM 400	250 x 250 x 300	400
		PBF (Laser)	RenAM 500M	250 x 250 x 350	500
Realizer	Germany	PBF (Laser)	SLM 250	250 x 250 x 300	100 - 400
		PBF (Laser)	SLM 300i	300 x 300 x 300	400 / 1000
Additive Industries	Netherlands	PBF (Laser)	MetalFAB1	420 x 420 x 400	1-4x500 / 1-4x1000
SLM Solutions	Germany	PBF (Laser)	SLM 125	125 x 125 x 125	400
		PBF (Laser)	SLM 280 HL	280 x 280 x 365	400 / 700 / 2x400 / 2x700 / 700+1000
		PBF (Laser)	SLM 500 HL	500 x 280 x 365	2-4x400 / 2-4x700
		PBF (Laser)	SLM 800	800 x 280 x 365	2-4x400 / 2-4x700
3D Systems	USA	PBF (Laser)	ProX DMP 100	100 x 100 x 100	50
		PBF (Laser)	ProX DMP 200	140 x 140 x 125	300
		PBF (Laser)	ProX DMP 300	250 x 250 x 330	500
		PBF (Laser)	ProX DMP 320	275 x 275 x 420	500
Wuhan Huake 3D	China	PBF (Laser)	HK M100	100 x 100 x 80	200
		PBF (Laser)	HK M250	250 x 250 x 250	400
Wuhan Binhu	China	PBF (Laser)	HRPM-II	250 x 250 x 250	200 / 400
Syndaya	China	PBF (Laser)	DiMetal-400	400 x 400 x 400	200 / 400
		PBF (Laser)	DiMetal-280	250 x 250 x 300	200 / 400
Trumpf	Germany	PBF (Laser)	TruPrint 1000	100 x 100 x 100	200
		PBF (Laser)	TruPrint 3000	300 x 300 x 400	500
Bright Laser Technologies	China	PBF (Laser)	S-200	150 x 150 x 200	200 / 500

		PBF (Laser)	S-300	250 x 250 x 500	500
Sodick	USA/Japan	Hybrid-PBF (Laser)	OPM250L	250x250x250	250
OR Laser	Germany	PBF (Laser)	ORLAS Creator	Ø 100 x 110	250
Shining 3D	China	PBF (Laser)	EP-M250	250 x 250 x 300	200 / 500
Farsoon	China	PBF (Laser)	FS271M	250 x 250 x 320	500
Sisma	Italy	PBF (Laser)	mysint300	ø 300x400 mm	500
DMG Mori	Germany/Japan	PBF (Laser)	LASERTEC 30 SLM	300 x 300 x 300	400 / 1000
AddUp	France	PBF (Laser)	FormUp 3D	350 x 350 x 350	1-2 x 500

**** MS - maraging/tool steels, SS - stainless steels, IN - Inconel, Al - aluminum, Ti - Titanium, CoCr - Cobalt chromium***

Company	**Machine**	**Materials ***	**Price [M€]**	**Other**
Matsuura	LUMEX Avance-60	MS, SS, Ti, CoCr, Ni, Al	N/A	Hybrid-PBF/CNC milling system, automatic powder sieving station
	LUMEX Avance-25	MS, SS, Ti, CoCr, Ni, Al	0,8	Hybrid-PBF/CNC milling system
Arcam	Q10plus	Ti, CoCr, IN	0,6	N/A
	Q20plus	Ti, CoCr, IN	0,8	N/A
	A2X	Ti, CoCr, IN	N/A	N/A
EOS Gmbh	M100	CoCr, SS, Ti	0,25	N/A
	M280	CoCr, Ti, SS, MS, IN, Al	0,4	Real-time process controlling
	M290	CoCr, Ti, SS, MS, IN, Al	0,9	Real-time process controlling & monitoring
	M400	CoCr, Ti, SS, MS, IN, Al	1,3	Real-time process controlling
ConceptLaser	M2 Cusing	SS, Al, Ti, MS, CoCr	0,8	Integrated filter system
	M2 Cusing Multilaser	SS, Al, Ti, MS, CoCr	N/A	Integrated filter system
	X line 2000 R	Al, Ti, Ni	N/A	Integrated filter system, set-up/dismantling module, rotating system for base plate
	ATLAS	N/A	N/A	Real-time process controlling
	M Line Factory	SS, Ti, Ni	N/A	Integrated filter system, set-up/dismantling module
Renishaw	AM 250	CoCr, Ti, SS, MS, IN, Al	N/A	N/A
	AM 400	CoCr, Ti, SS, MS, IN, Al	N/A	Real-time process controlling & monitoring
	RenAM 500M	CoCr, Ti, SS, MS, IN, Al	N/A	Integrated filter system, powder sieving station
Realizer	SLM 250	CoCr, Ti, SS, MS	N/A	N/A
	SLM 300i	CoCr, Ti, SS, MS	N/A	Powder recycling system
Additive Industries	MetalFAB1	N/A	N/A	Integrated powder sieving and handling system, heat treatment, set-up/dismantling stage, modular architecture
SLM Solutions	SLM 125	CoCr, Ti, SS, MS, IN, Al	N/A	Part removable unit, (removable build cylinder)
	SLM 280 HL	CoCr, Ti, SS, MS, IN, Al	0,7	Part removable unit, (removable build cylinder), Real-time process controlling & monitoring
	SLM 500 HL	CoCr, Ti, SS, MS, IN, Al	1,3	Integrated powder sieving station/powder supply unit, part removal station, removable build cylinder, Real-time process controlling & monitoring
	SLM 800	CoCr, Ti, SS, MS, IN, Al	N/A	Integrated part removal station, automated chamber switching
3D Systems	ProX DMP 100	CoCr, SS	N/A	Optional powder recycling system
	ProX DMP 200	CoCr, MS, SS, Al	N/A	Optional powder recycling system, semiautomatic material loading
	ProX DMP 300	CoCr, MS,SS, Al	N/A	Automatic powder recycling system, automatic material loading,
	ProX DMP 320	Ti,SS, IN, Al, (MS, CoCr)	0,7	Removable build cylinder, optional powder recycling system, optional module for fast material exchange
Wuhan Huake 3D	HK M100	N/A	N/A	N/A

	HK M250	N/A	N/A	N/A
Wuhan Binhu	HRPM-II	N/A	N/A	N/A
Syndaya	DiMetal-400	SS, Ti, CoCr, Al	N/A	N/A
	DiMetal-280	SS, Ti, CoCr, Al	N/A	N/A
Trumpf	TruPrint 1000	MS, SS, Ti, CoCr, Ni, Al, Bronze, precious metals	N/A	N/A
	TruPrint 3000	MS, SS, Ti, CoCr, Ni, Al, Bronze, precious metals	N/A	Part and powder handling automatization, removable build cylinder, simultaneous supply chamber applying
Bright Laser Technologies	S-200	Ti, SS, IN, Al, MS	N/A	N/A
	S-300	Ti, SS, IN, Al, MS	N/A	N/A
Sodick	OPM250L	MS, SS	N/A	Hybrid machine with CNC milling, powder recycling system
OR Laser	ORLAS Creator	N/A	N/A	Rotating recoater
Shining 3D	EP-M250	N/A	N/A	N/A
Farsoon	FS271M	N/A	N/A	N/A
Sisma	mysint300	CoCr, Ti, SS, MS, IN, Al, bronze	N/A	Automated unpacking station, filtering system, open system for parameters and process control
DMG Mori	LASERTEC 30 SLM	CoCr, Ti, SS, MS, IN, Al	N/A	Integrated glove box & powder removing, integrated sieving system, fast powder change (2 h)
AddUp	FormUp 3D	Ti, SS, IN, Al, MS	N/A	Real-time process controlling, automatic sieving system

Company	*Country*	*Process*	*Machine*	*Building area [mm x mm x mm]*	*Power [kW]*
DMG Mori	Japan/Germany	Hybrid-DED	Lasertec 65 3D	Ø600 x 400	2
Trumpf	Germany	DED	TruLaser 3000	800x600x400	8
		DED	TruLaser 7020	1540x2000x520	2-6
		DED	TruLaser 7040	3540x2000x520	2-6
BeAM	France	DED	Mobile	400x250x200	0,5
		DED	Modulo	650x400x400	0,5
		Hybrid-DED	Magic 2.0	1200x800x800	2
Sciaky	USA	Wire feed EB-DED	EBAM 68	1727x1727x2794	42
		Wire feed EB-DED	EBAM 88	2235x2235x2794	42
		Wire feed EB-DED	EBAM 110	2794x2794x2794	42
		Wire feed EB-DED	EBAM 150	3810x3810x3048	42
		Wire feed EB-DED	EBAM 300	7620x2743x3353	42
RPM Innovations	USA	DED	LMD 557	1500x1500x2100	3 / 4
		DED	LMD 535	1500x1000x1500	3 / 4
		DED	LMD 222	600x600x600	2
Optomec	USA	DED	LENS 450	100x100x100	0,4
		DED	LENS 450 XL	150x150x150	0,4
		DED	LENS MR-7	300x300x300	0,5 / 1
		DED	LENS 850-R	900x1500x900	1 / 2
		Hybrid-DED	LENS 3D Hybrid 20	500x350x500	0,5 / 1
InssTec	South Korea	DED	MX-400	400x450x300	0,5
		DED	MX-600	450x600x380	1
		DED	MX-1000	1000x800x650	2
		DED	MX-Grande	4000x1000x1000	5
Mazak	Japan	Hybrid-DED	Integrex i-400AM	N/A	N/A

Build rates in general:

0,5 kW = 0,1 kg/h

1 kW = 0,2 kg/h

2 kW = 0,5 kg/h

3 kW = 1 kg/h

Company	*Machine*	*Build rate [kg/h]*	*Materials*	*Price [M€]*	*Other*
DMG Mori	Lasertec 65 3D	1	SS, MS, Al, CoCr, Bronze, Ni, WC, Stellite, Noble alloys	> 0.6	Combined CNC machining center and DED processing chamber
Trumpf	TruLaser 3000		MS, SS, Ni, Ti, Al, Cu, TiC, WC, Co		Laser cutting & welding features in addition, Rotary two-stage table, additional automated loading/unloading, additional machine vision system for process monitoring
	TruLaser 7020		MS, SS, Ni, Ti, Al, Cu, TiC, WC, Co		Laser cutting & welding features in addition, Rotary two-stage table, additional automated loading/unloading, additional machine vision system for process monitoring; modular design
	TruLaser 7040		MS, SS, Ni, Ti, Al, Cu, TiC, WC, Co		Laser cutting & welding features in addition, Rotary two-stage table, additional automated loading/unloading, additional machine vision system for process monitoring; modular design
BeAM	Mobile	0,1 - 0,5			Controlled atmosphere
	Modulo				Controlled atmosphere
	Magic 2.0				Milling spindle (hybrid), controlled atmosphere
Sciaky	EBAM 68	5	Ti		Vacuum atmosphere
	EBAM 88	5	Ti		Vacuum atmosphere
	EBAM 110	5	Ti		Vacuum atmosphere
	EBAM 150	5	Ti		Vacuum atmosphere
	EBAM 300	5	Ti		Vacuum atmosphere
RPM Innovations	LMD 557	0,2 - 1	SS, Ni, Ti		Fume collection system, inert gas atmosphere
	LMD 535	0,2 - 1	SS, Ni, Ti		Fume collection system, inert gas atmosphere
	LMD 222	0,2 - 1	SS, Ni, Ti		Fume collection system, inert gas atmosphere
Optomec	LENS 450	0,5	SS, MS, TI, Al, Ni, IN, Co, MMC		Powder feeder unit
	LENS 450 XL	0,5	SS, MS, TI, Al, Ni, IN, Co, MMC		Powder feeder unit
	LENS MR-7	0,5	SS, MS, TI, Al, Ni, IN, Co, MMC		Dual powder feeder unit enables material alloying simultaneously, thermal imaging
	LENS 850-R	0,5	SS, MS, TI, Al, Ni, IN, Co, MMC		Rotating and tilting table with in/out cart on rails
	LENS 3D Hybrid 20	0,2	SS, MS, TI, Al, Ni, IN, Co, MMC	> 0,3	Hybrid DED machine with CNC milling
InssTec	MX-400		MS, SS, IN		Tilting & rotating table, process monitoring
	MX-600		MS, SS, IN		Tilting & rotating table, process monitoring
	MX-1000		MS, SS, IN		Tilting & rotating table, process monitoring
	MX-Grande		MS, SS, IN		Tilting & rotating table, process monitoring
Mazak	Integrex i-400AM				Hybrid-DED machine with CNC milling and laser marking and dual laser processing heads

Build rates in general:

0,5 kW = 0,1 kg/h

1 kW = 0,2 kg/h

2 kW = 0,5 kg/h

3 kW = 1 kg/h

DED process head suppliers by December 2017 Appendix III, 1/1

Company	*Country*	*Process*	*Process head*	*Power [kW]*	*Materials*	*Price [M€]*	*Other*
Trumpf	Germany	DED	BEO D 70				Mountable in robot or CNC machining center
Hybrid manufacturing technologies	USA	DED	AMBIT	1			Mountable in robot or CNC machining center
Optomec	USA	DED	LENS	0,5 - 3	SS, MS, TI, Al, Ni, IN, Co, metal matrix composites	0.2	Mountable in robot or CNC machining center
OR Laser	Germany	DED	Diodeline Robolaser		MS, SS, Ni, Co, WC, Ti, Al, metal matrix composites		Mountable in robot or CNC machining center

Build rates in general:

0,5 kW = 0,1 kg/h

1 kW = 0,2 kg/h

2 kW = 0,5 kg/h

3 kW = 1 kg/h